Mon. Not. R. Astron. Soc. **000**, 1–?? (2008) Printed 1 August 2008 (MN LaTeX style file v2.2)

arXiv:0808.0165v1 [astro-ph] 1 Aug 2008

The Combined NVSS-FIRST Galaxies (CoNFIG) Sample - I. Sample Definition, Classification and Evolution

M. A. Gendre[1]* and J. V. Wall[1]
[1] *Department of Physics and Astronomy, The University of British Colombia, 6224 Agricultural Rd, Vancouver, BC, V6T 1Z1, Canada*

Accepted . Received ; in original form

ABSTRACT
The CoNFIG (Combined NVSS-FIRST Galaxies) sample is a new sample of 274 bright radio sources at 1.4 GHz. It was defined by selecting all sources with $S_{1.4\ \mathrm{GHz}}{\geqslant}1.3$ Jy from the NRAO-VLA Sky Survey (NVSS) in the North field of the Faint Images of the Radio Sky at Twenty-cm (FIRST) survey. New radio observations obtained with the VLA for 31 of the sources are presented. The sample has complete FRI/FRII morphology identification; optical identifications and redshifts are available for 80% and 89% of the sample respectively, yielding a mean redshift of ∼0.71. One of the goals of this survey is to get better definitions of luminosity distributions and source counts of FRI/FRII sources separately, in order to determine the evolution of the luminosity function for each type of source. We present a preliminary analysis, showing that these data are an important step towards examining various evolutionary schemes for these objects and to confirm or correct the dual population unified scheme for radio AGN. Improving our understanding of radio galaxy evolution will give better insight into the role of AGN feedback in galaxy formation.

Key words:
Surveys - Radio Continuum: Galaxies - Galaxies: Active - Galaxies: Statistics - Galaxies: Luminosity Function

1 INTRODUCTION

Longair (1966) determined that powerful radio sources undergo strong differential evolution, the first indication of cosmic downsizing. Since then our understanding of the space density of AGN as a function of cosmic epoch has steadily continued to advance.

With the development of evolutionary models for radio sources came the idea of a dual-population model. The initial version of this dichotomy (Longair 1966) was in terms of low and high luminosities. But with high-frequency surveys, and the large number of flat/inverted spectrum sources revealed in them, an alternative classification emerged, based exclusively on the source spectra: sources with a spectral index $\alpha \leqslant -0.5$ (where $S_\nu^\alpha \propto \nu^\alpha$), corresponding to optically thin synchrotron radiation, were classified as steep-spectrum, whereas sources with lower spectral indices ($\alpha \geqslant -0.5$) inevitably showed features of synchrotron self-absorption and were classified as flat-spectrum. Initial indications suggested that these two populations underwent different evolution (Schmidt 1976; Masson & Wall 1977). However, Dunlop & Peacock (1990) studied the radio luminosity function (density of sources with a given luminosity per unit of co-moving volume) of these two classes of radio sources, and came to the conclusion that both populations were undergoing a similar evolution, implying that they might not actually be distinct.

The Fanaroff-Riley (FR) classification (Fanaroff & Riley 1974), originally a sub-classification for steep-spectrum objects, was employed to provide a further categorization of radio sources. This classification divides radio sources into two classes of double-lobed sources based on the appearance of their jets. The FRI objects have the highest brightness along the jets and core, reside in moderately rich cluster environments (Hill & Lilly 1991) and include sources with irregular structure (Parma et al. 1992). In contrast, FRII sources show hot spots in the lobes and more collimated jets, are found in more isolated environments and display stronger emission lines (Rawlings et al. 1989; Baum & Heckman 1989). Fanaroff & Riley (1974) found these two classes to be divided in radio power, with a break luminosity $P_{178\ \mathrm{MHz}} \sim 10^{25}\ \mathrm{WHz^{-1}sr^{-1}}$, with FRII sources lying above this limit. Subsequently Owen & Ledlow (1994) showed that the break was a function of both radio and optical luminosity.

During the 1980s the 'unification' hypothesis emerged to describe how viewing aspect could relate RQSOs, (Radio

---

* E-mail: mgendre@phas.ubc.ca; jvw@phas.ubc.ca

Quasi-Stellar Objects of either flat or steep-spectrum) to FRII radio galaxies (e.g. Peacock 1987; Scheuer 1987; Barthel 1989). However, the scheme did not include lower-luminosity AGNs such as FRI galaxies and BL Lac objects. The unifying connection between these was introduced by Marcha & Browne (1995). The unified model of AGN proposed by Wall & Jackson (1997) and Jackson & Wall (1999) assumes that the cosmic evolution of radio loud AGN is based on a division of the radio sources into a low-luminosity ($P_{178\ \mathrm{MHz}} < 10^{25}\ \mathrm{WHz}^{-1}\mathrm{sr}^{-1}$) component corresponding to FRIs, and a high-luminosity component corresponding to FRIIs. In this scheme, the various forms of AGN observed (FRI and FRII extended double sources, flat- and steep-spectrum RQSOs and BL Lac objects) result from the orientation of the extended parent objects with respect to the observer's line-of-sight. Indeed, because the double-sided ejection of synchrotron blobs in AGN is at relativistic speed, the orientation of the ejection axis to the line-of-sight becomes crucial: sources viewed side-on appear as double radio galaxies (FRI or FRII) and sources viewed along the jets appear as RQSOs (beamed counterparts of FRII sources) or BL Lac objects (beamed counterparts of FRI sources). The relativistically-boosted jet emission in the beamed counterparts of the extended sources dominates the extended emission, making the overall radio emission appear compact down to VLBI scales.

Initially, in modelling the space density of radio AGN, it was assumed for simplicity that the low-luminosity radio galaxies including FRI sources showed no cosmic evolution (Wall, Pearson & Longair 1980; Jackson & Wall 1999), the strong cosmic evolution confined only to the higher luminosities and the FRII galaxies. With the advent of large-scale redshift surveys for nearby galaxies, many authors, including Brown et al. (2001), Snellen & Best (2001), Willott et al. (2001), Sadler et al. (2007) and Rigby, Best & Snellen (2007), found significant evolution for low power sources – but mild evolution in comparison with that of the high-luminosity sources. Rigby, Best & Snellen (2007) argued that if both FRIs and FRIIs have similar evolution, the dual-population scheme could be reduced to a single-population model.

The FRI/FRII dual-population scheme has encountered several problems. One of these concerns the correspondence between FRI galaxies and BL Lac objects. Urry & Padovani (1995) noted that some BL Lac objects have non-FRI-like morphologies and that the density of FRI sources is too low to account for the entire BL Lac population, a concern also raised by Wall & Jackson (1997). Looking at BL Lac objects from another point of view, March et al. (1996) demonstrate that only about one third of low-luminosity core dominated radio sources - which are supposedly the beamed counterpart of FRI sources - are conventional BL Lac objects. Most of the remaining sources have optical classification such as Seyfert objects or elliptical galaxies.

A related issue concerns the existence of FRI RQSOs. Until recently, these objects were thought not to exist, leading to the hypothesis that FRI and FRII central engines were of different nature (Baum et al. 1995) and that the torus opening in FRI sources was too small to observe a quasar nucleus (Falcke et al. 1995). However, the discovery of an FRI QSO, E1821+643, by Blundell & Rawlings (2001) overthrew those assumptions. More recent VLA observations (Heywood, Blundell & Rawlings 2007) uncovered another 4 sources of this type.

Finally, if sources with different FR classes undergo different evolution, this might imply that their fundamental characteristics, such as the black hole spin or jet composition, are different too. However, the existence of hybrid sources, which display both FRI and FRII morphological characteristics (Capetti et al. 1995), then becomes puzzling. Based on observations of hybrid sources, Kaiser & Alexander (1997) argued that the FR dichotomy is based purely on the interaction between the jets and the environmental medium, and not on intrinsic properties of the central engine. This view is also supported by Gopal-Krishna & Wiita (2000) and Gawronski et al. (2006). However, Wang et al. (1992) suggested that some AGN engines could be capable of ejecting jets of unequal power, resolving the problem of hybrid sources. Gopal-Krishna & Wiita (2000) found no evidence for such a process in their sample.

Other schemes have been suggested to resolve these difficulties. Kaiser & Best (2007) explained the FR dichotomy by postulating that all sources start as FRII objects and used an analytical model in which the evolution of the radio sources is governed by energy losses from both radiating relativistic electrons in the lobes and turbulence in the jets.

Willott et al. (2001) used an approach to a dual-population unified scheme based on the luminosity of sources instead of morphology. Optical spectra of FRII sources are heterogeneous and they can display both strong and weak low-excitation emission lines (Laing 1994). Therefore, radio sources can also be grouped based on their emission lines, with one population composed of low-luminosity sources having weak emission lines (containing both FRI and FRII objects), and the other composed of high-luminosity sources with strong emission lines (containing only FRII objects). With this model, Willott et al. (2001) concluded that high luminosity objects undergo a stronger evolution with epoch than low luminosity sources, as found by by e.g. Longair (1966), Wall, Pearson & Longair (1980) and Urry & Padovani (1995), and that the radio luminosity function has the form of a broken power-law, similar to the conclusions of Dunlop & Peacock (1990). We note that, since conventional accretion-disk systems are expected to be strong X-ray sources, luminosity-based dual-population models are also used in modelling the luminosity function of X-ray selected RQSOs (Hardcastle et al. 2006).

Defining the relation between the different radio sub-populations together with their cosmic evolution is becoming fundamental to our understanding of galaxy formation.

The current paradigm for galaxy formation follows hierarchical build-up in a Cold Dark Matter (CDM) universe. Nevertheless, serious difficulties arise from this model in its simplest form, as discussed by Bower et al. (2006). It implies that current epoch galaxies must be the largest and bluest and have the highest star forming rate of all galaxies. Observations show that they are red, old galaxies, whereas the bulk of star formation is observed at earlier epochs. This is known as downsizing, first described by Cowie et al. (1996). AGN negative feedback could be the key to understanding this phenomenon. The ignition of the nucleus in a star forming galaxy could eject the gas into the inter-galactic medium, thus reducing or even stopping star formation, breaking the hierarchical buildup (Silk & Rees 1998; Granato et al. 2001; Quilis et al. 2001). Note that there is also some positive AGN feedback (van Breugel et al. 2004; Klamer et al. 2004) in which the pressure from the jets compresses the inter-stellar medium and induces star formation. The balance between these processes remains to be understood; establishing the cosmic behaviour of the radio AGN is important in revealing the precise role of the feedback mechanisms.

Although FRI and FRII sources show different evolution, they also lie in different luminosity ranges. There is therefore a possibility that both types may show similar evolution for overlapping luminosities (i.e. high-luminosity FRIs and low-luminosity FRIIs). In order to sort out the FR dichotomy and its details, accurate models of the evolution of each population are needed. This implies compiling accurate statistics, such as luminosity distributions and source counts, for both types separately. This is the goal of the CoNFIG (Combined NVSS-FIRST Galaxies) sample presented here, a new sample of bright radio sources with complete morphological identification.

The CoNFIG sample is defined as all sources with $S_{1.4\ \mathrm{GHz}}\geqslant 1.3$ Jy from the NRAO-VLA Sky Survey (NVSS, Condon et al. 1998) catalogue within the north region of the Faint Images of Radio Sources at Twenty-cm survey (FIRST, White et al. 1997), a 1.5 sr region defined roughly by $-8^\circ \leqslant$ Dec $\leqslant 64^\circ$ and 7 hr $\leqslant$ RA $\leqslant$ 17 hr. The flux density limit of 1.3 Jy was chosen so that the number of sources in the sample was of statistical significance while allowing us to identify the morphology for each source individually. Optical identifications were obtained from the SuperCOSMOS Sky Survey (SSS, Hambly et al. 2001) and redshift information extracted using the SIMBAD database. With the accompanying VLA observations described here, the sample has complete morphology information, a median flux density of $S_{1.4\ \mathrm{GHz}}\sim 1.96$ Jy and optical identifications and redshift information for ~80% and ~89% of the sources respectively.

The structure of this paper is as follows. The details of the construction of the CoNFIG sample are explained in §2 while §3 describes how the morphologies were determined. Optical identifications and redshift information are discussed in §4 and §5 outlines the computation of the morphology-dependent luminosity distributions. Finally, §6 describes and discusses the FRI/FRII source counts.

Throughout this paper, we assume a standard ΛCDM cosmology with $H_0=70$ km s^{-1} Mpc^{-1}, $\Omega_M=0.3$ and $\Omega_\Lambda=0.7$.

2 THE CONFIG SAMPLE

2.1 Radio Surveys

2.1.1 NVSS

The NRAO-VLA Sky Survey (NVSS) is a 1.4 GHz continuum survey covering the entire sky north of -40° declination (corresponding to an area of 10.3 sr). The completeness limit is about 2.5 mJy with an rms brightness fluctuation of about 0.45 mJy/beam. The survey has yielded over 1.8 million sources, implying a surface density of ~50 sources per square degree. It was carried out with the Very Large Array (VLA) in D and DnC configuration (the D configuration being the most compact VLA configuration with a maximum antenna separation of ~1 km), providing an angular resolution of about 45 arcsec FWHM (Condon et al. 1998).

Since the median angular size of faint extragalactic sources at these flux density levels is $\lesssim$10 arcsec (Condon et al. 1998), most sources are unresolved, and the NVSS flux density measurements are quite accurate. However, the large beam size does not allow one to determine precise structure of sources or to determine positions accurate enough to establish optical counterparts.

2.1.2 FIRST

The Faint Images of the Radio Sky at Twenty-cm (FIRST) is another 1.4 GHz continuum survey, covering an area of ~9030 deg^2 over the North Galactic Pole. The completeness limit is about 1 mJy with a typical rms of 0.15 mJy. The survey yielded ~811,000 sources, implying a surface density of ~90 sources per square degree. It was carried out with the VLA in B configuration (the B configuration having a maximum antenna separation of ~10 km), which provides an angular resolution of about 5 arcsec FWHM (White et al. 1997). This survey complements the NVSS survey well, providing a beam size small enough to resolve the structure of most nearby extended radio sources.

2.2 Sample Definition

The CoNFIG sample is defined as all sources with $S_{1.4\ \mathrm{GHz}}\geqslant 1.3$ Jy from the NVSS catalogue within the north region of the FIRST survey (1.5 sr region defined roughly by $-8^\circ \leqslant$ Dec $\leqslant 64^\circ$ and 7 hr $\leqslant$ RA $\leqslant$ 17 hr), resulting in a sample of 261 objects.

Very large sources resolved in NVSS within this initial sample, such as 3CRR sources (Laing, Riley & Longair 1983), need to be considered. In these cases, two or more NVSS sources with $S_{1.4\ \mathrm{GHz}}\geqslant 1.3$ Jy are actually components of a much larger resolved source. After collecting the resolved source components together, the refined sample contains 248 sources.

Multi-component sources, where each component has $S_{1.4\ \mathrm{GHz}}<1.3$ Jy but with a total flux density $S_{1.4\ \mathrm{GHz}}\geqslant 1.3$ Jy, also need to be considered. For this purpose, NVSS sources with 0.1 Jy$\leqslant S_{1.4\ \mathrm{GHz}}\leqslant$1.3 Jy were selected and, if any other source in the catalogue was located within 4 arcmin of the listed sources, they were set aside as candidate extended sources. The final decision on whether or not the sources are actually components of a resolved source was made by visual inspection of the NVSS contour plot. In this manner, 32 more sources were added to the sample.

Finally, after looking at the NVSS and FIRST contour plots and optical information of all the sources, 7 sources[1] were deleted, either because the source is a globular cluster, or because the source actually consists of independent sources, each with $S_{1.4\ \mathrm{GHz}}$<1.3 Jy.

The final sample, referred to as the CoNFIG Sample, consists of 274 sources. Details of the sources can be found in Appendix A.

3 MORPHOLOGY

3.1 Initial Classification

76 sources in the sample appear in the 3CRR catalogue (Laing, Riley & Longair 1983) in which the morphology type of each 3CRR source has been determined. These sources are marked by a star next to their 3C name in Appendix A.

For other sources, the morphology was determined by looking at the FIRST and NVSS radio contour plots, obtained from the NASA virtual observatory Skyview (`http://skyview.gsfc.nasa.gov`). The contour plots are shown in Figure 3 and Appendix C.

If the contour plot displays distinct hot spots at the edge of the lobes (as in Figure 2), and the lobes are aligned, the source was classified as FRII. On the contrary, sources with collimated jets showing hot spots near the core and jets were classified as FRI (see Figure 1). Most irregular-looking sources were also classified as FRI (Parma et al. 1992).

Contour plots were obtained for all but one (CoNFIG-225) of the CoNFIG sources. 53 sources were identified as extended but the resolution is too low to confirm their exact morphological types. Additional VLA observations were obtained for 31 of these sources (see §3.2) while for the other 22 sources, data were found in the VLA archives.

As specified in §2.2, 7 sources were deleted from the sample after examination of their contour plots. In one case, the source is a globular cluster and in another case, the source has no FIRST or NVSS contours. The other 5 NVSS 'sources', when observed with FIRST, actually consist of separate and independent sources, each with $S_{1.4\ \mathrm{GHz}}$<1.3 Jy. The NVSS radio positions of these sources can be found in Table 1.

3.2 VLA Observations

Radio observations of 31 extended sources with uncertain morphological classification were taken at 8 GHz using the VLA in A configuration on July 29, 2007. The observations used the standard two IFs of 8435.1 and 8485.1 GHz, with a bandwidth of 50 MHz. The A configuration is the configuration with the largest spacing between antennas (∼36 km), providing a synthesized beam of 0.24 arcsec FWHM at 8 GHz.

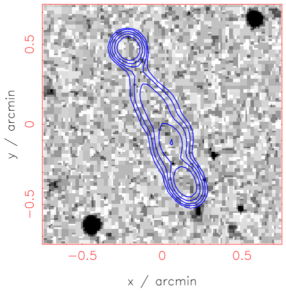

Figure 1. Typical FIRST contour plot of FRI source (here, 3C 284) against SSS grey-scale optical background. The hot spots are located along the jets and more towards the core of the source.

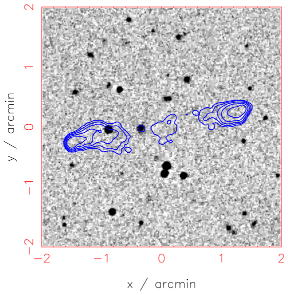

Figure 2. Typical FIRST contour plot of FRII source (here, 3C 223) against SSS grey-scale optical background. The hot spots are located at the edge of the lobes.

Table 1. Sources deleted from the original sample.

Source	Reason deleted
08 14 43.59 +12 58 10.0	2 separate sources
08 30 04.12 +07 45 45.0	2 separate sources
10 34 05.09 +11 12 32.1	2 separate sources
12 30 35.69 +12 19 18.2	globular cluster
13 23 02.33 +29 41 34.0	3 separate sources
14 17 00.49 +07 10 50.2	2 separate sources
15 40 30.42 −05 03 17.4	no contours

The 8 GHz flux density of each source was derived from the 1.4 GHz NVSS flux density and spectral index (see details in §5), and the exposure time was computed for each source such as to provide a signal-to-noise ratio of at least 5. The sources were placed accordingly into 4 different exposure time groups (5, 10, 20 and 30 min), except for CoNFIG-227 (60 min) and CoNFIG-257 (40 min). For observations with a 30 min exposure time, the exposure was split into two separate 15 min scans to improve *uv* coverage. The primary calibrator 3C174 (0542+498) was observed at the beginning of the run while 3C286 (1331+305) was observed twice during the run, once in the middle and once at the end. These calibrate the flux density scale assuming a flux density of 4.84 Jy at 8435.1 MHz and 4.81 Jy at 8485.1 MHz for 3C174 and 5.18 Jy at 8435.1 MHz and 4.99 Jy at 8485.1 MHz for 3C286, based on the scale of Baars et al. (1977). Nearby secondary calibrators were observed approximately every 30 min to provide phase calibration. Details of the observations are shown in Appendix D.

---

[1] Note that 3 of these sources (CoNFIG-015, 076 and 225) were deleted later in the sample construction process, based on the 8 GHz VLA observations described in §3.2.

Figure 3. Contour plots from NVSS (outermost contours) and FIRST (innermost contours) of sources in the CoNFIG sample. The complete set of images can be found in Appendix C.

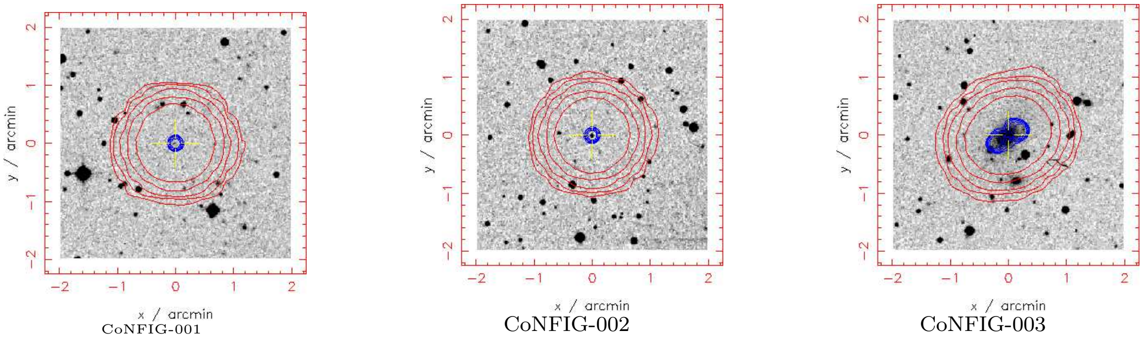

CoNFIG-001
07 13 38.15 +43 49 17.20

CoNFIG-002
07 14 24.80 +35 34 39.90

CoNFIG-003
07 16 41.09 +53 23 10.30

Figure 4. Contour plots from FIRST 1.4GHz (outermost contours) and VLA 8 GHz observations (innermost contours). The complete set of images can be found in Appendix D.

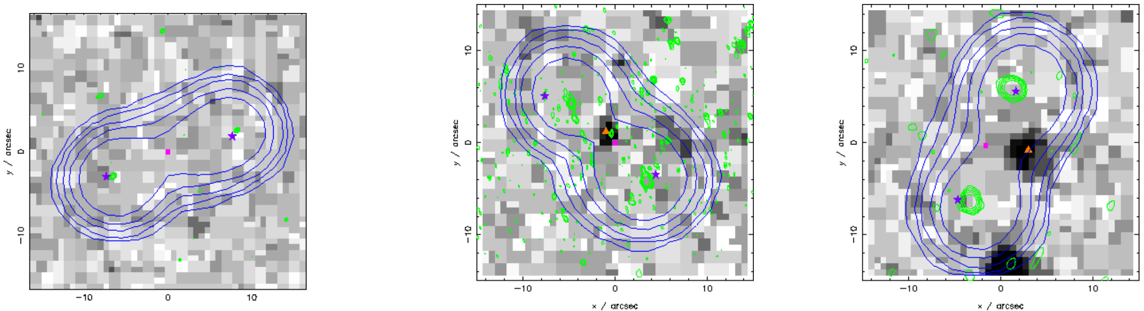

CoNFIG-009
8 GHz, A configuration

CoNFIG-010
8 GHz, A configuration

CoNFIG-012
8 GHz, A configuration

3.3 Final Classification

Data were extracted from the VLA archives at other frequencies and configurations for some sources for which the 8 GHz contours were not satisfactory. All data were reduced using standard procedures incorporated within the AIPS software provided by NRAO, and the resulting images are grouped in Appendix D.

Over 60% of sources in the CoNFIG sample are classified either as FRI or FRII. The rest of the sources are classified as compact or deleted from the sample (see Table 1). Some sources in this group will be unresolved high redshift FRIIs, and some others are confirmed as truly compact from the VLBA calibrator list (Beasley et al. 2002; Fomalont et al. 2003; Petrov et al. 2005, 2006; Kovalev et al. 2007) or from the Pearson-Readhead survey (Pearson & Readhead 1988). Some of these confirmed compact sources show a steep ($\alpha \leqslant -0.6$) spectral index and are possible Compact Steep Sources (CSS) (Fanti & Fanti 1994).

After looking at optical counterparts from the SuperCOSMOS Sky Survey (as discussed in §4), two particular subclasses of compact and FRII sources are identified.

(1) Some compact sources show no optical counterpart. These sources can be classified either as CSS or as unresolved FRII. When confirmed as a compact source from the VLBA calibrator list (see Beasley et al. 2002; Fomalont et al. 2003; Petrov et al. 2005, 2006; Kovalev et al. 2007) or the Pearson-Readhead survey (Pearson & Readhead 1988), the source is classified as CSS and is included in the compact sources statistics. Otherwise, the source is assumed to be an unresolved FRII. Their inclusion into the FRII group has a low impact on the FRII statistics, as seen in Figure 8.

(2) Other sources are classified as FRII and present a stellar type optical identification. These sources are - on the basis of the unified model - steep-spectrum RQSOs, which occur when the line of sight of the observer is oriented at less than 45° with respect to the jets, enabling the observer to look inside the dusty torus.

The final classification for each source is shown in Table A and the distribution of morphological types is presented in Table 2. Errors in flux density measurements are well defined for point sources in the catalogues, but corresponding error estimates for the extended sources were too uncertain to be worth including here.

Table 2. Morphology of the sources in the CoNFIG sample. The morphology of each source is determined by looking at FIRST and NVSS contour plots or from VLA observations as described in §3.1 and §3.2 respectively.

FRI	FRII	Unres.	Comp.	CSS
36 13.1%	135 49.3%	22 8.0%	75 27.4%	6 2.2%

Table 3. Details of the extra samples constructed to better define the FRI/FRII source counts. The total number of sources as well as the number FRI, FRII and unresolved extended, compact and Compact Steep Spectrum sources, are shown here.

	S_{lim} (mJy)	Area (deg^2)	Number of sources FRI	FRII	C	Tot.
CoNFIG-2	800	2915.25	27	149	67	243
CoNFIG-3	200	370.00	41	205	45	291
CoNFIG-4	50	64.00	42	119	73	234

3.4 CoNFIG-2, 3 and 4

In order to improve the FRI/FRII statistics, three more samples of about 250 sources each, and complete to 0.8 Jy (CoNFIG-2), 0.2 Jy (CoNFIG-3) and 50 mJy (CoNFIG-4), were constructed from the NVSS catalogue over various areas, all included in the FIRST northern region. For each sample, the morphologies of the sources were determined as described in §3.1. Details of the samples are given in Table 3 while the data for the samples are shown in Tables B1 and B2. Optical identification and redshifts were retrieved for CoNFIG-2 only, as described in the next section.

Because the morphology information is not complete for all sources in the CoNFIG-2, 3 and 4 samples, these objects were only used to compute the FRI/FRII source count (see §6.2).

4 OPTICAL IDENTIFICATIONS AND REDSHIFTS

To determine core coordinates in order to retrieve redshifts, optical identifications (together with B_j, R1, R2 and I magnitudes) were obtained for 79% of the sources in the CoNFIG sample and 61% of the sources in the CoNFIG-2 sample from the SuperCOSMOS Sky Survey (SSS, Hambly et al. 2001).

Redshifts were retrieved for 230 CoNFIG sources and 161 CoNFIG-2 sources, using the SIMBAD (`http://simbad.u-strasbg.fr/simbad`) and NED (`http://nedwww.ipac.caltech.edu/`) databases.

Redshift and magnitude information are listed in Table 6 and Appendix A for CoNFIG, and in Table B1 for CoNFIG -2.

When spectroscopic redshifts were not available, we estimated photometric redshifts via an empirical R - z relation derived from extended sources in the CoNFIG sample with galaxy identifications and $15 \leqslant R \leqslant 21$, as shown in Figure 5. A simple fit to these data is

$$R = 20.70 + 5.24 \log z + 1.28(\log z)^2 \qquad (1)$$

Photometric redshift estimate is given to 14 CoNFIG objects falling into this category, but with no spectroscopic redshift information, bringing the redshift coverage to 244 sources (89% of the sample).

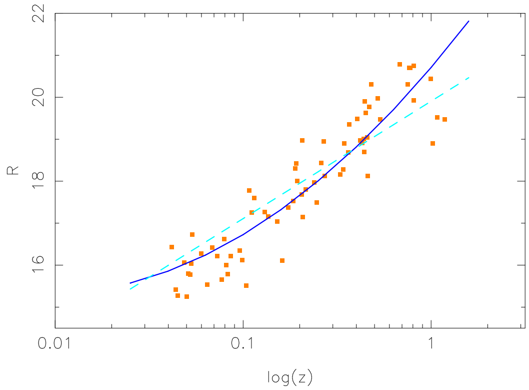

Figure 5. R-z relation from CoNFIG data for extended sources with $15 \leqslant R \leqslant 21$. The squares represent objects classified as FRI or FRII (excluding unresolved sources) with optical ID and spectroscopic redshift information. The solid line shows the quadratic fit ($R = 20.70 + 5.24 \log z + 1.28(\log z)^2$) from which photometric redshifts are estimated. For comparison, the linear fit is also shown (dashed line).

Table 4. Redshift completeness in the CoNFIG and CoNFIG-2 samples. Redshift information was retrieved from the SIMBAD database. CSS and unresolved sources from Table 2 are regrouped with Compact and FRII sources respectively.

	CoNFIG FRI	FRII	Compact
with z	34	142	68
% of group with z	94.4%	90.4%	83.9%
% of sample with z	12.4%	51.8%	24.8%
	CoNFIG-2 FRI	**FRII**	**Compact**
with z	22	97	52
% of group with z	81.5%	65.1%	77.6%
% of sample with z	9.0%	39.9%	21.4%

For the CoNFIG sample, redshifts range from z=0.0033 to z=3.522 with a mean redshift of z=0.715 and a median redshift of z=0.580. The morphology-dependent distribution is shown in Figure 6 and details of the redshift distributions are given in Tables 4 and 5. The FRI distribution is concentrated at low redshifts ($z \leqslant 0.5$) while the FRII distribution covers a wider range, up to z=2.5.

Note that for 38 CoNFIG and 34 CoNFIG-2 sources, redshift information was retrieved from the literature using the radio position of the object, but no counterpart was found in SSS.

Table 5. Redshift distribution information for the CoNFIG sample.

Type	% of group with ID	redshift: min	max	mean	med.
all	79.6%	0.0034	3.522	0.715	0.580
FRI	97.2%	0.0034	1.191	0.157	0.053
FRII	75.1%	0.0456	2.474	0.712	0.572
Comp.	80.2%	0.0336	3.5220	1.001	0.909

Table 6. Optical identification table for CoNFIG (example). The complete table can be found in Table A1.

ID	Rad. Type	Optical Position (J2000)	Opt. Type	B_j	R1	R2	I
1	C*	07 13 38.15 +43 49 17.20	g	21.79	19.79	19.93	18.62
2	C*	07 14 24.80 +35 34 39.90	s	18.74	17.59	18.42	17.50
3	II	07 16 41.09 +53 23 10.30	g	15.43	15.54	14.22	13.30
4	C	07 35 55.54 +33 07 09.60	s	21.22		20.34	18.55
5	C*	07 41 10.70 +31 12 00.40	s	16.52	16.28	16.32	15.83
6	II	07 45 42.13 +31 42 52.60	s	15.76	15.55	15.56	15.11
8	I	07 58 28.60 +37 47 13.80	g	14.51	15.42	14.06	12.23
10	II	08 01 35.32 +50 09 43.00	s	21.79		20.17	
11	II	08 05 31.31 +24 10 21.30	g	17.28	16.28	15.60	15.16
12	II	08 10 03.67 +42 28 04.00	g	21.08	19.47	18.91	17.38
13	II	08 12 59.48 +32 43 05.60	g	21.19	19.76	19.19	18.64
14	II	08 13 36.07 +48 13 01.90	s	18.45	17.79	17.82	17.54
16	II	08 19 47.55 +52 32 29.50	g	20.37	18.31	18.26	17.80
17	II	08 21 33.77 +47 02 35.70	g	18.55	17.26	17.07	16.26

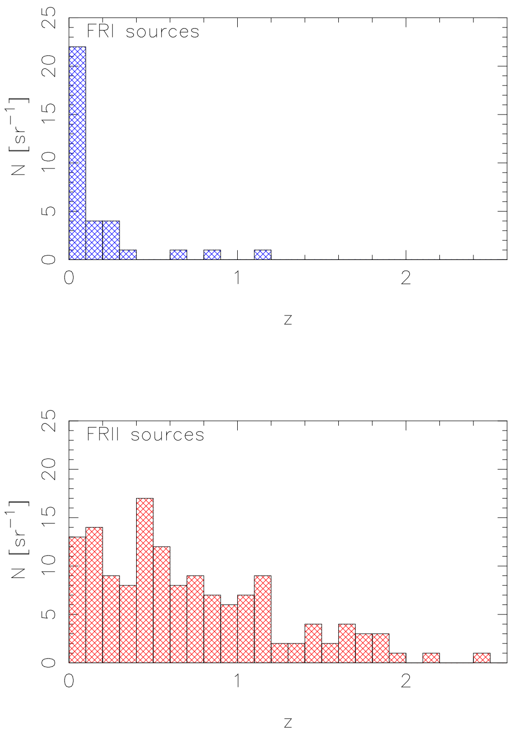

Figure 6. Redshift distributions for the CoNFIG sample. Details are given in Table 4. The FRI distribution is concentrated at low redshifts ($z \leqslant 0.5$) while the FRII distribution lies over a wider range, up to z∼2.5.

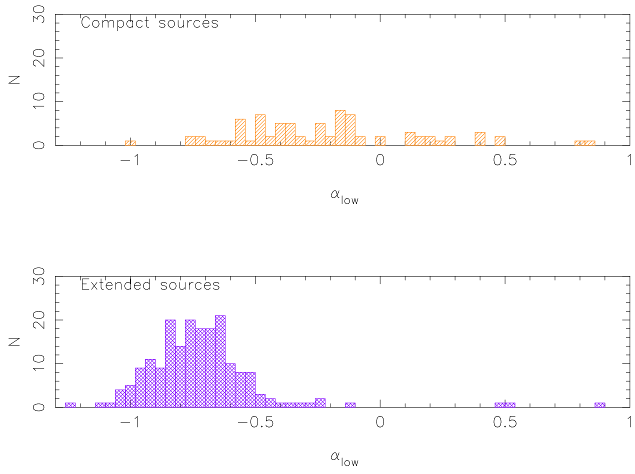

Figure 7. Spectral index distribution (using frequencies 178 MHz $\leqslant \nu \leqslant$ 1.4 GHz). The distribution peaks around -0.7, which is the usual value for extended sources, but has a long tail to flat/inverted spectra.

5 LUMINOSITY DISTRIBUTIONS

In order to compute the radio luminosity, the spectral index α (defined as $S_\nu \propto \nu^\alpha$) of each source needs to be determined. To achieve this, flux densities at different frequencies for each source were compiled and the spectral index computed following the relation:

$$\alpha = \frac{\Delta \log(S)}{\Delta \log(\nu)} \tag{2}$$

A summary of the different frequencies and corresponding surveys used to retrieve the flux density information is given in Table 8.

We made independent estimates for the low- and high-frequency spectral indices (with 178 MHz $\leqslant \nu \leqslant$ 1.4 GHz and 1.4 GHz $\leqslant \nu \leqslant$ 5 GHz respectively). The low frequency spectral indices are used to compute the luminosities; since $\nu_{rest} = \nu_{obs}(z+1)$, the luminosity emitted at $\nu_{rest} = 1.4$ GHz will correspond to an observed flux at frequency $\nu_{obs} < 1.4$ GHz.

Values for spectral indices are listed in Table A. The median value is $\alpha = -0.67$. However, the extended sources are grouped around a median value of $\alpha = -0.73$ as seen in Figure 7, while the compact sources, as is well known, show a broader distribution.

Figure 8 presents the luminosity distributions for FRI and FRII objects. The distribution of FRII sources only (excluding unresolved sources) is shown as a solid-line distribution on the plot. As stated in §3.3, the inclusion of the unresolved sources with the FRII sources has very little effect on the structure of the distribution.

Data table for CoNFIG (example). The complete table can be found in Appendix A.

CoNFIG ID	Name	RA (J2000)	DEC (J2000)	Type	Red.	$S_{178\ \mathrm{MHz}}$ (Jy)	$S_{365\ \mathrm{MHz}}$ (mJy)	$S_{408\ \mathrm{MHz}}$ (Jy)	$S_{1.4\ \mathrm{GHz}}$ (mJy)	$S_{2.7\ \mathrm{GHz}}$ (Jy)	$S_{5.0\ \mathrm{GHz}}$ (Jy)	α	Ref. and Comments	
1	QSO B0710+439	07 13 38.15	+43 49 17.20	C*	0.5180		655.0	0.75	2011.4		1.60	$0.82^{\dagger}$	1	
2	QSO B0711+35	07 14 24.80	+35 34 39.90	C*	1.6260		840.0		1467.1		0.89	$0.41^{\dagger}$	1	
3	4C 53.16	07 16 41.09	+53 23 10.30	II	0.0643	5.4	3913.0		1501.4		0.63	−0.63	2	
4	4C 33.21	07 35 55.54	+33 07 09.60	C		7.4	6750.0		2473.1		0.92	−0.56		
5	QSO J0741+3111	07 41 10.70	+31 12 00.40	C*	0.6300		1365.0		2284.3		2.68	0.38	3	
6	4C 31.30	07 45 42.13	+31 42 52.60	II	0.4620	4.4	2448.0		1357.8		1.02	−0.55	3	S
7	4C 56.16	07 49 48.10	+55 54 21.00	I	0.0360	4.2	2636.0		1660.4			−0.44	4	N
8	NGC 2484	07 58 28.60	+37 47 13.80	I	0.0438	11.3		5.39	2717.9		1.33	−0.68	5	
9	4C 37.21	07 59 47.26	+37 38 50.20	II			5374.0	4.54	1691.2		0.46	−0.84		NV
10	TXS 0757+503	08 01 35.32	+50 09 43.00	II			5810.0		1471.7		0.47	−1.02		SV
11	3C 192*	08 05 31.31	+24 10 21.30	II	0.0600	21.0		13.10	5330.6	3.30	2.60	−0.67	3	
12	3C 194	08 10 03.67	+42 28 04.00	II	1.1840	9.9	6734.0	5.68	2056.6	1.07	0.61	−0.78	6	A
13	4C 32.24	08 12 59.48	+32 43 05.60	II	0.4700	5.1	4266.0		1522.5		0.47	−0.68	7	
14	3C 196*	08 13 36.07	+48 13 01.90	II	0.8710	68.2	49023.0		15010.0	7.66	4.36	−0.75	3	S
16	4C 52.18	08 19 47.55	+52 32 29.50	II	0.1890	7.2	6037.0		2104.2		0.80	−0.62	8	V^{1}
17	3C 197.1	08 21 33.77	+47 02 35.70	II	0.1300	8.1	5534.0	4.68	1787.1	1.16	0.86	−0.75	8	A
18	4C 17.44	08 21 44.02	+17 48 20.50	C		5.8	4566.0	4.56	1875.1	1.11	0.68	−0.57		
19	4C 22.21	08 23 24.72	+22 23 03.70	C*	0.9510	4.5	4086.0		2272.4		1.59	−0.34	9	
20	4C 56.16A	08 24 47.27	+55 52 42.60	C*	1.4170		2028.0		1449.4		1.20	−0.25	10	

Table 7. Data for CoNFIG-2 sample (example). The complete table can be found in Table B1. Data for CoNFIG-3 and CoNFIG-4 can be found in Table B2

RA	DEC (J2000)	Radio Type	$S_{1.4\ \mathrm{GHz}}$ (mJy)	B-mag.	Opt. Type	z	Ref.
09 20 11.16	+17 53 25.00	S	1070.6				
09 20 58.48	+44 41 53.70	C*	1017.2	17.20	2	2.180	2
09 21 07.54	+45 38 45.70	II	8101.6	18.61	1	0.174	1
09 21 47.05	+37 54 16.10	II	826.4	20.24	2	1.108	3
09 22 49.93	+53 02 21.20	S	1597.8				
09 27 03.04	+39 02 20.70	C*	2884.6	17.06	2	0.698	1
09 30 33.45	+36 01 23.60	II	1875.1	18.98	2	1.157	1
09 30 54.27	+58 55 16.60	II	1082.9				
09 34 15.80	+49 08 21.00	C*	800.5			2.582	2
09 35 04.06	+08 41 37.30	S	1037.6				
09 35 06.62	+39 42 07.60	I	1029.5				
09 36 32.02	+04 22 10.80	S	971.1			1.340	4
09 39 50.20	+35 55 53.10	II	3719.0	18.59	1	0.137	1

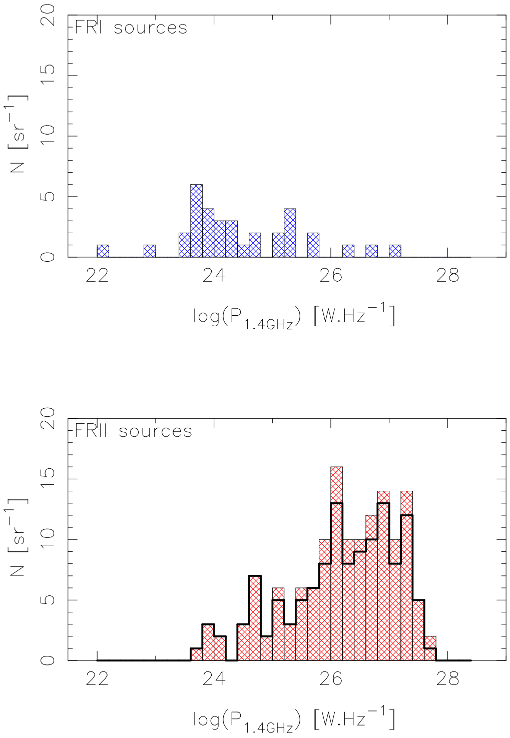

Figure 8. Luminosity distributions for FRI and FRII sources. The solid-line histogram in the FRII luminosity distribution plot corresponds to the distribution we would get if the unresolved sources were excluded from the FRII grouping.

6 FRI/FRII SOURCE COUNTS

One of the challenges in modelling the space densities of FRI and FRII sources is to compute an accurate source count for each morphological type. This implies determining the morphological type of all sources used.

To increase the number of sources with morphology information, five samples at different flux density limits were combined with the CoNFIG sample. These samples include the CENSORS (Best et al. 2003)and BDFL (Bridle, Davis, Fomalont & Lequeux 1972) samples, as well as the 3 extra CoNFIG samples (see details in §3.4 and Table 3). The morphologies of the sources in each sample were determined by looking at the FIRST and NVSS contour plots as described in §3, (with the exception of the CENSORS sources and some of the BDFL sources, as described in the next section).

Table 8. Surveys used to retrieve flux density information.

Frequency	Survey	Reference
178 MHz	3C	Kellermann et al. (1969)
	4C	Pilkington & Scott (1965)
365 MHz	Texas	Douglas et al. (1996)
408 MHz	Parkes	Wright & Otrupcek (1990)
	B3	Ficarra et al. (1985)
2.7 GHz	3C	Kellermann et al. (1969)
	Parkes	Wright & Otrupcek (1990)
5.0 GHz	3C	Kellermann et al. (1969)
	Parkes	Wright & Otrupcek (1990)
	MIT-Greenbank	Bennett et al. (1986)

6.1 The CENSORS and BDFL samples

6.1.1 The CENSORS sample

The CENSORS (Combined EIS-NVSS Survey Of Radio Sources) sample (Best et al. 2003; Brookes et al. 2005, 2007) contains 150 sources complete to $S_{1.4\ \mathrm{GHz}}$=7.2 mJy, selected from NVSS over the ESO Imaging Survey (EIS) Patch D. The sample has a median flux density of $S_{1.4\ \mathrm{GHz}}\sim$15 mJy and optical identifications for 68% of the sources.

The wide field EIS comprises a relatively wide-angle survey of four distinct patches of sky up to 6 deg^2 each (Nonino et al. 1999). Patch D is the most northerly, with a limiting magnitude of I∼23 (Benoist et al. 1999) and an area of 2×3 deg^2 centred on $09^h51^m36.0^s$-$21°00'00''$ (J2000).

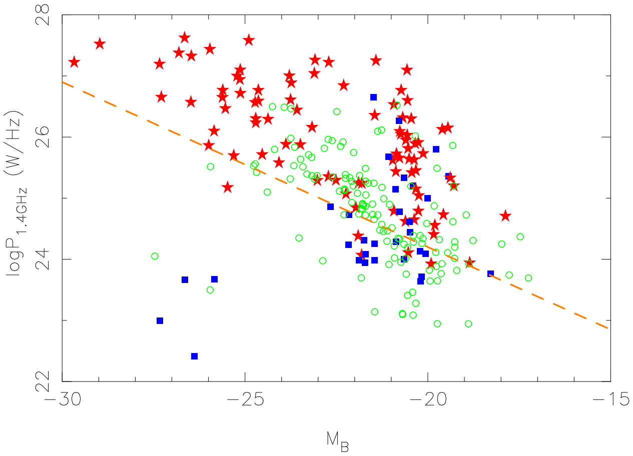

Figure 9. Radio power-optical B-magnitude relation for the CoNFIG and CoNFIG-2 sources. FRIs (filled squares) seem to take over FRIIs (stars) below the dash line $logP_{1.4\ GHz} = -0.27M_B + 18.8$. This relation is used to determine the FRI/FRII classification for non-QSO sources from CENSORS (open circles).

The goals of the CENSORS sample (Best et al. 2003) are to constrain evolution of the top end of the black hole mass function, study the environments around radio sources at different luminosities, test the K-z relation for radio sources and test the dual-population models.

Little classification of the CENSORS sources has been done, although Brookes et al. (2007) presented a list of the possible RQSOs. To attempt a preliminary morphological classification, we used the NVSS images to determine the morphology of the sources; in most cases though, the resolution is far too low to determine the morphology of the extended sources. In the case of the CoNFIG sample, this was solved by using FIRST images together with supplementary VLA observations. However, the CENSORS sample does not overlap with the FIRST survey, or any other higher resolution samples. Ledlow & Owen (1996) showed that FRI and FRII sources are separated on a radio power-optical magnitude diagram. Following this idea, we used radio flux densities and B-magnitude data from CoNFIG and CoNFIG-2 to determine a line in the radio power-optical B-magnitude diagram below which FRI morphology dominates. The line is defined as (as shown in Figure 9):

$$logP_{1.4\ GHz} = -0.27M_B + 18.8 \qquad (3)$$

This relation was then applied to the 136 sources from CENSORS using the flux density and magnitude information from Best et al. (2003), using a K-correction value of $K_{corr} = 1.122$ z. As a result, 49 sources were classified as FRI and 87 as FRII. Note that, for 63 CENSORS sources, B-magnitude information were not available and a B-z relation similar to the R-z relation defined in §4 was then used to determine M_B.

6.1.2 The BDFL sample

The BDFL sample (Bridle, Davis, Fomalont & Lequeux 1972) contains 424 sources and is complete to $S_{1.4\ \mathrm{GHz}} \geqslant 1.7$ Jy in the area of sky $-5° < \delta < +70°$, $|b| > 5°$.

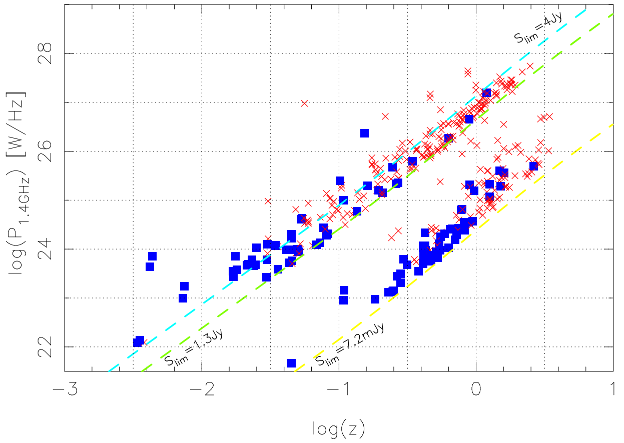

Figure 10. P-z plane for the CoNFIG sources. FRIs and FRIIS are represented by squares and crosses respectively. The flux-density limit lines for the BDFL (down to 4.0 Jy), CENSORS (at 7.2 mJy) and CoNFIG (at 1.3 Jy) samples are represented as dashed lines respectively. The plane is divided into sections of $\Delta log(P) = 1$ and $\Delta log(z) = 0.5$ to illustrate the poor coverage of some regions.

To improve definition of the high flux-density ends of the morphological source counts, sources from this sample with $S_{1.4\ \mathrm{GHz}} \geqslant 4.0$ Jy were selected, yielding a total number of 90 sources. The morphology of each source was determined from either Laing, Riley & Longair (1983) or Kharb & Shastri (2004), or by looking at the NVSS contours. As a result, of the 90 sources, 21 sources are classified as FRI, 38 as FRII and 31 as compact.

6.2 Compiling the Source Count

In total, there are ∼500 sources from the combined BDFL (down to 4.0 Jy), CENSORS (at 7.2 mJy) and CoNFIG (at 1.3 Jy) samples. Still, as illustrated in Figure 10, large areas of the P-z plane are not covered.

To improve coverage, the three other CoNFIG samples described in 3.4 were used. In all three of these samples, sources with $S_{1.4\ \mathrm{GHz}} \geqslant 1.3$ Jy were removed as they are already present in the CoNFIG sample.

The relative differential source counts $\Delta N/\Delta N_0$ for FRI and FRII sources were then computed from the combined sample of 244 FRI and 736 FRII sources. Data for the source count presented in Figure 11 can be found in Table B3.

It is seen that FRII sources dominate the total count, except at low flux densities ($\log S_{1.4\ \mathrm{GHz}} \lesssim -1.6$), where the FRI sources suddenly take over. Since most of the FRI count at low flux densities is composed of low-luminosity sources at low redshift, our results show that FRI objects must undergo some mild evolution. This is consistent with the results of Sadler et al. (2007), who studied low power sources in the 2SLAQ survey (Richards et al. 2005) and found evidence that FRIs undergo significant evolution over $0 < z < 0.7$. Our results also show that FRIs undergo less evolution than FRIIs, and they do not participate much in the source-count "evolution bump" around $S_{1.4\ \mathrm{GHz}} \sim 1$Jy. This is in agreement with previous investigations stretching back to Longair

(1966).

An illustrative exponential evolution model of space density, as described by Wall, Pearson & Longair (1980), was used to fit the data, as shown in Figure 11. In the case of both FRI and FRII sources, the luminosity distribution obtained for the CoNFIG sample was used as starting points. This approach, as detailed in Wall, Pearson & Longair (1980), assumes that the luminosity function $\rho(P,z)$ can be factorized as $\rho(P,z) = F(P,z)\rho_0(P)$, where $\rho_0(P)$ is the local luminosity function and $F(P,z)$ an evolution function transforming $\rho_0(P)$ into the redshift and luminosity-dependent $\rho(P,z)$. The details of the evolution function $F(P,z)$ successfully fitting the two morphology counts (with the same set of parameters) are as follows:

$$F(P,z) = \begin{cases} e^{M(P)\tau} & z \leqslant z_c \\ 0 & z > z_c \end{cases} \tag{4}$$

where z_c is the redshift cutoff (maximum redshift at which a population exists) and τ is the look-back time

$$\tau = \frac{1}{H_0}\int_0^z \frac{dz'}{(1+z)\sqrt{\Omega_M(1+z)^3 + \Omega_K(1+z)^2 + \Omega_\Lambda}} \tag{5}$$

with M(P) defined as

$$M = \begin{cases} M_1 & P < P_1 \\ \frac{(M_2-M_1)(logP_1 - logP)}{logP_1 - logP_2} + M_1 & P_1 \leqslant P \leqslant P_2 \\ M_2 & P > P_2 \end{cases} \tag{6}$$

The best fit values for this model are $z_c = 4.37$, $M_1 = 2.38$, $M_2 = 11.63$, $logP_1 = 26.0$ and $logP_2 = 26.9$.
This is only an illustrative model. Accurate modelling of the FRI/FRII source counts and luminosity functions will be the subject of a future study.

The morphological counts and the model fit raise two points:

(1) If a single model, albeit one with differential evolution, can describe both populations, are the populations separate, or necessarily one (Snellen & Best 2001; Rigby, Best & Snellen 2007)? At present the question is a semantic one: we do not have an immediate hypothesis to test requiring FRIs and FRIIs to be one population or two. What is of interest in this is whether FRIs and FRIIs at the same radio luminosity show exactly the same evolution, and our single model successfully fitting the data suggests that they do. This question will be examined in more detail in subsequent analyses.

(2) Our model is a hands-off best-fit to the composite and morphologically-divided source counts at 1.4 GHz – down to 10 mJy. It is not a valid model, because it predicts far too many sources in total at lower flux densities. A valid model needs a rapid downturn to be achieved at about 0.01 Jy, and it must be that further modelling details need introducing to achieve this. What seems clear however is that a large proportion of sources at a level of 1 mJy (i.e. at "mJy corner") must be FRIs. In fact starburst galaxies are usually thought to account for the sub-mJy part of the source count. However, analysis of several radio sources from the VLA-CDFS survey by Padovani et al. (2007) shows that over two thirds of the sub-mJy sources are faint radio galaxies, mostly FRIs. Our results support this finding. The next paper of this short series will examine the combined data and space density models in more detail.

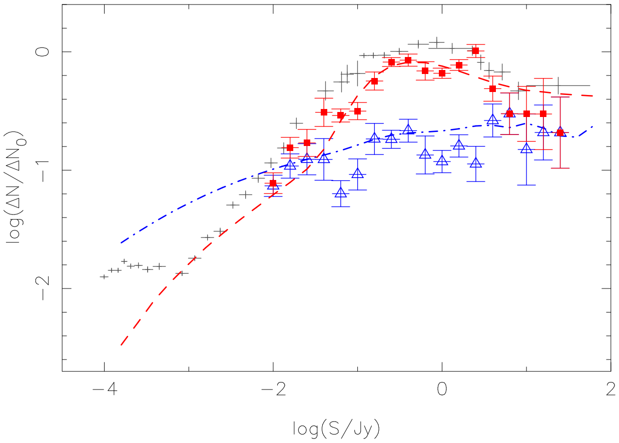

Figure 11. Relative differential source count for FRI (triangles) and FRII (squares) sources. A 1.4 GHz source count, compiled from the data of Bridle, Davis, Fomalont & Lequeux (1972), Machalski (1978), Hopkins et al. (2003) and Prandoni et al. (2001), is represented by the grey crosses for comparison. Here, $\Delta N_0 = 200\Delta(S^{-1.5})$ and the error bars correspond to $\sqrt{N}$ where N is the number of objects in each bin. The counts are fitted by an illustrative model (FRI: dot-dashed line, FRII: dash line), the details of which are described in §6.2. The FRII sources mostly dominate the count, except at low flux densities, where FRI sources take over. Our results show that FRI objects must undergo some mild evolution and that many of the mJy sources are radio galaxies, mostly FRIs.

7 SUMMARY

The CoNFIG sample is constructed as a sample of 274 radio sources from NVSS with $S \geqslant 1.3$ Jy. Redshift information is available for ∼80% of the sample, and morphological classifications were obtained for all of the sources, either from NVSS and FIRST contour plots, or, for 46 sources, from 8 GHz VLA observations. These data allow us to compute morphology-dependent luminosity distributions and source counts.

To increase the number of sources with morphology information, three more samples were constructed in sub-areas of the main region with flux density limits of 0.8 Jy, 0.2 Jy and 50 mJy. Morphological identifications were obtained only from NVSS and FIRST contour plots for those sources. Morphological information for the CENSORS and BDFL sample were obtained from the Ledlow-Owen relation between radio power and optical magnitude and from published classification respectively. Combining these six samples allowed us to compile source counts for FRI and FRII sources separately. A simple, single evolution model for space density was then fitted to these data.

Our data show mild evolution of the FRI sources at low redshift; however, they do not participate in the "evolution bump" around $S_{1.4\ \mathrm{GHz}}\sim1$ Jy. The results also support the observation that a large number of mJy sources are FRIs galaxies and not starburst galaxies as previously assumed.

ACKNOWLEDGEMENTS

We are very grateful to Jim Dunlop for many helpful suggestions, and to Rick Perley and Eric Greison for their precious help with the VLA observation and data reduction. We also thank the referee for very helpful comments.
This work was supported by the National Sciences and Engineering Research Council of Canada.
The National Radio Astronomy Observatory is a facility of the National Science Foundation operated under cooperative agreement by Associated Universities, Inc. This research has made use of the SIMBAD database, operated at CDS, Strasbourg, France.

REFERENCES

Abazajian, K., et al., 2003, *Astron. J.*, 126, 2081
Abazajian, K., et al., 2004, *Astron. J.*, 128, 502
Abazajian, K., et al., 2005, *Astron. J.*, 129, 1755
Adelman-McCarthy, J. K. et al., 2006, *Astroph. J.*, 162, 38
Baars, J. W. M. et al., 1977, *Astron. Astrophys.*, 61, 99
Barkhouse, W. A. & Hall, P. B., 2001, *Astron. J.*, 121, 2843
Barthel, P. D., 1989, *Astroph. J.*, 336, 606
Bauer, F. ., Condon, J. J., Thuan, T. X., *Astroph. J. Sup.*, 129, 547
Baum, S. A. & Heckman, T. M., 1989, *Astroph. J.*, 336, 681
Baum, S. A., Zirbel, E. L. & O'Dea, C. P., 1995, *Astroph. J.*, 451, 88
Beasley, A. J., et al., 2002, *Astroph. J. Sup.*, 141, 13
Beckmann, V., Gehrels, N., Shrader, C. R. & Soldi, S., 2006, *Astroph. J.*, 638, 642
Bennett C. L. et al., 1986, *Astr. J. Sup.*, 61, 1
Benoist C. et al., 1999, *Astron. Astrophys.*, 346, 58
Best, P. N., Röttgering, H. J. A. & Lehnert, M. D., 1999, *Mon. Not. R. Astr. Soc.*, 310, 223
Best, P. N., Arts, J. N., Röttgering, H. J. A., et al. 2003, *Mon. Not. R. Astr. Soc.*, 346, 627
Blundell, K. M. & Rawlings, S., 2001, *Astroph. J. Lettres*, 562, 5
Bongiovanni, A. et al., 2005, *Mon. Not. R. Astr. Soc.*, 359, 930
Bower, R. G. et al., 2006, *Mon. Not. R. Astr. Soc.*, 370, 645
van Breugel, W. J. M. & Dey, A., 1993, *Astroph. J.*, 414, 563
Brinkmann, W., et al., 1995, *Astron. Astrophys. Sup.*, 109, 147
Bridle, A.H., Davis, M.M., Fomalont, E.B. & Lequeux, J., 1972, *Astron. J.*, 77, 1401
Brookes, M. H. et al., 2005, *Mon. Not. R. Astr. Soc.*, 00, 1
Brookes, M. H. et al., 2008, *Mon. Not. R. Astr. Soc.*, 385, 1297
Brown, M. J. I., Webster, R. L. & Boyle, B. J., 2001, *Astron. J.*, 121, 2381
Cannon, R., et al., 2006, *Mon. Not. R. Astr. Soc.*, 372, 425
Capetti, A. et al., 1995, *Astron. Astrophys.*, 300, 643
Cappi, A., Benoist, C. & da Costa, L. N., 2003, *Astron. Astrophys.*, 408, 905
Clewley, L. & Jarvis, M. J., 2004, *Mon. Not. R. Astr. Soc.*, 352, 909
Colless M. et al., 2001, *Mon. Not. R. Astr. Soc.*, 328, 1039
Condon, J. J., et al., 1998, *Astroph. J.*, 115, 1693
Cowie, L. L. et al., 1996, *Astron. J.*, 112, 839
Croom, S. M. et al., 2004, *Mon. Not. R. Astr. Soc.*, 349, 1397
Daly, R. A. & Djorgovski, S. G., 2004, *Astroph. J.*, 612, 652
Douglas J.N., et al., 1996, *Astron. J.*, 111, 1945
Dunlop, J. S. & Peacock, J. A., 1990, *Mon. Not. R. Astr. Soc.*,247, 19
Ellingson, E. & Yee, H. K. C., 1994, *Astroph. J.*, 92, 33
Enya, K., et al., 2002, *Astroph. J.*, 141, 23
Falcke, H., Gopal-Krishna & Biermann, P.L., 1995, *Astron. Astrophys.*, 298, 395
Falco, E. E., et al., 1999, *Publi. Astr. Soc. Pac.*, 111, 438
Fanaroff, B. L. & Riley, J. M., 1974, *Mon. Not. R. Astr. Soc.*, 167, 31P
Fanti, C. & Fanti, R., 1994, *Astr. Soc. Pac. Conf. Ser.*, 54, 341
Ficarra A., Grueff G., Tomassetti G., 1985, *Astron. Astroph. Sup. Ser.*, 59, 255
Fomalont, E., et al., 2003, *Astron. J.*, 126, 2562
Gandhi, P., Fabian, A. C. & Crawford, C. S., 2006, *Mon. Not. R. Astr. Soc.*, 369, 1566
Gawronski, M. P. et al., 2006, *Astron. Astrophys.*, 447, 63
Gopal-Krishna & Wiita, P. J., 2000, *Astron. Astrophys.*, 363, 507
Gopal-Krishna et al., 2005, *Astron. Astrophys.*, 436, 457
Gregory, S. A. & Burns, J. O., 1982, *Astroph. J.*, 255, 373
Granato, G. L. et al., 2001, *Mon. Not. R. Astr. Soc.*, 324, 757
de Grijp, M. H. K. et al., 1992, *Astron. Astrophys.*, 96, 389
Grimes, J. A., Rawlings, S. & Willott, C. J., 2005, *Mon. Not. R. Astr. Soc.*, 359, 1345
Hambly, N. C. et al., 2001, *Mon. Not. R. Astr. Soc.*, 326, 1279
Hardcastle, M.J., Evans, D. A. & Croston, J.H., 2006, *Mon. Not. R. Astr. Soc.*, 370, 1893
Heckman, T. M. et al. ,1994, *Astroph. J.*, 428, 65
Herbig, T. & Readhead, A. C. S., 1992, *Astroph. J.*, 81, 83
Hewett, P. C., Folts, C. B. & Chaffee, F. H., 2001, *Astron. J.*, 122, 518
Hewitt, A. & Burbidge, G., 1989, *Astroph. J.*, 69, 1
Hewitt, A. & Burbidge, G., 1991, *Astroph. J.*, 75, 297
Heywood, I., Blundell, K.M. & Rawlings, S., 2007, *Mon. Not. R. Astr. Soc.*, 381, 1093
Hill, G. J. & Lilly, S. J., 1991, *Astroph. J.*, 367, 1
Hill, G. J., Goodrich, R. W. & Depoy, D. L., 1996, *Astroph. J.*, 462, 163
Holt, J., Tadhunter, C. N. & Morganti, R., 2003, *Mon. Not. R. Astr. Soc.*, 342, 227
Hopkins, A. M., et al., 2003, *Astron. J.*, 125, 465
Jackson, C. A. & Wall, J. V., 1999, *Mon. Not. R. Astr. Soc.*, 304, 160
Jones, D. L. & Preston, R. A., 2001, *Astron. J.*, 122, 2940
Kaiser, C. R. & Alexander, P., 1997, *Mon. Not. R. Astr. Soc.*, 286, 215
Kaiser, C. R. & Best, P. N., 2007, *Mon. Not. R. Astr. Soc.*, 381, 1548
Kellermann, K. I., Pauliny-Toth, I. I. K. & Williams, P. J. S., 1969, *Astroph. J.*, 157, 1
Kharb, P. & Shastri, P., 2004, *Astron. Astrophys.*, 425, 825

Klamer, I. J., Ekers, R. D., Sadler, E. M. & Hunstead, R. W., *Astroph. J.*, 612, 97

Kovalev, Y. Y., et al., 1999, *Astron. Astrophys. Sup.*, 139, 545

Kovalev, Y. Y., et al., 2007, *Astron. J.*, 133, 1236

Lahulla, J. E., Merighi, R., Vettolani G. & Vigotti, M., 1991, *Astron. Astrophys. Sup.*, 88, 525

Laing, R. A., Riley, J. M. & Longair, M. S., 1983, *Mon. Not. R. Astr. Soc.*, 204, 151

Laing, R. A., 1994, in The Physics of Active Galaxies, eds. G. V. Bicknell, M. A. Dopita, and P. J. Quinn, *Astr. Soc. Pac. Conf. Ser.*, 54, 201

Lara, L. et al., 2001, *Astron. Astrophys.*, 370, 409

Ledlow, M. J. & Owen, F. N., 1996, *Astroph. J.*, 112, 9

Liu, F. K. & Zhang, Y. H., 2002, *Astron. Astrophys.*, 381, 757

Longair, M. S., 1966, *Mon. Not. R. Astr. Soc.*, 133, 421

Lu, N. Y., et al., 1993, *Astroph. J. Sup.*, 88, 383

Machalski, J., 1978, *Astron. Astrophys.*, 65, 157

Machalski, J., 1998, *Astron. Astrophys. Sup.*, 128, 153

Madore, B. F. et al., 1992, *Astr. Soc. Pac. Conf. Ser.*, 25, 47

Marcha, M. J. M. & Browne, I. W. A., 1995, *Mon. Not. R. Astr. Soc.*, 275, 951

March, M. J. M. et al, 1996, *Mon. Not. R. Astr. Soc.*, 281, 425

Marzke, R. O. & Huchra, J. P., 1996, *Astron. J.*, 112, 1803

Masson, C. R.& Wall, J. V., 1977, *Mon. Not. R. Astr. Soc.*, 180, 193

Mathez, G., 1969, *Astron. Astrophys.*, 3, 127

Maxfield, L. et al., 1995, *Publi. Astr. Soc. Pac.*, 107, 369

Miller, N. A., Ledlow, M. J., Owen, F. N. & Hill, J. M., 2002, *Astron. J.*, 123, 3018

Nilsson, K., 1998, *Astron. Astrophys.*, 132, 31

Nonino, M., et al., 1999, *Astron. Astrophys.*Supp, 137, 51

Owen, F. N. & Ledlow, M. J., 1994, in The Physics of Active Galaxies, eds. G. V. Bicknell, M. A. Dopita, and P. J. Quinn, *Astr. Soc. Pac. Conf. Ser.*, 54, 319

Owen, F. N., Ledlow, M. J. & Keel, W. C., 1995, *Astron. J.*, 109, 140

Padovani, P. et al., 2007, , 380, 205

Parma, P., et al., 1992, in Astrophysical Jets, Poster Papers from the Space Telescope Science Institute Symposium, eds. D. Burgarella, M. Livio, and C. O'Dea (Baltimore, Space Telescope Science Institute), p. 30

Peacock, J. A., 1987, in Astrophysical Jets and Their Engines, ed. W. Kundt (Dordrecht, Reidel), p. 185

Pearson, T. J. & Readhead, A.C.S., 1988, *Astroph. J.*, 328, 114

Petrov, L., et al., 2005, *Astron. J.*, 129, 1163

Petrov, L., et al., 2006, *Astron. J.*, 131, 1872

Pihlstroem Y. M., Conway J. E.; Vermeulen R.C., *Astron. Astrophys.*, 404, 871

Pilkington J. D. H. & Scott P. F., 1965, *Mon. Not. R. Astr. Soc.*, 69, 183

Pinkney, J. et al., 2000, *Astron. J.*, 120, 2269

Polatidis, A. G. et al., 1995, *Astroph. J.*, 98, 1

Polatidis, A. G. & Conway, J. E., 2003, P.A.S.A., 20, 69

Prandoni, I., et al., 2001, *Astron. Astrophys.*, 365, 392

Quilis, V., Bower, R. G. & Balogh, M. L., 2001, *Mon. Not. R. Astr. Soc.*, 328, 1091

Rawlings, S. et al. , 1989, *Mon. Not. R. Astr. Soc.*, 240, 701

Richards, G. T. et al., 2005, *Mon. Not. R. Astr. Soc.*, 360, 839

Rigby, E. E., Best, P. N. & Snellen, I. A. G., 2008, *Mon. Not. R. Astr. Soc.*, 385, 310

Rines, K. et al., 2001, *Astroph. J.*, 561, 41

Roche, N., Eales, S. & Hippelein, H., 1998, *Mon. Not. R. Astr. Soc.*, 295, 946

Ryabinkov, A. I., Kaminker, A. D. & Varshalovich, D. A., 2003, A& A, 412, 707

Sadler E.M. et al., 2007, *Mon. Not. R. Astr. Soc.*381, 211

Saripalli, L., Gopal-Krishna & Reich, W., 1986, *Astron. Astrophys.*, 170, 20

Scheuer, P. A. G., 1987, in Superluminal Radio Sources, eds. J. A. Zensus and T. J. Pearson (Cambridge, Cambridge University Press), p. 104

Schmidt, M., 1976, *Astroph. J.*, 209, 55

Schneider, D. P. et al., 2007, *Astron. J.*, 134, 102

Schneider, D. P. et al., 2005, *Astron. J.*, 130, 367

Schneider, D. P. et al., 2001, *Astron. Astrophys.*, 198, 7801

Silk, J. & Rees, M. J., *Astron. Astrophys.*, 331, 1

Singal, A. K., 1993, *Mon. Not. R. Astr. Soc.*, 263, 139

Smith, H. E., Smith, E. O. & Spinrad, H., 1976, *Publi. Astr. Soc. Pac.*, 88, 621

Smith, R. J. et al., 2000, *Mon. Not. R. Astr. Soc.*, 313, 469

Snellen, I. A. G. & Best, P. N., 2001, *Mon. Not. R. Astr. Soc.*, 328, 897

Snellen I. A. G., et al., 2002, *Mon. Not. R. Astr. Soc.*, 329, 700

Spinrad, H., Marr, J., Aguilar, L. & Djorgovski, S., 1985, *Publi. Astr. Soc. Pac.*, 97, 932

Stickel, M., Fried, J. W. & Kuehr, H., 1993, *Astron. Astrophys. Sup.*, 98, 393

Stickel, M. & Kuehr, H., 1994, *Astron. Astrophys.*, 103, 349

Stickel, M. & Kuehr, H., 1994, *Astron. Astrophys.*, 105, 67

Strom, R. G. et al., 1990, *Astron. Astrophys.*, 227, 19

Thimm, G. J., Roeser, H. J., Hippelein, H. & Meisenheimer, K., 1994, *Astron. Astrophys.*, 285, 785

Thompson, D. J., Djorgovski, S. & de Carvalho, R., 1990, *Publi. Astr. Soc. Pac.*, 102, 1235

Tinti, S. & de Zotti, G., 2006, *Astron. Astrophys.*, 445, 889

Trager, S. C., Faber, S. M., Worthey, G. & Gonzlez, J. J., 2000, *Astron. J.*, 119, 1645

Urry, C. M. & Padovani, P., 1995, *Publi. Astr. Soc. Pac.*, 107, 803

van Breugel, W. et al., 2004, *Int. Astr. Un. Symp. Proc.*, 222, 485

Vermeulen, R. C. & Taylor, G. B., 1995, *Astron. J.*, 109, 1983

Wall, J.V., Pearson, T. J. & Longair, M.S., 1980, *Mon. Not. R. Astr. Soc.*, 193, 683

Wall, J.V. & Jackson, C. A., 1997, *Mon. Not. R. Astr. Soc.*, 290, 17

Wang, J. C. L., Sulkanen, M. E. & Lovelace, R. V. E., 1992, *Astroph. J.*, 390, 46

Wegner, G. et al., 2001, *Astron. J.*, 122, 2893

White, R. L., et al., 1997, *Astroph. J.*, 475, 479

Wills, D. & Wills, B. J., 1976, *Astroph. J. Sup.*, 31, 143

Willott, C. J., Rawlings, S. & Jarvis, M. J., 2000, *Mon. Not. R. Astr. Soc.*, 313, 237

Willott, C. J., Rawlings, S., Blundell, K. M. & Lacy, M., 2001, *Mon. Not. R. Astr. Soc.*, 322, 536

Willott C. J., Rawlings S., Archibald E.N. & Dunlop J.S., *Mon. Not. R. Astr. Soc.*, 331, 435
Wills, D. & Wills, B. J., 1976, *Astroph. J.*, 31, 63
Woo, J. et al., 2005, *Astroph. J.*, 631, 762
Wright A. & Otrupcek R., 1990, *Publi. Astr. Soc. Pac.*, 41, 47
Xu, W., Lawrence, C. R., Readhead, A. C. S. & Pearson, T. J., *Astron. J.*, 108, 395
Zensus, J. A., et al., 2002, *Astron. J.*, 124, 662

APPENDIX A: CONFIG SAMPLE

Data for CoNFIG sample. The 3CRR sources from Laing, Riley & Longair (1983) are indicated by stars. The RA and DEC gives the NVSS position of the source. Note that 3 sources (CoNFIG-015, 076 and 225) were deleted later in the sample construction process and therefore do not appear here.

The sources of C* type are confirmed compact sources from the VLBA calibrator list (see Beasley et al. 2002; Fomalont et al. 2003; Petrov et al. 2005, 2006; Kovalev et al. 2007) or the Pearson-Readhead survey (Pearson & Readhead 1988). Sources of S* type are confirmed compact sources which show a steep ($\alpha \leqslant -0.6$) spectral index. These are probably CSS sources. Finally, sources of S type look compact with a steep spectral index, but are not confirmed compact. They are probably unresolved FRII sources. Designations I and II are Fanaroff & Riley (1974) types.

The values for $S_{178\ \mathrm{MHz}}$, $S_{365\ \mathrm{MHz}}$, $S_{408\ \mathrm{MHz}}$, $S_{2.7\ \mathrm{GHz}}$and $S_{5.0\ \mathrm{GHz}}$were retrieved from the samples listed in Table 8. References for the redshift information and comments are given in the last two column.

The spectral index α (where $S_{\nu}^{\alpha} \propto \nu^{\alpha}$) corresponds to α_{low} as defined in §5. The α values with † sign correspond to sources for which the value is derived from a non-satisfactory single-power-low fit of the $logS - log\nu$ relation.

Comments are as follow:

N - No optical counterpart identified above the SSS limit.

V - One of the 52 sources with uncertain morphology from the 1.4 GHz FIRST contours. Contours were obtained from our VLA A−configuration observations.

A - One of the 52 sources with uncertain morphology from the 1.4 GHz FIRST contours. Contours were obtained from NRAO archives.

S - Steep-spectrum QSO, since the source has a stellar-type optical counterpart and is classified as FRII.

[1] Because of the very low quality of the data for this source, its morphology remains uncertain.

[2] At first, this source looked like a steep-spectrum source with an FRI morphology. However, it is actually a well known radio loud QSO used as a VLBA calibrator.

[3] This source's contours probably show a QSO with a suggestion of a jet.

[p] photometric redshifts derived from the R-z relation; see §4

References: (1) Liu & Zhang (2002); (2) Cappi, Benoist & da Costa (2003); (3) Enya et al. (2002); (4) Saripalli, Gopal-Krishna & Reich (1986); (5) Marzke & Huchra (1996); (6) Strom et al. (1990); (7) Machalski (1998); (8) Nilsson (1998); (9) Stickel, Fried & Kuehr (1993); (10) Snellen et al. (2002); (11) Abazajian et al. (2004); (12) Falco et al. (1999); (13) Hewitt & Burbidge (1989); (14) Spinrad et al. (1985); (15) Barkhouse & Hall (2001); (16) Hewitt & Burbidge (1991); (17) Ellingson & Yee (1994); (18) Abazajian et al. (2005); (19) Daly & Djorgovski (2004); (20) Gandhi, Fabian & Crawford (2006); (21) Polatidis & Conway (2003); (22) Best, Röttgering & Lehnert (1999); (23) Croom et al. (2004); (24) Mathez (1969); (25) Tinti & de Zotti (2006); (26) Madore et al. (1992); (27) Wegner et al. (2001); (28) Singal (1993); (29) Roche, Eales & Hippelein (1998); (30) Maxfield et al. (1995); (31) Lara et al. (2001); (32) Hewett, Foltz & Chaffee (2001); (33) Stickel & Kuehr (1) (1994); (34) Ryabinkov, Kaminker & Varshalovich (2003); (35) Vermeulen & Taylor (1995); (36) Trager et al. (2000); (37) Adelman-McCarthy et al. (2006); (39) Beckmann et al. (2006); (40) Smith et al. (2000); (41) Owen, Ledlow & Keel (1995); (42) Rines et al. (2001); (43) Pinkney et al. (2000); (44) van Breugel & Dey (1993); (45) Herbig & Readhead (1992); (46) Colless et al. (2001); (47) Thompson, Djorgovski & de Carvalho (1990); (48) Holt, Tadhunter & Morganti (2003); (49) Thimm et al. (1994); (50) Miller, Ledlow & Owen (2002); (51) Woo et al. (2005); (52) Gregory & Burns (1982); (53) Schneider et al. (2001); (54) Willott, Rawlings & Jarvis (2000); (55) Heckman et al. (1994); (56) de Grijp et al. (1992); (57) Grimes, Rawlings & Willott (2005); (58) Hill, Goodrich & Depoy (1996); (59) Stickel & Kuehr (2) (1994); (60) Polatidis et al. (1995); (61) Jones & Preston (2001); (62) Smith, Smith & Spinrad (1976); (63) Wills & Wills (1976); (64) Abazajian et al. (2003); (65) (2005); (66) Cannon et al. (2006)

CoNFIG	Name	RA	DEC	Type	z	$S_{178\ \mathrm{MHz}}$	$S_{365\ \mathrm{MHz}}$	$S_{408\ \mathrm{MHz}}$	$S_{1.4\ \mathrm{GHz}}$	$S_{2.7\ \mathrm{GHz}}$	$S_{5.0\ \mathrm{GHz}}$	α_{low}	Ref. and Comments	
ID		(J2000)				(Jy)	(mJy)	(Jy)	(mJy)	(Jy)	(Jy)			
1	QSO B0710+439	07 13 38.15	+43 49 17.20	C*	0.5180		655.0	0.75	2011.4		1.60	$0.82^\dagger$	1	
2	QSO B0711+35	07 14 24.80	+35 34 39.90	C*	1.6260		840.0		1467.1		0.89	$0.41^\dagger$	1	
3	4C 53.16	07 16 41.09	+53 23 10.30	II	0.0643	5.4	3913.0		1501.4		0.63	−0.63	2	
4	4C 33.21	07 35 55.54	+33 07 09.60	C		7.4	6750.0		2473.1		0.92	−0.56		
5	QSO J0741+3111	07 41 10.70	+31 12 00.40	C*	0.6300		1365.0		2284.3		2.68	0.38	3	
6	4C 31.30	07 45 42.13	+31 42 52.60	II	0.4620	4.4	2448.0		1357.8		1.02	−0.55	3	S
7	4C 56.16	07 49 48.10	+55 54 21.00	I	0.0360	4.2	2636.0		1660.4			−0.44	4	N
8	NGC 2484	07 58 28.60	+37 47 13.80	I	0.0438	11.3		5.39	2717.9		1.33	−0.68	5	
9	TXS 0756+377	07 59 47.26	+37 38 50.20	II			5374.0	4.54	1691.2		0.46	−0.84		NV
10	TXS 0757+503	08 01 35.32	+50 09 43.00	II			5810.0		1471.7		0.47	−1.02		SV
11	3C 192*	08 05 31.31	+24 10 21.30	II	0.0600	21.0		13.10	5330.6	3.30	2.60	−0.67	3	
12	3C 194	08 10 03.67	+42 28 04.00	II	1.1840	9.9	6734.0	5.68	2056.6	1.07	0.61	−0.78	6	A
13	4C 32.24	08 12 59.48	+32 43 05.60	II	0.4700	5.1	4266.0		1522.5		0.47	−0.68	7	
14	3C 196*	08 13 36.07	+48 13 01.90	II	0.8710	68.2	49023.0		15010.0	7.66	4.36	−0.75	3	S
16	4C 52.18	08 19 47.55	+52 32 29.50	II	0.1890	7.2	6037.0		2104.2		0.80	−0.62	8	V^1
17	3C 197.1	08 21 33.77	+47 02 35.70	II	0.1300	8.1	5534.0	4.68	1787.1	1.16	0.86	−0.75	8	A
18	4C 17.44	08 21 44.02	+17 48 20.50	C		5.8	4566.0	4.56	1875.1	1.11	0.68	−0.57		
19	4C 22.21	08 23 24.72	+22 23 03.70	C*	0.9510	4.5	4086.0		2272.4		1.59	−0.34	9	
20	4C 56.16A	08 24 47.27	+55 52 42.60	C*	1.4170		2028.0		1449.4		1.20	−0.25	10	
21	4C 39.23	08 24 55.43	+39 16 41.80	C*	1.2160	4.8		2.59	1480.8		1.00	−0.56	11	
22	3C 200*	08 27 25.40	+29 18 44.80	II	0.4580	14.0	6407.0		2043.1	1.10	0.76	−0.92	1	
23	4C 37.24	08 31 10.00	+37 42 09.90	S	0.9140	8.5	5808.0	5.17	2259.6		0.77	−0.65	11	
24	4C 51.25	08 33 18.80	+51 03 07.80	II	0.4700	6.8	4219.0		1313.5		0.32	−0.81	7	N
25	3C 202	08 34 48.37	+17 00 46.10	II	0.7587^p	8.0	5641.0	5.15	1882.8	1.00	0.55	−0.72		V
26	4C 55.16	08 34 54.91	+55 34 21.00	C	0.2420	8.1	9744.0		8283.1		5.80	$-0.01^\dagger$	10	
27	4C 45.17	08 37 53.51	+44 50 54.60	I	0.2072	6.4	1366.0	3.35	1528.9			$-0.60^\dagger$	11	
28	3C 205*	08 39 06.50	+57 54 13.40	II	1.5360	12.5	9276.0		2257.7	1.11	0.67	−0.86	1	S
29	3C 207*	08 40 47.70	+13 12 23.90	II	0.6840	13.6	8922.0	7.03	2613.0	1.70	1.30	−0.81	3	S
30	B3 0840+424A	08 43 31.63	+42 15 29.70	C*			2504.0	2.28	1409.7		0.59	−0.41		N
31	NGC 2656	08 47 53.83	+53 52 36.80	I	0.0453	5.3	2918.0		1542.3		0.66	−0.58	12	
32	4C 31.32	08 47 57.00	+31 48 40.50	II	1.8340	5.7	841.0		1482.0		0.29	$-0.52^\dagger$	13	
33	3C 208*	08 53 08.83	+13 52 55.30	II	1.1100	17.0	10332.0	7.75	2364.3	1.10	0.53	−0.97	14	S
34	3C 208.1	08 54 39.35	+14 05 52.10	II	1.0200	9.0	6437.0	5.50	2163.8	1.20	0.77	−0.71	15	SV
35	QSO J0854+2006	08 54 48.87	+20 06 30.70	C*	0.3060		1134.0		1511.8		2.61	$0.21^\dagger$	10	
36	3C 211	08 57 40.64	+34 04 06.40	II	0.7500	8.5	6054.0		1798.4		0.55	−0.77	7	V
37	3C 210	08 58 10.07	+27 50 50.80	II	1.1690	9.5	6740.0		1807.8	0.93	0.49	−0.83	6	NV
38	3C 212*	08 58 41.51	+14 09 43.80	II	1.0430	14.1	8337.0	7.01	2370.8	1.40	0.83	−0.87	15	S
39	3C 213.1	09 01 05.40	+29 01 45.70	I	0.1940	6.6	4393.0		2003.4	1.01	0.88	−0.58	16	
40	4C 47.29	09 03 04.04	+46 51 04.70	C*	1.4620	3.9	3205.0	2.81	1754.9		1.30	−0.39	11	

CoNFIG ID	Name	RA	DEC (J2000)	Type	z	$S_{178\ \mathrm{MHz}}$ (Jy)	$S_{365\ \mathrm{MHz}}$ (mJy)	$S_{408\ \mathrm{MHz}}$ (Jy)	$S_{1.4\ \mathrm{GHz}}$ (mJy)	$S_{2.7\ \mathrm{GHz}}$ (Jy)	$S_{5.0\ \mathrm{GHz}}$ (Jy)	α_{low}	Ref. and Comments	
41	3C 215*	09 06 31.88	+16 46 13.00	II	0.4115	11.4	5064.0	6.30	1586.2	0.70	0.42	−0.95	17	S
42	4C 41.19	09 07 34.92	+41 34 53.80	II	0.5272^p	5.4	5070.0	4.25	1394.5		0.46	−0.70		
43	3C 217*	09 08 50.56	+37 48 20.20	II	0.8980	14.5	8372.0	7.09	2086.4	1.00	0.56	−0.95	8	N
44	3C 216*	09 09 33.53	+42 53 47.40	S*	0.6700	20.1	13932.0	11.90	4233.8	3.39	1.81	−0.77	11	
45	4C 16.27	09 12 04.00	+16 18 29.70	II		6.4	4429.0	4.48	1374.6	0.60	0.35	−0.77		NV
46	4C 17.48	09 14 04.83	+17 15 52.40	II		6.7	4612.0	4.44	1527.3	0.84	0.45	−0.74		
47	3C 219*	09 21 07.54	+45 38 45.70	II	0.1742	41.2		23.50	8101.6	4.35	2.29	−0.79	11	
48	4C 53.18	09 22 49.93	+53 02 21.20	II		7.4	6013.0		1597.8		0.43	−0.77		NV
49	4C 39.25	09 27 03.04	+39 02 20.70	C*	0.6980	5.4	3922.0	3.33	2884.6		11.20	$-0.29^{\dagger}$	3	
50	3C 220.2	09 30 33.45	+36 01 23.60	II	1.1570	7.2	5740.0		1875.1	0.99	0.59	−0.68	18	SA
51	3C 223*	09 39 50.20	+35 55 53.10	II	0.1368	14.2			3719.0	2.06	1.29	−0.65	7	
52	3C 223.1	09 41 23.62	+39 44 14.10	II	0.1073	6.0	3958.0	4.88	1976.8	1.23	0.87	−0.54	11	
53	[HB91] 0939+140	09 42 08.40	+13 51 52.20	C	1.5650				1338.5		0.38		16	
54	3C 225	09 42 15.35	+13 45 49.60	S	0.5800	28.9	10165.0	9.13	3336.4	2.22	1.26	−1.01	14	A
55	4C 02.29	09 43 12.74	+02 43 27.50	II	0.5920	3.0	3148.0	2.73	1331.5	0.83	0.54	−0.43	64	NV
56	3C 226*	09 44 16.40	+09 46 19.20	II	0.8178	15.7	9341.0	8.19	2393.7	1.22	0.64	−0.93	16	S
57	3C 227	09 47 47.27	+07 25 13.80	II	0.0865	30.4	12000.0	22.10	7617.0	4.16	2.60	$-0.64^{\dagger}$	11	
58	4C 40.24	09 48 55.36	+40 39 44.80	C*	1.2520	2.5	2940.0	2.43	1599.5		1.60	$-0.25^{\dagger}$	11	
59	3C 228*	09 50 10.77	+14 19 57.30	II	0.5520	21.8	10438.0	9.29	3711.6	1.90	1.11	−0.84	8	N
60	3C 230	09 51 58.83	−00 01 26.80	II	1.4870	21.1	12659.0	12.30	3152.1	1.94	0.69	−0.94	16	SA
61	3C 229	09 52 00.52	+24 22 29.70	II		6.5	4952.0		1788.6	1.20	0.63	−0.64		
62	4C 28.24	09 52 06.14	+28 28 33.20	C		3.5	2978.0		1362.7		0.58	−0.47		
63	4C 55.17	09 57 38.18	+55 22 57.40	C*	0.9090	6.4	5255.0		3079.2		2.30	−0.36	10	
64	3C 234*	10 01 46.73	+28 46 56.50	II	0.1849	31.4	15782.0		5597.0	2.92	1.54	−0.83	16	
65	3C 236*	10 06 01.74	+34 54 10.40	II	0.0989	11.3	7600.0		3236.6	2.01	1.41	−0.61	1	
66	4C 44.19	10 07 18.92	+44 25 01.40	II		5.7	4492.0	4.18	1413.7			−0.70		N
67	3C 237	10 08 00.04	+07 30 16.20	C	0.8800	20.9	18051.0	15.40	6522.1	3.66	2.01	−0.59	1	
68	3C 238	10 11 00.36	+06 24 40.20	II	1.4050	16.3	11081.0	9.32	2964.2	1.35	1.58	−0.85	16	NA
69	3C 239*	10 11 45.46	+46 28 20.10	II	1.7900	13.0	7367.0	6.55	1557.2	0.65	0.33	−1.05	19	N
70	4C 39.29	10 17 14.15	+39 01 24.00	S	0.2060	6.1	3807.0	3.08	1392.2		0.49	−0.72	20	A
71	4C 48.29A	10 20 49.61	+48 32 04.20	II	0.0530	4.5	677.0		1700.1			$-0.32^{\dagger}$	8	
72	3C 241*	10 21 54.58	+21 59 30.90	II	1.6170	11.1	7184.0		1686.2	0.80	0.35	−0.94	8	N
73	S4 1020+59	10 23 38.71	+59 04 49.50	S			4756.0		1609.3		0.47	−0.81		
74	4C 46.21	10 27 14.97	+46 03 21.90	I		6.5	3310.0	4.09	1437.4			−0.72		
75	3C 244.1*	10 33 33.87	+58 14 37.90	II	0.4300	20.2	13889.0		4187.9	1.95	1.12	−0.78	19	
77	4C 50.30	10 34 17.86	+50 13 30.20	S		6.4	5250.0		1545.2		0.44	−0.72		
78	QSO B1031+567	10 35 07.04	+56 28 47.30	C*	0.4597		1773.0		1801.9		1.30	0.01	21	N
79	4C 06.41	10 41 17.16	+06 10 16.50	C*	1.2700		1594.0	1.63	1405.2		1.40	−0.10	10	
80	4C 03.18	10 41 39.01	+02 42 33.00	II	0.5350	7.4	6797.0	6.38	2710.1	1.67	0.99	−0.52	22	V

CoNFIG ID	Name	RA (J2000)	DEC (J2000)	Type	z	$S_{178\ \mathrm{MHz}}$ (Jy)	$S_{365\ \mathrm{MHz}}$ (mJy)	$S_{408\ \mathrm{MHz}}$ (Jy)	$S_{1.4\ \mathrm{GHz}}$ (mJy)	$S_{2.7\ \mathrm{GHz}}$ (Jy)	$S_{5.0\ \mathrm{GHz}}$ (Jy)	α_{low}	Ref. and Comments	
81	3C 245*	10 42 44.54	+12 03 31.80	S*	1.0285	14.4	9449.0	8.90	3305.7	2.00	1.46	−0.73	11	
82	4C 20.23	10 52 26.06	+20 29 48.00	C		2.3	2771.0		1727.5		0.69	−0.17†		
83	4C 20.24	10 58 17.46	+19 52 09.50	II	1.1100	9.5	5535.0		2143.0	1.65	1.13	−0.72	11	NA
84	4C 01.28	10 58 29.62	+01 33 58.20	C*	0.8880	4.2	4275.0	4.47	3220.2	3.15	3.16	−0.14†	23	A
85	3C 247*	10 58 58.69	+43 01 23.70	II	0.7490	16.8	7612.0	7.01	2875.1	1.63	0.95	−0.84	19	N
86	3C 249	11 02 03.91	−01 16 18.30	II	0.3110	16.9	9990.0	8.04	2799.6	1.35	0.68	−0.88	24	NV
87	4C 14.40	11 08 08.31	+14 35 35.80	C		3.0	2961.0	2.72	1348.7	0.82	0.53	−0.42		N
88	PKS 1107+10	11 09 46.04	+10 43 43.40	C	0.5500		2430.0	2.40	1481.3	0.80	0.40	−0.38†	25	N
89	4C 37.29	11 09 52.06	+37 38 43.90	I	0.3456	7.5	5426.0	5.35	2214.1		0.72	−0.61	26	
90	3C 252*	11 11 31.56	+35 40 45.50	II	1.1050	10.8	6559.0		1336.3	0.58	0.30	−1.03	8	N
91	4C 43.21	11 12 38.36	+43 26 27.10	II	1.6800	6.2	4690.0	4.52	1717.0			−0.64	18	S
92	3C 253	11 13 32.13	−02 12 55.20	II	0.1251	7.7	4846.0	4.58	1595.6	0.91	0.50	−0.77	65	
93	3C 254*	11 14 38.43	+40 37 20.80	II	0.7340	19.9	12568.0	10.92	3127.9	1.45	0.79	−0.92	18	S
94	4C 29.41	11 16 34.70	+29 15 20.50	II	0.0487	5.5	3164.0		1927.9		0.86	−0.49	27	
95	3C 255	11 19 25.22	−03 02 51.60	S	1.3550	12.5	9251.0	7.73	1730.4	0.57	0.20	−1.00	28	N
96	4C 14.41	11 20 27.81	+14 20 54.40	C	0.3620	3.2	3819.0	3.50	2446.9	1.50	1.02	−0.16†	10	
97	3C 256	11 20 43.07	+23 27 55.30	S	1.8190	9.2	5483.0		1362.0	0.62	0.34	−0.94	16	
98	3C 257	11 23 09.10	+05 30 20.30	S	2.4740	9.7	5903.0	5.08	1721.1	0.90	0.52	−0.85	16	NA
99	4C 33.26	11 26 23.65	+33 45 27.10	C	1.2300	2.8			1376.8		0.41	−0.34†	29	N
100	B3 1128+455	11 31 38.90	+45 14 51.50	S	0.4040		5046.0	4.37	2048.8		0.66	−0.65	15	
101	4C 43.22	11 34 38.46	+43 28 00.50	II	0.5724	6.6	4218.0	3.90	1567.1		0.47	−0.70	30	SV
102	B3 1133+432	11 35 55.93	+42 58 44.80	C			708.0	0.88	1448.8		0.45	0.48†		N
103	4C 61.23	11 37 16.95	+61 20 38.40	II	0.1110	3.8	1719.0		1314.0			−0.55†	31	
104	4C 12.42	11 40 27.69	+12 03 07.60	I	0.0812	5.5		3.49	1527.0	0.90	0.46	−0.62		
105	4C 59.16	11 40 49.54	+59 12 26.00	C		6.6	5384.0		2179.4		0.86	−0.56		N
106	4C 01.32	11 41 08.23	+01 14 17.70	II	0.4430	9.1	6656.0	5.72	2690.8	1.60	0.97	−0.60	22	V
107	3C 263.1*	11 43 25.04	+22 06 56.00	II	0.3660	18.3	16963.0		3128.7	1.49	0.78	−0.91	8	S
108	4C 37.32B	11 44 34.45	+37 10 16.90	II	0.1148	3.7	6792.0	2.36	2065.4		0.25	−0.56†	11	
109	3C 264*	11 45 05.23	+19 36 37.80	I	0.0214	26.0		19.30	5689.0	3.10	2.00	−0.76	12	
110	3C 265*	11 45 31.03	+31 33 37.00	II	0.8105	19.5	12184.0		2890.9	1.39	0.63	−0.94	14	
111	3C 266*	11 45 43.41	+49 46 08.40	II	1.2750	11.1	6910.0		1424.5	0.58	0.32	−1.02	8	N
112	3C 267*	11 49 55.54	+12 47 15.90	II	1.1440	14.6	9068.0	6.97	2519.9	1.29	0.59	−0.86	19	N
113	4C −00.47	11 50 43.88	−00 23 54.30	C*	1.9760		3433.0	3.43	2773.9	2.40	1.90	−0.16	32	
114	4C 49.22	11 53 24.51	+49 31 09.50	S*	0.3340	5.6	3944.0		1572.2		1.00	−0.62	18	A
115	4C 29.44	11 54 13.01	+29 16 08.50	II	0.3292	6.7	5337.0		1620.3		0.54	−0.71	16	V
116	4C 55.22	11 55 26.63	+54 54 13.60	I	0.0500	3.6	3697.0		2195.7			−0.26†	33	
117	S4 1153+590	11 56 03.67	+58 47 05.40	S	0.2730^{p}		4352.0		1591.7		0.54	−0.75		
118	4C 31.38	11 56 18.74	+31 28 05.00	C	0.4180	7.5	7197.0		2978.3		1.24	−0.47	34	
119	4C 54.25	11 59 13.79	+53 53 07.40	C		5.3	4508.0		1740.6		0.69	−0.56		N
120	4C 29.45	11 59 31.80	+29 14 44.30	C*	0.7290	2.8	3106.0		2030.8		2.17	−0.18†	3	

CoNFIG	Name	RA	DEC	Type	z	$S_{178\ \mathrm{MHz}}$	$S_{365\ \mathrm{MHz}}$	$S_{408\ \mathrm{MHz}}$	$S_{1.4\ \mathrm{GHz}}$	$S_{2.7\ \mathrm{GHz}}$	$S_{5.0\ \mathrm{GHz}}$	α_{low}	Ref. and	
ID		(J2000)				(Jy)	(mJy)	(Jy)	(mJy)	(Jy)	(Jy)		Comments	
121	3C 268.2	12 00 59.77	+31 33 57.90	II	0.3620	9.7	2886.0		1301.6	0.73	0.38	−0.93	8	
122	4C −04.40	12 04 02.13	−04 22 43.90	II		8.3	4264.0	4.57	2141.3	1.32	0.97	−0.64		SV
123	4C 04.40	12 06 19.93	+04 06 12.20	I	0.6285^{p}	8.3	4362.0	4.67	1501.2	0.87	0.43	−0.83		
124	3C 268.4*	12 09 13.52	+43 39 18.70	II	1.4000	10.3	6585.0	5.69	1979.9	1.06	0.60	−0.81	18	S
125	4C 20.27	12 12 56.06	+20 32 37.90	S	0.4649^{p}	6.5	4680.0		1417.9	0.80	0.36	−0.76		
126	4C 13.46	12 13 32.13	+13 07 20.40	C*	1.1410	3.1	2515.0	2.38	1344.2	0.95	0.88	−0.41	10	
127	B2 1211+33	12 14 04.08	+33 09 45.50	C*	1.5980		1639.0		1403.6			−0.12	15	
128	4C 53.24	12 15 29.80	+53 35 54.10	II	1.0650	8.7	7962.0		2755.0		0.93	−0.59	11	SV
129	4C 35.28	12 15 55.60	+34 48 15.10	C*	0.8570	2.2	2316.0		1506.8		1.10	−0.20	35	A
130	PKS 1214+038	12 17 29.83	+03 36 44.00	I	0.0770		5573.0	7.80	2411.5	1.19	0.53	−0.76	11	
131	3C 270	12 19 15.33	+05 49 40.40	I	0.0073	51.8		41.50	10445.0	12.65	8.32	$-0.80^{\dagger}$	36	
132	3C 270.1*	12 20 33.88	+33 43 10.90	II	1.5190	13.6	9742.0		2845.9	1.49	0.87	−0.78	37	S
133	3C 272*	12 24 30.20	+42 06 24.00	II	0.9440	10.3	4754.0	4.02	1352.3	0.70	0.36	−0.98	6	N
134	4C 21.35	12 24 54.62	+21 22 47.20	C*	0.4350	6.6	3475.0		2094.4	1.10	0.81	−0.53	13	[2]
135	M84*	12 25 03.78	+12 52 35.20	I	0.0034	19.5		12.20	6012.8	3.91	2.86	−0.57	36	
136	QSO B1225+368	12 27 58.78	+36 35 11.60	C*	1.9730		1200.0		2098.4		0.80	$0.42^{\dagger}$	10	
137	3C 273	12 29 06.41	+02 03 05.10	C*	0.1583	62.8	66452.0	55.10	54991.2	41.80	44.90	−0.07	39	[3]
138	PKS 1227+119	12 29 51.84	+11 40 24.20	I	0.0830			4.31	1519.0	1.04	0.49	−0.85	18	
139	M87*	12 30 49.46	+12 23 21.60	I	0.0042	1050.0		519.00	141949.3	120.00	67.60	−0.98	40	
140	4C −02.55	12 32 00.13	−02 24 04.10	C*	1.0450	7.4	4124.0	3.87	1646.7	1.19	0.90	−0.72	32	A
141	3C 274.1*	12 35 22.97	+21 20 18.30	II	0.4220	16.5			2918.5	1.44	0.76	−0.84	8	S
142	4C 16.33	12 36 29.13	+16 32 32.10	I	0.0684	7.0	1857.0	3.88	1383.9	1.00	0.71	−0.72	41	
143	3C 275	12 42 19.68	−04 46 19.70	S	0.4800	14.2	10765.0	10.20	3672.1	1.83	0.98	−0.68	8	
144	3C 275.1*	12 43 57.63	+16 22 52.70	II	0.5570	18.3	10883.0	9.35	2895.8	1.56	0.95	−0.91	15	S
145	S4 1242+41	12 44 49.18	+40 48 06.50	C*	0.8130		2039.0	2.01	1341.8		0.71	−0.32	10	
146	4C 09.44	12 51 44.47	+08 56 27.80	II	0.2720^{p}	6.1	3697.0	3.99	1684.4	1.00	0.51	−0.62		
147	3C 277.1	12 52 26.33	+56 34 19.70	S*	0.3205	8.9	7444.0		2288.3	1.53	1.05	−0.69	11	
148	4C 02.34	12 53 03.55	+02 38 22.30	II	0.3398^{p}	5.0	4674.0	4.13	1604.9	0.95	0.55	−0.59		V
149	3C 277.2*	12 53 32.70	+15 42 27.30	II	0.7660	12.0	7092.0	5.83	1952.2	0.91	0.58	−0.89	8	
150	3C 277.3*	12 54 11.68	+27 37 32.70	II	0.0858	12.4	6047.0		2923.9	1.93	1.24	−0.68	42	
151	3C 279	12 56 11.15	−05 47 20.10	C*	0.5362	20.9	15461.0	14.50	9711.2	12.00	13.00	$-0.37^{\dagger}$	39	A
152	3C 280*	12 56 57.38	+47 20 19.80	II	0.9960	23.7	14941.0	13.71	5099.6	2.83	1.53	−0.75	19	
153	3C 280.1*	13 00 32.87	+40 09 09.20	II	1.6670	11.9	5720.0	4.51	1368.9	0.62	0.36	−1.05	15	S
154	4C 09.45	13 05 36.05	+08 55 15.90	II	1.4090	9.8	6175.0	5.21	1461.8	0.70	0.32	−0.94	22	NA
155	4C 00.46	13 09 49.66	−00 12 36.60	II	0.4190	9.5	4525.0	5.10	1636.7	0.86	0.47	−0.85	22	
156	QSO B1308+326	13 10 28.70	+32 20 44.30	C*	0.9970		1157.0		1686.6		1.68	$0.28^{\dagger}$	3	
157	3C 284*	13 11 08.56	+27 27 56.50	II	0.2394	11.4	7070.0		2044.6	1.07	0.63	−0.85	14	
158	TXS 1311+552	13 13 37.88	+54 58 24.30	C*			1645.0		1304.6		0.54	$-0.17^{\dagger}$		N
159	4C 07.32	13 16 20.51	+07 02 54.30	I	0.0507	3.1	1924.0	5.50	1884.2	1.20	0.82	$-0.24^{\dagger}$	43	
160	4C 29.47	13 19 06.83	+29 38 33.80	I	0.0729	3.2	583.0		1372.5		0.55	$-0.28^{\dagger}$	27	

CoNFIG ID	Name	RA (J2000)	DEC (J2000)	Type	z	$S_{178\ \mathrm{MHz}}$ (Jy)	$S_{365\ \mathrm{MHz}}$ (mJy)	$S_{408\ \mathrm{MHz}}$ (Jy)	$S_{1.4\ \mathrm{GHz}}$ (mJy)	$S_{2.7\ \mathrm{GHz}}$ (Jy)	$S_{5.0\ \mathrm{GHz}}$ (Jy)	α_{low}	Ref. and Comments	
161	4C −00.50	13 19 38.73	−00 49 40.90	C*	0.8920	4.4	3749.0	3.37	1468.9	1.01	0.63	−0.56	11	
162	4C 17.56	13 20 21.45	+17 43 12.40	II		5.4	4084.0	3.83	1573.2	1.10	0.62	−0.62		NV
163	4C 11.45	13 21 18.84	+11 06 49.40	II	2.1710	8.1	6214.0	5.90	2238.0	1.38	0.75	−0.65	1	SA
164	3C 285*	13 21 21.28	+42 35 15.20	II	0.0794	11.4		5.03	2085.0	1.23	0.76	−0.81	44	
165	4C 03.27	13 23 21.04	+03 08 02.80	I	0.2690	5.9	2659.0	3.68	1385.2	0.79	0.41	−0.68	11	
166	4C 32.44	13 26 16.51	+31 54 09.70	C*	0.3700	5.8	7486.0		4861.9		2.15	$-0.12^{\dagger}$	45	
167	4C 32.44B	13 27 31.71	+31 51 27.30	I	0.2600		3328.0		1415.1		0.70	−0.64	7	
168	3C 287*	13 30 37.69	+25 09 11.00	C*	1.0550	16.0	14959.0		7052.2	4.60	3.26	−0.42	14	
169	3C 286*	13 31 08.31	+30 30 32.40	C*	0.8490	24.0	27475.0		14902.7	10.26	7.49	$-0.26^{\dagger}$	10	
170	3C 287.1	13 32 56.37	+02 00 46.50	II	0.2155	8.2	4772.0	5.29	2648.5	1.93	1.43	−0.54	46	
171	QSO J1338−0627	13 38 08.07	−06 27 11.20	II	0.6250	18.1	9912.0	9.74	2958.5	1.79	0.98	−0.88	11	SA
172	3C 288*	13 38 49.67	+38 51 11.10	I	0.2460	18.7	11741.0	10.06	3358.9	1.76	0.99	−0.85	1	
173	3C 288.1	13 42 13.13	+60 21 42.30	II	0.9610	9.0	5069.0		1493.3	0.81	0.40	−0.88	11	SA
174	4C 05.57	13 42 43.57	+05 04 31.50	I	0.1360	5.5	3681.0	3.83	1600.9	1.10	0.78	−0.61	47	
175	4C 14.49	13 44 23.75	+14 09 15.30	S		6.8	4676.0	3.54	1302.8	0.68	0.35	−0.82		
176	3C 289*	13 45 26.38	+49 46 32.70	II	0.9670	11.8	8103.0		2398.3	1.17	0.60	−0.79	19	N
177	4C 12.50	13 47 33.42	+12 17 24.10	C*	0.1213	4.6	8309.0	8.78	5397.2	3.88	2.89	$0.80^{\dagger}$	48	
178	3C 293*	13 52 17.81	+31 26 46.70	I	0.0450	12.7	11207.0		4844.2	2.89	1.87	−0.49	11	
179	4C 11.46	13 52 56.36	+11 07 07.70	C	0.6500	3.4	3441.0	3.62	1537.9	0.78	0.41	$-0.42^{\dagger}$	25	N
180	4C 01.39	13 57 01.51	+01 04 39.70	II	0.8190	9.6	7363.0	6.59	2400.4	1.35	0.71	−0.70	22	N
181	4C 19.44	13 57 04.37	+19 19 08.10	II	0.7200	7.6	5290.0	6.00	2585.6	1.50	1.49	−0.53	13	S
182	PKS 1355+01	13 57 53.77	+00 46 32.80	S			4739.0	4.73	1921.6	1.00	0.49	−0.70		N
183	4C 62.22	14 00 28.65	+62 10 38.60	C*	0.4310	2.9	5564.0		4307.6		1.84	$0.14^{\dagger}$	1	
184	3C 294*	14 06 44.10	+34 11 26.20	II	1.7790	10.3	6123.0		1316.1	0.54	0.28	−1.02	8	N
185	3C 295*	14 11 20.63	+52 12 09.00	II	0.4610	83.5			22720.1	11.83	6.53	−0.63	49	
186	4C−05.60	14 13 48.34	−05 59 54.20	II	1.0940	9.3	6255.0	5.49	1520.8	0.64	0.35	−0.90	22	N
187	S4 1413+34	14 16 04.18	+34 44 36.50	C*	1.0000		2162.0		1863.7		0.95	$-0.11^{\dagger}$	11	N
188	NGC 5532*	14 16 53.50	+10 48 40.20	I	0.0240	13.0		8.30	4445.4	2.70	1.70	−0.52	50	
189	3C 297	14 17 23.95	−04 00 46.60	S	1.4060	10.3	4584.0	4.17	1687.2	1.00	0.63	−0.86	14	A
190	3C 298	14 19 08.18	+06 28 36.30	S*	1.4400	47.5	29025.0	23.40	6100.3	2.71	1.46	−1.02	1	
191	3C 299*	14 21 05.73	+41 44 49.70	S	0.3670	11.8	8047.0	8.17	3146.9	1.59	0.90	−0.65	8	
192	3C 300*	14 23 00.81	+19 35 22.80	II	0.2720	17.9	10471.0	10.90	3738.8	1.92	1.11	−0.76	1	
193	4C 20.33	14 24 56.93	+20 00 22.70	II	0.8710	7.4	5544.0		1808.5	1.14	0.60	−0.70	13	SA
194	4C 24.31	14 25 50.67	+24 04 06.70	II	0.6490	7.7	4453.0		1558.7	1.00	0.51	−0.77	37	SV
195	3C 300.1	14 28 31.22	−01 24 08.70	II	1.1590	14.1	8810.0	7.21	3157.4	1.83	0.94	−0.73	16	NA
196	4C 07.36	14 30 03.34	+07 15 01.30	I		3.5		5.80	1719.6	1.06	0.66	$-0.39^{\dagger}$		
197	4C 03.30	14 36 57.07	+03 24 12.30	C	1.4380	7.3	6081.0	5.16	2797.3	1.97	1.28	−0.48	22	V
198	QSO B1437+6224	14 38 44.71	+62 11 54.50	C*	1.0900		2912.0		2410.4		0.80	$-0.14^{\dagger}$	15	
199	3C 303*	14 43 01.45	+52 01 38.20	II	0.1410	11.2	7244.0		2543.0	1.55	0.94	−0.73	1	
200	PKS 1442+101	14 45 16.48	+09 58 36.00	C	3.5220		1799.0	1.90	2417.6	1.77	1.15	$0.21^{\dagger}$	10	

CoNFIG ID	Name	RA (J2000)	DEC (J2000)	Type	z	$S_{178\ \mathrm{MHz}}$ (Jy)	$S_{365\ \mathrm{MHz}}$ (mJy)	$S_{408\ \mathrm{MHz}}$ (Jy)	$S_{1.4\ \mathrm{GHz}}$ (mJy)	$S_{2.7\ \mathrm{GHz}}$ (Jy)	$S_{5.0\ \mathrm{GHz}}$ (Jy)	α_{low}	Ref. and Comments	
201	4C 00.52	14 48 39.98	+00 18 17.90	II	0.4381	6.2	4154.0	4.12	1651.5	1.00	0.55	−0.65	66	V
202	3C 305*	14 49 21.74	+63 16 13.90	I	0.0416	15.7	9820.0		3006.0	1.64	0.92	−0.81	50	
203	4C −04.53	14 55 01.43	−04 20 22.50	II	0.4403	11.4	5414.0	6.72	2104.3	0.90	0.53	−0.81	51	
204	3C 311	15 04 09.27	+60 00 55.50	S	1.0220	7.4	5224.0		1553.1		0.44	−0.78	13	
205	B2 1502+28	15 04 19.50	+28 35 34.30	I	0.0432^p		499.0		1626.5		0.37	$0.88^\dagger$		
206	PKS 1502+106	15 04 25.03	+10 29 38.50	C*	1.8390		1388.0	1.55	1774.2	1.74	2.04	0.15	10	
207	3C 310*	15 04 58.98	+25 59 49.00	I	0.0535	56.0			7613.4	3.10	1.26	−0.97	52	
208	4C −05.64	15 10 53.55	−05 43 07.10	I	1.1910	10.5	7409.0	7.72	3569.3	2.90	2.33	−0.53	34	SV
209	3C 313	15 10 57.03	+07 51 24.80	II	0.4610	20.6	15190.0	11.50	3799.1	2.07	1.39	−0.85	8	S
210	4C 01.42	15 12 25.35	+01 21 08.70	II	0.7920	8.4	6858.0	5.56	2262.7	1.28	0.68	−0.66	22	NV^1
211	3C 315*	15 13 39.90	+26 07 33.70	I	0.1080	18.8			4332.7	2.36	1.27	−0.71	16	
212	4C 23.41	15 13 40.20	+23 38 35.30	C*		2.1	2402.0		1767.5	1.20	0.75	$-0.10^\dagger$		
213	4C 00.56	15 16 40.21	+00 15 02.40	II	0.0523	3.9	1267.0	3.19	2593.1	1.87	1.37	$-0.11^\dagger$	53	
214	3C 317	15 16 44.58	+07 01 18.10	I	0.0344	49.0	23691.0	25.20	5499.3	2.11	0.87	−1.07	40	
215	3C 316	15 16 56.61	+18 30 21.60	S	0.5795^p	5.9	4057.0	3.40	1335.2	0.72	0.40	−0.73		
216	3C 318*	15 20 05.50	+20 16 05.70	S*	1.5740	12.3	9212.0		2688.0	1.33	0.75	−0.76	54	
217	4C 04.51	15 21 14.51	+04 30 20.00	C*	1.2960	2.0	3404.0	3.30	3927.2	2.30	1.03	$0.29^\dagger$	55	N
218	3C 319*	15 24 05.64	+54 28 18.40	II	0.1920	15.3	7662.0		2624.0	1.25	0.65	−0.85	8	
219	4C 03.33	15 25 48.92	+03 08 26.50	C		4.7	4174.0	4.15	1960.0	1.22	0.69	−0.45		N
220	3C 320	15 31 25.36	+35 33 40.60	II	0.3420	9.1	6590.0		1820.7	0.91	0.50	−0.80	8	N
221	3C 321*	15 31 50.71	+24 02 43.30	II	0.0962	13.5	8434.0		3577.3	2.00	1.22	−0.64	56	
222	QSO B1532+016	15 34 52.45	+01 31 03.30	C*	1.4350		1138.0		1320.4		1.30	0.11	10	
223	3C 322*	15 35 01.27	+55 36 49.80	II	1.6810	10.2	6938.0		1846.9	0.85	0.46	−0.85	6	N
224	4C 13.56	15 37 32.39	+13 44 47.70	I	0.8879^p	6.7	4943.0	4.21	1805.6	1.10	0.61	−0.65		V
226	4C 14.60	15 40 49.51	+14 47 46.70	C*	0.6050	3.6	2792.0	2.35	1386.8	1.98	1.73	$-0.47^\dagger$	9	
227	3C 323	15 41 45.64	+60 15 36.20	II	0.6790	8.4	5430.0		1337.4	0.65	0.33	−0.91	6	V
228	PKS 1543+005	15 46 09.50	+00 26 24.60	C*	0.5500		2279.0	2.13	1830.3	1.24	0.84	$-0.15^\dagger$	10	
229	3C 323.1	15 47 44.23	+20 52 41.00	II	0.2640	9.7	5042.0		2396.2	1.29	0.92	−0.66	1	S
230	3C 324*	15 49 48.98	+21 25 39.10	II	1.2061	15.8	8911.0		2522.0	1.26	0.61	−0.90	14	N
231	3C 325*	15 49 58.54	+62 41 20.90	II	1.1350	15.6	12124.0		3563.7	1.84	0.83	−0.74	57	S
232	4C 05.64	15 50 35.26	+05 27 10.60	C*	1.4220	2.7	2668.0	2.74	2303.3	1.83	2.18	−0.08	13	
233	3C 326*	15 52 26.86	+20 05 01.80	II	0.0900	12.1			3214.1	2.07	0.41	$-0.64^\dagger$	8	N
234	3C 326.1	15 56 10.06	+20 04 21.20	II	1.8250	8.2	6032.0		2313.7	1.30	0.86	−0.63	8	NV^1
235	4C 43.35	15 56 36.35	+42 57 09.60	II		7.6	4465.0	4.77	1656.4		0.52	−0.74		
236	4C 33.38	16 02 07.27	+33 26 53.10	C	1.1000	2.4	2470.0		2990.6		2.00	$0.11^\dagger$	25	N
237	3C 327	16 02 17.21	+01 58 19.40	II	0.1041	35.3		16.10	8298.7	5.21	2.76	−0.69	58	
238	4C 10.45	16 08 46.13	+10 29 08.20	C*	1.2260	2.7		2.11	1392.0	1.10	1.70	$-0.32^\dagger$	59	
239	PKS 1607+26	16 09 13.31	+26 41 29.20	C	0.4730		2529.0		4908.2	3.04	1.56	$0.49^\dagger$	1	
240	3C 329	16 10 07.74	+32 58 35.10	II	1.7810	7.2	7100.0		2027.1		0.85	−0.65	57	N

CoNFIG ID	Name	RA (J2000)	DEC	Type	z	$S_{178\ \mathrm{MHz}}$ (Jy)	$S_{365\ \mathrm{MHz}}$ (mJy)	$S_{408\ \mathrm{MHz}}$ (Jy)	$S_{1.4\ \mathrm{GHz}}$ (mJy)	$S_{2.7\ \mathrm{GHz}}$ (Jy)	$S_{5.0\ \mathrm{GHz}}$ (Jy)	α_{low}	Ref. and Comments
241	3C 331	16 12 19.02	+22 22 15.60	S	0.6362^p	7.1	5360.0		1401.9	0.70	0.37	−0.81	
242	QSO B1611+3420	16 13 41.08	+34 12 47.70	C*	1.4010		2928.0		4024.1		2.54	$0.24^\dagger$	10
243	PKS 1614+26	16 16 38.29	+26 47 01.60	C			1711.0		1484.4	1.20	0.96	$-0.11^\dagger$	N
244	3C 333	16 17 15.75	+21 07 29.40	II		6.9	5309.0		1748.5	1.00	0.55	−0.69	NV
245	NGC 6109*	16 17 38.89	+35 00 48.00	I	0.0296	4.3	1513.0		1706.2		0.66	$-0.38^\dagger$	11
246	3C 332	16 17 43.28	+32 23 02.40	II	0.1517	9.5			2598.5	1.46	0.83	−0.63	37
247	3C 334*	16 20 21.40	+17 36 29.30	II	0.5550	10.9	6708.0	6.80	1993.9	1.32	0.57	−0.84	15 S
248	3C 336*	16 24 39.42	+23 45 17.50	II	0.9270	11.5	7883.0		2612.7	1.40	0.69	−0.73	37 S
249	4C 41.32	16 25 57.66	+41 34 41.20	C*	2.5500	2.5	2471.0	1.99	1677.4		1.40	−0.20	13 N
250	3C 341*	16 28 03.57	+27 41 36.10	II	0.4480	10.8	6350.0		1998.6	1.08	0.57	−0.82	1
251	3C 338*	16 28 38.34	+39 33 04.70	I	0.0298	46.9	17385.0	16.73	3678.7	1.24	0.49	−1.23	12
252	3C 337*	16 28 53.30	+44 19 05.20	II	0.6300	11.8	9977.0	8.21	3155.8	1.57	0.91	−0.67	19 N
253	3C 340*	16 29 37.52	+23 20 13.40	II	0.7750	10.1	7789.0		2599.0	1.30	0.69	−0.68	8
254	4C 12.59	16 31 45.29	+11 56 03.30	C	1.7920	4.4	3575.0	3.71	1733.7	1.04	0.80	−0.47	15
255	3C 343*	16 34 33.86	+62 45 35.70	C*	0.9880	12.4	13907.0		5001.9	2.68	1.49	−0.48	14
256	4C 38.41	16 35 15.51	+38 08 04.80	C*	1.8140	2.2	2430.0	1.90	2726.0		3.83	0.11	10
257	3C 342	16 36 37.38	+26 48 06.60	S	0.5610	6.9	4343.0		1336.1	0.80	0.34	−0.81	13 A
258	3C 343.1*	16 38 28.22	+62 34 43.90	C*	0.7500	11.5	14155.0		4610.8	2.23	1.20	$-0.49^\dagger$	60
259	3C 345*	16 42 58.77	+39 48 37.00	C*	0.5928	11.9	9559.0	8.73	7098.6		8.48	$-0.24^\dagger$	10
260	3C 344	16 43 05.93	+37 29 34.40	II	0.5200	8.6	4949.0	4.21	1418.1		1.38	$-0.88^\dagger$	61
261	3C 346*	16 43 48.69	+17 15 48.80	I	0.1617	10.9	9025.0	8.62	3666.2	2.33	1.63	−0.55	62
262	4C 17.71	16 47 41.83	+17 20 11.50	C*	0.3140	3.2	3750.0	3.67	2130.2		2.79	$-0.23^\dagger$	16
263	4C 39.49	16 53 52.24	+39 45 36.60	C	0.0336	2.0	1920.0	1.81	1558.0		1.28	−0.12	11
264	3C 349*	16 59 27.57	+47 03 13.10	II	0.2050	13.3	9947.0	8.55	3358.4	1.88	1.14	−0.69	60
265	4C 29.50	17 04 07.21	+29 46 59.50	S	1.9270	6.6	3659.0		1413.9		0.50	−0.74	1
266	3C 351*	17 04 43.03	+60 44 49.60	II	0.3715	13.7	8367.0		3259.0	2.03	1.21	−0.70	53 S
267	3C 350	17 05 06.57	+38 40 37.60	I	0.6187^p	7.4	5134.0	3.85	1302.4		0.32	−0.86	
268	3C 352*	17 10 44.11	+46 01 30.30	II	0.8060	11.3	7847.0	6.44	1865.5	0.95	0.47	−0.90	1
269	4C 34.47	17 23 20.85	+34 17 57.30	II	0.2060	5.0	2467.0		1610.2		1.25	$-0.52^\dagger$	63 S
270	3C 356*	17 24 18.40	+50 57 54.00	II	1.0790	11.3	6388.0		1509.1	0.66	0.38	−0.99	19
271	4C 61.34	17 42 51.84	+61 45 51.00	II	0.5230	5.2	3831.0		1354.7		0.53	−0.67	13 S
272	4C 45.13	07 14 35.25	+45 40 00.10	II	0.1559^p	3.6	3188.0	2.91	1386.4			−0.49	
273	3C 306	14 54 20.30	+16 20 55.80	II	0.0456		711.0		1391.3		0.46	0.50	18
274	4C 32.25A	08 31 20.33	+32 18 37.00	II	0.0512		871.0		1773.5		0.76	0.53	11
275	4C 06.32	08 48 41.94	+05 55 35.00	II	0.7977^p			2.54	1319.5	0.70	0.36	−0.53	
276	4C 20.29	12 28 11.77	+20 23 19.10	II	0.6800	4.3	3080.0		1333.9	0.83	0.39	−0.57	44 S
277	4C 38.21	07 44 17.50	+37 53 16.90	S	1.0630	13.0	6582.0		1341.8	0.255	−1.11	1	

Table A1. Optical identifications for the CoNFIG sources. The optical type (g for galaxy and s for stellar) as well as the B_j, R1, R2 and I magnitudes were retrieved from the SuperCosmos Sky Survey (Hambly et al. 2001). The radio type is as described in the previous table. Sources marked by a ^{z} have an optical identification but no spectroscopic redshift.

ID	Rad. Type	Optical Position (J2000)	Opt. Type	B_j	R1	R2	I
1	C*	07 13 38.15 +43 49 17.20	g	21.79	19.79	19.93	18.62
2	C*	07 14 24.80 +35 34 39.90	s	18.74	17.59	18.42	17.50
3	II	07 16 41.09 +53 23 10.30	g	15.43	15.54	14.22	13.30
4^z	C	07 35 55.54 +33 07 09.60	s	21.22		20.34	18.55
5	C*	07 41 10.70 +31 12 00.40	s	16.52	16.28	16.32	15.83
6	II	07 45 42.13 +31 42 52.60	s	15.76	15.55	15.56	15.11
8	I	07 58 28.60 +37 47 13.80	g	14.51	15.42	14.06	12.23
10^z	II	08 01 35.32 +50 09 43.00	s	21.79		20.17	
11	II	08 05 31.31 +24 10 21.30	g	17.28	16.28	15.60	15.16
12	II	08 10 03.67 +42 28 04.00	g	21.08	19.47	18.91	17.38
13	II	08 12 59.48 +32 43 05.60	g	21.19	19.76	19.19	18.64
14	II	08 13 36.07 +48 13 01.90	s	18.45	17.79	17.82	17.54
16	II	08 19 47.55 +52 32 29.50	g	20.37	18.31	18.26	17.80
17	II	08 21 33.77 +47 02 35.70	g	18.55	17.26	17.07	16.26
18^z	C	08 21 44.02 +17 48 20.50	g	20.40	17.92	18.01	17.58
19	C*	08 23 24.72 +22 23 03.70	s	20.77	18.31	20.01	19.17
20	C*	08 24 47.27 +55 52 42.60	s	18.22	17.88	17.93	17.92
21	C*	08 24 55.43 +39 16 41.80	s	18.37	18.29	17.55	17.55
22	II	08 27 25.40 +29 18 44.80	g	20.96	19.04	18.89	18.82
23	S	08 31 10.00 +37 42 09.90	s	18.10	18.52	17.78	18.63
25^z	II	08 34 48.37 +17 00 46.10	g	22.06	20.09	20.08	
26	C	08 34 54.91 +55 34 21.00	g	18.92	17.36	16.86	16.21
27	I	08 37 53.51 +44 50 54.60	g	18.99	17.15	17.30	16.45
28	II	08 39 06.50 +57 54 13.40	s	18.15	17.62	17.23	16.90
29	II	08 40 47.70 +13 12 23.90	s	18.09	17.49	17.62	16.67
31	I	08 47 53.83 +53 52 36.80	g	18.18	10.37	16.58	15.16
32	II	08 47 57.00 +31 48 40.50	g	15.85	10.28	14.50	13.28
33	II	08 53 08.83 +13 52 55.30	s	18.88	16.87	18.05	17.37
34	II	08 54 39.35 +14 05 52.10	s	20.04	20.30	19.22	18.46
35	C*	08 54 48.87 +20 06 30.70	s	15.54	13.98	15.19	13.59
36	II	08 57 40.64 +34 04 06.40	g			20.31	19.10
38	II	08 58 41.51 +14 09 43.80	s	20.04	19.22	18.79	18.04
39	I	09 01 05.40 +29 01 45.70	g	19.31	18.01	17.77	17.07
40	C*	09 03 04.04 +46 51 04.70	s	19.13	18.54	18.66	18.48
41	II	09 06 31.88 +16 46 13.00	s	17.99	18.60	18.24	17.63
42^z	II	09 07 34.92 +41 34 53.80	g	21.51	19.34	19.06	18.72
44	S*	09 09 33.53 +42 53 47.40	g	19.52	18.54	17.43	17.55
46^z	II	09 14 04.83 +17 15 52.40	g		19.28	19.39	18.78
47	II	09 21 07.54 +45 38 45.70	g	18.61	17.38	16.86	16.16
49	C*	09 27 03.04 +39 02 20.70	s	17.06	17.53	16.49	16.35
50	II	09 30 33.45 +36 01 23.60	s	18.98	18.67	18.23	17.74
53	C	09 42 08.40 +13 51 52.20	g	20.08	19.49	18.82	
54	S	09 42 15.35 +13 45 49.60	s			19.95	
56	II	09 44 16.40 +09 46 19.20	s	22.45	20.21		
58	C*	09 48 55.36 +40 39 44.80	s	19.00	17.80	18.13	17.66
60	II	09 51 58.83 −00 01 26.80	s	15.88		14.88	14.41
6^z1	II	09 52 00.52 +24 22 29.70	g		18.67	17.78	17.25
62^z	C	09 52 06.14 +28 28 33.20	s	21.59	19.62	19.78	
63	C*	09 57 38.18 +55 22 57.40	s	18.28	17.31	17.36	16.98
64	II	10 01 46.73 +28 46 56.50	g	18.64	17.52	17.32	16.15
65	II	10 06 01.74 +34 54 10.40	g	17.27	16.12	15.64	15.04
67	C	10 08 00.04 +07 30 16.20	g	21.53			
70	S	10 17 14.15 +39 01 24.00	g	20.83	18.97	18.72	
71	II	10 20 49.61 +48 32 04.20	g	17.95	16.04	16.02	15.64
73^z	S	10 23 38.71 +59 04 49.50	s	20.95	19.39	20.02	18.93
74^z	I	10 27 14.97 +46 03 21.90	g		19.58	19.71	
75	II	10 33 33.87 +58 14 37.90	g	20.89	18.92	19.21	17.93

ID	Rad. Type	Optical Position (J2000)	Opt. Type	B_j	R1	R2	I
77^z	S	10 34 17.86 +50 13 30.20	s		20.78	20.28	
79	C*	10 41 17.16 +06 10 16.50	s	17.40	15.06	16.49	16.69
80	II	10 41 39.01 +02 42 33.00	g	21.65		19.47	19.04
81	S*	10 42 44.54 +12 03 31.80	s	18.03	17.10	17.01	17.00
82^z	C	10 52 26.06 +20 29 48.00	g	21.62	18.96	18.90	18.15
84	C*	10 58 29.62 +01 33 58.20	s	18.75	17.60	17.63	16.71
89	I	11 09 52.06 +37 38 43.90	g	21.28	18.90	18.65	18.18
91	II	11 12 38.36 +43 26 27.10	s	22.15	19.93	20.40	18.36
92^z	II	11 13 32.13 −02 12 55.20	g	20.84	19.15	19.51	18.05
93	II	11 14 38.43 +40 37 20.80	s	18.27	16.97	17.33	17.24
94	II	11 16 34.70 +29 15 20.50	g	16.72	16.06	15.43	13.90
96	C	11 20 27.81 +14 20 54.40	s		19.45	19.49	
97	S	11 20 43.07 +23 27 55.30	s	22.63			
100	S	11 31 38.90 +45 14 51.50	g	21.58	19.48	19.34	18.97
101	II	11 34 38.46 +43 28 00.50	s	22.52	20.35	20.62	
103	II	11 37 16.95 +61 20 38.40	g	18.53	17.25	16.78	16.17
104^z	I	11 40 27.69 +12 03 07.60	g	16.88	16.00	14.98	14.65
106	II	11 41 08.23 +01 14 17.70	g	22.04	19.90	19.34	18.81
107	II	11 43 25.04 +22 06 56.00	s		19.43	20.60	
108^z	II	11 44 34.45 +37 10 16.90	g	18.95		17.59	16.67
109	I	11 45 05.23 +19 36 37.80	g	8.98	14.10	13.04	6.55
110	II	11 45 31.03 +31 33 37.00	g	20.86	19.93	19.28	
113	C*	11 50 43.88 −00 23 54.30	s	17.24		16.94	16.34
114	S*	11 53 24.51 +49 31 09.50	s	17.02	16.49	16.23	15.79
115	II	11 54 13.01 +29 16 08.50	g	20.56	18.16	18.54	18.36
116	I	11 55 26.63 +54 54 13.60	g	16.03	15.25	14.09	13.67
11^z7	S	11 56 03.67 +58 47 05.40	g	20.39	18.15	18.35	18.08
118	C	11 56 18.74 +31 28 05.00	g	19.18	18.55	18.45	17.63
120	C*	11 59 31.80 +29 14 44.30	s	17.49	16.56	17.65	13.10
121	II	12 00 59.77 +31 33 57.90	g	20.39	18.68	18.61	17.81
122^z	II	12 04 02.13 −04 22 43.90	s	17.75	16.17	16.69	15.72
123^z	I	12 06 19.93 +04 06 12.20	g	21.72	19.70	19.09	
124	II	12 09 13.52 +43 39 18.70	s	18.49	17.54	17.22	17.10
125^z	S	12 12 56.06 +20 32 37.90	g	21.69		19.10	18.75
126	C*	12 13 32.13 +13 07 20.40	s	17.87	17.58	17.10	17.08
127	C*	12 14 04.08 +33 09 45.50	s	17.91	17.10	17.64	17.05
128	II	12 15 29.80 +53 35 54.10	s	18.67	17.77	18.19	17.86
129	C*	12 15 55.60 +34 48 15.10	s	20.08	19.58	19.17	19.35
130	I	12 17 29.83 +03 36 44.00	g	17.16	15.65	15.57	14.43
131	I	12 19 15.33 +05 49 40.40	g	5.16	14.72	4.51	10.37
132	II	12 20 33.88 +33 43 10.90	s	18.96	18.13	18.12	17.49
134	C*	12 24 54.62 +21 22 47.20	s	16.01	18.03	15.94	15.62
135	I	12 25 03.78 +12 52 35.20	g			16.31	14.23
136	C*	12 27 58.78 +36 35 11.60	s	22.11	19.86		
137	C*	12 29 06.41 +02 03 05.10	s	11.74	9.82	11.12	10.58
138	I	12 29 51.84 +11 40 24.20	g	16.06	15.78	14.87	14.08
139	I	12 30 49.46 +12 23 21.60	g	11.08		15.49	14.76
140	C*	12 32 00.13 −02 24 04.10	s	17.35		16.32	16.17
141	II	12 35 22.97 +21 20 18.30	s	22.08	18.89	19.08	19.02
142	I	12 36 29.13 +16 32 32.10	g	17.31	16.42	15.30	14.41
143	S	12 42 19.68 −04 46 19.70	g	21.28		20.31	
144	II	12 43 57.63 +16 22 52.70	s	18.63	18.77	18.50	17.44
145	C*	12 44 49.18 +40 48 06.50	s	20.37	19.49	19.80	
146^z	II	12 51 44.47 +08 56 27.80	g	20.17	18.15	18.01	17.84
147	S*	12 52 26.33 +56 34 19.70	s	17.93	16.57	17.09	17.09
148^z	II	12 53 03.55 +02 38 22.30	g	20.50	18.53	18.33	17.18
149	II	12 53 32.70 +15 42 27.30	g	22.46		20.69	
150	II	12 54 11.68 +27 37 32.70	g	17.27	16.22	15.93	15.14
151	C*	12 56 11.15 −05 47 20.10	s	17.57	15.36	15.62	13.67
152	II	12 56 57.38 +47 20 19.80	g	22.29		20.44	19.57
153	II	13 00 32.87 +40 09 09.20	s	18.74	19.34	18.58	17.49
155	II	13 09 49.66 −00 12 36.60	g	21.17		18.97	18.18
156	C*	13 10 28.70 +32 20 44.30	s	20.08	19.20	17.68	17.79
157	II	13 11 08.56 +27 27 56.50	g	19.32	17.97	17.51	17.07
159	I	13 16 20.51 +07 02 54.30	g	14.99	14.70	14.52	13.08

ID	Rad.	Optical Position	Opt.	B_j	R1	R2	I
	Type	(J2000)	Type				
160	I	13 19 06.83 +29 38 33.80	g	17.30	16.22	15.52	14.86
161	C*	13 19 38.73 −00 49 40.90	s	18.20	17.40	16.96	17.23
163	II	13 21 18.84 +11 06 49.40	s	19.45	18.78	18.65	18.11
164	II	13 21 21.28 +42 35 15.20	g	17.87	16.62	16.20	15.65
165^{z}	I	13 23 21.04 +03 08 02.80	g	21.03		18.94	18.00
166	C*	13 26 16.51 +31 54 09.70	g	21.37	19.42	18.88	18.33
167	I	13 27 31.71 +31 51 27.30	g	19.74	18.43	17.81	17.18
168	C*	13 30 37.69 +25 09 11.00	g	19.12	17.86	17.45	17.24
169	C*	13 31 08.31 +30 30 32.40	s	17.55	17.20	17.11	16.66
170	II	13 32 56.37 +02 00 46.50	g	19.51	17.80	17.40	16.79
171	II	13 38 08.07 −06 27 11.20	s	17.77	16.88	18.03	17.57
172	I	13 38 49.67 +38 51 11.10	g	19.18	17.49	17.03	16.57
173	II	13 42 13.13 +60 21 42.30	s	18.48	17.83	17.45	17.52
174	I	13 42 43.57 +05 04 31.50	g	18.13	17.15	16.56	15.65
177	C*	13 47 33.42 +12 17 24.10	g	16.61	16.50	15.72	14.78
178	I	13 52 17.81 +31 26 46.70	g	11.06	15.27	14.28	13.52
181	II	13 57 04.37 +19 19 08.10	s	16.37	15.44	16.18	15.79
183	C*	14 00 28.65 +62 10 38.60	g	22.14	19.83	19.53	18.48
185	II	14 11 20.63 +52 12 09.00	g	21.17	18.13	18.47	17.78
188	I	14 16 53.50 +10 48 40.20	g	8.43	14.20	16.17	6.39
189	S	14 17 23.95 −04 00 46.60	g	21.88			
190	S*	14 19 08.18 +06 28 36.30	s	16.97	16.43	16.36	15.60
191	S	14 21 05.73 +41 44 49.70	g	20.50	19.36	18.43	18.42
192	II	14 23 00.81 +19 35 22.80	g	19.95	18.13	18.21	17.92
193	II	14 24 56.93 +20 00 22.70	s	17.73	17.07	17.02	16.71
194	II	14 25 50.67 +24 04 06.70	s	17.88	17.22	17.15	16.64
196^{z}	I	14 30 03.34 +07 15 01.30	g	5.61	15.12	14.30	13.49
197	C	14 36 57.07 +03 24 12.30	g	21.98			19.31
198	C*	14 38 44.71 +62 11 54.50	s	19.45	18.80	18.65	18.43
199	II	14 43 01.45 +52 01 38.20	g		20.97	20.60	
200	C	14 45 16.48 +09 58 36.00	s	18.93	17.76	17.72	17.27
201^{z}	II	14 48 39.98 +00 18 17.90	g	21.36	19.01	18.52	17.86
202	I	14 49 21.74 +63 16 13.90	g	14.82	16.43	14.17	13.28
203	II	14 55 01.43 −04 20 22.50	g	20.89	18.70	18.96	18.16
204	S	15 04 09.27 +60 00 55.50	g	19.95	18.90	19.24	19.60
205^{z}	I	15 04 19.50 +28 35 34.30	g	16.19	15.93	15.06	15.10
206	C*	15 04 25.03 +10 29 38.50	s	19.56	19.46	18.76	18.46
207	I	15 04 58.98 +25 59 49.00	g	16.33	16.73	15.15	14.72
208	I	15 10 53.55 −05 43 07.10	s	17.28		16.77	16.52
209	II	15 10 57.03 +07 51 24.80	s	20.29	18.05	17.91	16.74
211	I	15 13 39.90 +26 07 33.70	g	18.38	17.78	16.91	16.31
212^{z}	C*	15 13 40.20 +23 38 35.30	s			20.84	
213	II	15 16 40.21 +00 15 02.40	g	16.25	15.78	15.15	14.18
214	I	15 16 44.58 +07 01 18.10	g	14.16	13.96	16.14	12.15
215^{z}	S	15 16 56.61 +18 30 21.60	g	21.22	19.53	19.93	18.49
216	S*	15 20 05.50 +20 16 05.70	g	20.57	18.73	19.40	18.53
218	II	15 24 05.64 +54 28 18.40	g	20.30	18.42	18.44	17.68
220	II	15 31 25.36 +35 33 40.60	g	20.90	18.28	18.14	17.33
221	II	15 31 50.71 +24 02 43.30	g		16.35	15.99	15.35
222	C*	15 34 52.45 +01 31 03.30	s	19.44	18.70	18.15	16.27
224^{z}	I	15 37 32.39 +13 44 47.70	g	21.91		20.43	19.17
226	C*	15 40 49.51 +14 47 46.70	s	17.66	15.55	17.43	16.81
227	II	15 41 45.64 +60 15 36.20	g			20.79	
228	C*	15 46 09.50 +00 26 24.60	g			19.92	19.04
229	II	15 47 44.23 +20 52 41.00	s	16.35	16.14	15.86	15.11
231	II	15 49 58.54 +62 41 20.90	s	21.36	19.71	19.59	19.05
232	C*	15 50 35.26 +05 27 10.60	s	20.07	17.59	18.56	18.63
235^{z}	II	15 56 36.35 +42 57 09.60	g			20.68	
237	II	16 02 17.21 +01 58 19.40	g	16.42		15.52	15.13
238	C*	16 08 46.13 +10 29 08.20	s	18.95	18.05	18.16	17.36
239	C	16 09 13.31 +26 41 29.20	g			20.38	19.17
241^{z}	S	16 12 19.02 +22 22 15.60	g	22.04	19.72	20.18	
242	C*	16 13 41.08 +34 12 47.70	s	18.06	17.60	17.02	16.63
245	I	16 17 38.89 +35 00 48.00	g	10.43	14.25	13.71	12.77
246	II	16 17 43.28 +32 23 02.40	g	18.58	17.04	16.81	16.06

ID	Rad. Type	Optical Position (J2000)	Opt. Type	B_j	R1	R2	I
247	II	16 20 21.40 +17 36 29.30	s	16.72	16.17	16.70	16.16
248	II	16 24 39.42 +23 45 17.50	s	18.57	18.39	18.06	17.88
250	II	16 28 03.57 +27 41 36.10	g	22.17	19.63	19.76	
251	I	16 28 38.34 +39 33 04.70	g	13.92	17.08	16.30	6.17
253	II	16 29 37.52 +23 20 13.40	g	22.62		20.70	
254	C	16 31 45.29 +11 56 03.30	s	18.73	18.29	18.20	17.52
255	C*	16 34 33.86 +62 45 35.70	g	21.42	20.00	20.25	19.36
256	C*	16 35 15.51 +38 08 04.80	s	18.37	17.80	17.43	16.49
258	C*	16 38 28.22 +62 34 43.90	s		20.62	20.55	
259	C*	16 42 58.77 +39 48 37.00	s	17.72	15.71	16.89	16.59
260	II	16 43 05.93 +37 29 34.40	g	21.33	19.98	20.17	
261	I	16 43 48.69 +17 15 48.80	g	18.26	16.11	16.36	15.93
262	C*	16 47 41.83 +17 20 11.50	g	20.41	18.39	18.32	17.79
263	C	16 53 52.24 +39 45 36.60	g	15.03	14.03	13.29	12.97
264	II	16 59 27.57 +47 03 13.10	g	19.93	17.68	17.69	16.74
265	S	17 04 07.21 +29 46 59.50	s	19.42	19.11	18.96	18.73
266	II	17 04 43.03 +60 44 49.60	s	15.10	14.74	14.53	14.34
267^z	II	17 05 06.57 +38 40 37.60	g	21.58	19.67	19.71	
268	II	17 10 44.11 +46 01 30.30	g			20.75	
269	II	17 23 20.85 +34 17 57.30	s	15.92	15.25	15.83	14.95
270	II	17 24 18.40 +50 57 54.00	g		19.52	20.71	
271	II	17 42 51.84 +61 45 51.00	s	18.20	18.19	18.11	17.85
272^z	II	07 14 35.25 +45 40 0.10	g	18.43	17.30	16.79	16.20
273	II	14 54 20.30 +16 20 55.80	g	14.91	14.71	13.59	12.80
274^z	II	08 31 20.33 +32 18 37.00	g	16.22	15.80	15.11	14.15
275^z	II	08 48 41.94 +05 55 35.00	g	22.03	20.20		
276	II	12 28 11.77 +20 23 19.10	s	18.40	18.00	17.77	17.56
277	S	07 44 17.50 +37 53 16.90	s	18.07	17.59	17.64	17.76

APPENDIX B: CONFIG-2, 3 AND 4 SAMPLES

Table B1. Data for CoNFIG-2 sample. The RA and DEC gives the NVSS position of the source. The sources of C* type are confirmed compact sources from the VLBA calibrator list (see Beasley et al. 2002; Fomalont et al. 2003; Petrov et al. 2005, 2006; Kovalev et al. 2007) or the Pearson-Readhead survey (Pearson & Readhead 1988). Unresolved sources (type S) are probably unresolved FRII sources. Designations I and II are Fanaroff & Riley (1974) types.
References:
(1) See Table A; (2) Snellen et al. (2002); (3) Lahulla et al. (1991); (4) Heckman et al. (1994); (5) Hewitt & Burbidge (1991); (6) Bauer, Condon & Thuan (2000); (7) Enya et al. (2002); (8) Abazajian et al. (2003); (9) Brinkmann et al. (1995); (10) Madore et al. (1992); (11) Machalski (1998); (12) Willis & Willis (1976); (13) Xu et al. (1994); (14) Kovalev et al. (1999); (15) Liu & Zhang (2002); (16) Willott et al. (2002); (17) Tinti & de Zotti (2006); (18) Barkhouse & Hall (2001); (19) Pihlstroem, Conway & Vermeulen (2003); (20) Hewitt & Burbidge (1989); (21) Abazajian et al. (2005); (22) Strom et al. (1990); (26) Lu et al. (1993); (27) Schneider et al. (2007); (28) Zensus et al. (2002); (29) Maxfield et al. (1995); (30) Pinkney et al. (2000); (31) Schneider et al. (2005); (32) Hewitt & Burbidge (1989); (33) Nilsson (1998); (35) (2005); (38) Gopal-Krishna et al. (2005)

RA	DEC (J2000)	Radio Type	$S_{1.4\ \mathrm{GHz}}$ (mJy)	B-mag.	Opt. Type	z	Ref.
09 20 11.16	+17 53 25.00	S	1070.6				
09 20 58.48	+44 41 53.70	C*	1017.2	17.20	2	2.180	2
09 21 07.54	+45 38 45.70	II	8101.6	18.61	1	0.174	1
09 21 47.05	+37 54 16.10	II	826.4	20.24	2	1.108	3
09 22 49.93	+53 02 21.20	S	1597.8				
09 27 03.04	+39 02 20.70	C*	2884.6	17.06	2	0.698	1
09 30 33.45	+36 01 23.60	II	1875.1	18.98	2	1.157	1
09 30 54.27	+58 55 16.60	II	1082.9				
09 34 15.80	+49 08 21.00	C*	800.5			2.582	2
09 35 04.06	+08 41 37.30	S	1037.6				
09 35 06.62	+39 42 07.60	I	1029.5				
09 36 32.02	+04 22 10.80	S	971.1			1.340	4
09 39 50.20	+35 55 53.10	II	3719.0	18.59	1	0.137	1
09 41 22.70	−01 43 01.00	II	830.0			0.382	5
09 41 23.62	+39 44 14.10	II	2064.7	18.00	1	0.107	1
09 42 08.40	+13 51 52.20	C	1338.5	20.08	1	1.565	1
09 42 15.35	+13 45 49.60	S	3336.4			0.580	1
09 43 12.74	+02 43 27.50	II	1331.5			0.592	8
09 43 19.16	−00 04 22.30	S	1188.9	21.27	1		
09 44 16.40	+09 46 19.20	II	2393.7	22.45	2	0.818	1
09 45 13.81	+16 55 21.70	II	1062.1				
09 47 47.27	+07 25 13.80	II	7617.0	17.65	1	0.086	1
09 47 44.60	+00 04 37.20	II	935.8	20.62	2		
09 48 55.36	+40 39 44.80	C*	1599.5	19.00	2	1.252	1
09 50 10.77	+14 19 57.30	II	3711.6			0.552	1
09 51 58.83	−00 01 26.80	II	3152.1	15.88	2	1.487	1
09 52 00.52	+24 22 29.70	II	1788.6				
09 52 06.14	+28 28 33.20	C	1362.7				
09 53 38.99	+25 16 24.60	S	993.1			0.146	2
09 54 56.81	+17 43 31.50	C*	1158.5	16.94	2	1.472	2
09 54 04.03	+21 22 28.10	II	948.8	17.66	2	0.295	6
09 56 49.88	+25 15 15.90	C*	1080.1	18.13	2	0.712	2
09 57 38.18	+55 22 57.40	C*	3079.2	18.28	2	0.909	1
09 58 20.92	+32 24 01.60	S*	1247.1	15.57	2	0.530	7
09 58 28.78	−01 39 59.30	S	1213.7				
10 00 17.51	+00 05 23.00	II	923.7	17.92	2	0.907	8
10 00 21.95	+22 33 18.20	II	1116.3	16.98	2	0.419	9
10 00 28.11	+14 01 34.10	II	1166.4				
10 01 24.45	−00 26 02.80	II	1221.0				
10 01 46.73	+28 46 56.50	II	5597.0	18.64	1	0.185	1
10 02 57.12	+19 51 53.50	I	1226.5	16.73	1	0.168	1
10 04 32.94	+31 51 51.50	II	1263.8			0.900	11
10 06 01.74	+34 54 10.40	II	3236.6	17.27	1	0.099	1
10 07 18.92	+44 25 01.40	II	1413.7				
10 07 27.54	+12 48 40.90	II	1216.1	14.73	2	0.240	7
10 07 41.51	+13 56 29.30	C*	936.3	18.27	2	2.707	12
10 07 42.54	+59 08 09.90	II	1082.8	19.46	2		
10 08 00.04	+07 30 16.20	C	6522.1	21.53	1	0.880	1

RA (J2000)	DEC	Radio Type	$S_{1.4\ \mathrm{GHz}}$ (mJy)	B-mag.	Opt. Type	z	Ref.
10 09 55.50	+14 01 54.10	S	994.6	17.50	1	0.215	12
10 11 00.36	+06 24 40.20	II	2964.2			1.405	1
10 11 45.46	+46 28 20.10	II	1557.2			1.790	1
10 14 16.03	+10 51 06.30	II	902.2			0.388	21
10 14 47.05	+23 01 12.70	I	1095.5	13.00	2	0.565	7
10 14 48.92	+08 52 58.80	C	877.4				
10 16 01.90	+40 46 57.40	II	1078.5	16.69	1	0.128	21
10 17 14.15	+39 01 24.00	S	1392.2	20.83	1	0.206	1
10 17 49.77	+27 32 07.70	II	1274.7	17.90	2	0.469	12
10 21 54.58	+21 59 30.90	II	1686.2			1.617	1
10 22 30.31	+30 41 05.80	C*	967.8	17.61	2	1.316	2
10 23 11.60	+39 48 17.20	C*	1122.6	17.02	2	1.254	13
10 23 38.71	+59 04 49.50	S	1609.3				
10 24 29.63	−00 52 55.20	C*	986.2	17.95	2	2.552	14
10 25 20.72	+20 10 21.30	I	1250.3				
10 25 29.87	+42 57 43.10	II	852.4				
10 26 31.96	+06 27 32.70	II	851.5	17.93	2	1.699	15
10 27 14.64	+46 2 20.10	I	1437.4				
10 27 32.89	+48 17 51.40	II	985.3	18.76	1	0.280	11
10 28 20.08	+15 11 29.50	S	824.5				
10 30 09.91	+00 37 40.20	S	1077.1				
10 31 43.55	+52 25 37.90	I	921.6	17.21	1	0.166	8
10 33 28.31	+17 42 44.70	II	929.0				
10 33 33.87	+58 14 37.90	II	4187.9	20.89	1	0.430	1
10 34 17.86	+50 13 30.20	S	1545.2				
10 35 07.04	+56 28 47.30	C*	1801.9			0.460	1
10 41 17.16	+06 10 16.50	C*	1405.2	17.40	2	1.270	1
10 41 39.01	+02 42 33.00	II	2710.1	21.65	1	0.535	1
10 42 36.53	+29 49 45.60	C	841.2				
10 42 44.54	+12 03 31.80	S*	3305.7	18.03	2	1.028	1
10 46 18.04	+54 59 37.50	II	1032.7				
10 46 34.99	+15 43 47.20	S	1071.9				
10 48 34.23	+34 57 25.50	S	1034.4	20.70	2	1.594	16
10 49 26.18	−02 54 52.70	I	956.5				
10 51 48.80	+21 19 52.80	C*	1253.1	17.40	2	1.300	12
10 52 26.06	+20 29 48.00	C	1727.5	21.62	1		1
10 57 15.77	+00 12 03.80	C*	898.1			0.650	17
10 58 17.46	+19 52 09.50	II	2143.0			1.110	1
10 58 29.62	+01 33 58.20	C*	3220.2	18.75	2	0.888	1
10 58 58.69	+43 01 23.70	II	2875.1			0.749	1
11 00 02.02	+30 27 42.00	II	991.4				
11 02 03.91	−01 16 18.30	II	2799.6			0.311	1
11 02 24.97	−02 35 34.10	S	838.4				
11 02 26.19	+55 50 03.30	I	1206.4	18.47	1		
11 05 26.17	+20 52 17.40	S	985.6				
11 06 31.77	−00 52 51.50	II	1065.6	16.25	2	0.426	7
11 07 15.02	+16 28 01.50	I	868.6	16.53	2	0.632	7
11 08 08.31	+14 35 35.80	C	1348.7				
11 08 36.10	+38 58 58.10	II	919.7	18.69	2	0.781	18
11 08 51.79	+25 00 52.10	II	1090.0				
11 09 28.86	+37 44 31.40	C*	1221.6			2.290	14
11 09 46.04	+10 43 43.40	C	1481.3			0.550	1
11 09 47.74	+37 38 16.50	I	2214.1	21.28	1	0.346	1
11 11 20.09	+19 55 36.10	C*	1194.8	18.56	2	0.299	19
11 11 22.71	+03 09 10.40	II	1017.7				
11 11 31.56	+35 40 45.50	II	1336.3			1.105	1
11 11 38.98	+40 50 15.30	II	819.2	15.69	1	0.074	15
11 12 38.36	+43 26 27.10	II	1433.0	22.15	2	1.680	1
11 13 32.13	−02 12 55.20	II	1595.6	20.84	1	0.125	35
11 14 38.43	+40 37 20.80	II	3127.9	18.27	2	0.734	1
11 16 34.70	+29 15 20.50	II	1927.9	16.72	1	0.049	1
11 17 33.85	−02 36 00.60	S	996.1				
11 18 11.85	+53 19 44.70	II	919.2	17.92	2	0.235	2
11 18 57.28	+12 34 42.20	S*	1112.2	18.12	2	2.118	21

RA	DEC (J2000)	Radio Type	$S_{1.4\ \mathrm{GHz}}$ (mJy)	B-mag.	Opt. Type	z	Ref.
11 19 25.22	−03 02 51.60	S	1730.4			1.355	1
11 20 27.81	+14 20 54.40	C	2446.9			0.362	1
11 20 43.07	+23 27 55.30	S	1362.0	22.63	2	1.819	1
11 23 09.10	+05 30 20.30	S	1721.1			2.474	1
11 24 37.45	+04 56 18.80	II	1145.4	17.86	1	0.283	8
11 24 43.90	+19 19 29.70	S	874.7	18.82	1	0.165	22
11 25 53.70	+26 10 20.10	C*	921.2	18.79	2	2.341	2
11 26 08.53	+30 03 36.50	II	933.6	18.19	2		
11 26 23.65	+33 45 27.10	C	1376.8			1.230	1
11 26 26.88	+12 20 37.40	II	1110.5	19.35	2		
11 29 35.97	+00 15 17.50	II	979.5	18.75	1	0.211	
11 29 47.93	+50 25 51.90	S	926.9				
11 31 38.90	+45 14 51.50	S	2048.8	21.58	1	0.404	1
11 32 59.49	+10 23 42.70	S	879.1	16.60	2	0.540	8
11 33 09.56	+33 43 12.60	II	886.6	17.70	1	0.190	11
11 33 13.18	+50 08 39.90	II	844.9	18.28	1	0.310	11
11 34 38.46	+43 28 00.50	II	1567.1	22.52	2	0.572	1
11 34 54.61	+30 05 25.20	II	1145.5	19.28	1	0.614	7
11 35 13.04	−00 21 19.40	S	1267.8	16.85	2	0.160	17
11 35 55.93	+42 58 44.80	C	1448.8				
11 37 29.68	+01 16 13.30	S	1059.7	19.32	1	0.430	1
11 40 17.03	+17 43 39.00	I	1143.3	7.05	1	0.011	26
11 40 27.69	+12 03 07.60	I	1527.0	16.88	1	0.081	21
11 40 49.54	+59 12 26.00	C	2179.4				
11 41 08.23	+01 14 17.70	II	2690.8	22.04	1	0.443	1
11 42 57.23	+21 29 12.50	II	921.0	17.91	1		
11 42 58.78	+48 51 19.70	II	958.6	19.91	2		
11 43 25.04	+22 06 56.00	II	3128.7			0.366	1
11 43 39.63	+46 21 20.70	II	863.2	16.66	1	0.117	21
11 44 21.23	+29 58 25.30	II	837.3				
11 44 34.45	+37 10 16.90	II	1998.9	18.95	1	0.115	21
11 44 54.01	−00 31 36.50	II	947.6				
11 45 05.23	+19 36 37.80	I	5689.0	8.98	1	0.021	1
11 45 31.03	+31 33 37.00	II	2890.9	20.86	1	0.811	1
11 45 43.41	+49 46 08.40	II	1424.5			1.275	1
11 47 14.71	+25 23 20.20	II	879.0				
11 48 47.51	+04 55 27.70	II	827.9			0.420	38
11 49 55.54	+12 47 15.90	II	2519.9			1.144	1
11 50 43.88	−00 23 54.30	C*	2773.9	17.24	2	1.976	1
11 53 03.11	+11 07 20.40	II	853.5				
11 53 12.54	+09 14 02.50	C*	809.2	17.36	2	0.698	8
11 53 24.51	+49 31 09.50	S*	1572.2	17.02	2	0.334	1
11 53 54.65	+40 36 52.90	C*	1135.6	20.16	1	0.916	27
11 54 13.01	+29 16 08.50	II	1620.3	20.56	1	0.329	1
11 55 13.61	+54 52 50.40	II	1233.3				
11 55 34.69	+54 53 40.40	I	2226.9	16.03	1	0.050	1
11 56 03.67	+58 47 05.40	S	1591.7	20.39	1		
11 56 18.74	+31 28 05.00	C	2978.3	19.18	1	0.418	1
11 57 34.91	+16 38 59.30	C*	813.2	17.26	2	1.050	2
11 58 25.80	+24 50 17.70	C*	1021.2	18.19	1	0.202	28
11 59 13.79	+53 53 07.40	C	1740.6				
11 59 31.80	+29 14 44.30	C*	2030.8	17.49	2	0.729	1
11 59 48.83	+58 20 20.80	C	1191.3	19.56	1		
12 00 31.19	+45 48 43.20	S	1156.5			0.743	29
12 00 57.78	+31 32 52.90	II	1301.6	20.39	1	0.362	1
12 01 25.01	+25 20 24.00	II	862.9				
12 02 04.19	+58 02 01.90	I	843.2	16.10	1	0.102	3
12 02 32.27	−02 40 03.20	S	906.1				
12 03 21.95	+04 14 17.70	C*	1146.1	18.39	2	1.212	31
12 04 02.13	−04 22 43.90	II	2141.3	17.75	2		
12 04 18.46	+52 02 18.80	C	962.3				
12 04 52.31	+29 29 12.40	II	1230.6	18.57	1		
12 06 19.93	+04 06 12.20	I	1501.2	21.72	1		
12 09 13.52	+43 39 18.70	II	1979.9	18.49	2	1.400	1

RA	DEC (J2000)	Radio Type	$S_{1.4\ \mathrm{GHz}}$ (mJy)	B-mag.	Opt. Type	z	Ref.
12 12 56.06	+20 32 37.90	S	1417.9	21.69	1		
12 13 32.13	+13 07 20.40	C*	1344.2	17.87	2	1.141	1
12 14 04.08	+33 09 45.50	C*	1403.6	17.91	2	1.598	1
12 14 47.73	−01 00 12.10	II	1092.5				
12 15 14.69	+17 30 02.20	S*	1010.2				
12 15 29.80	+53 35 54.10	II	2755.0	18.67	2	1.065	1
12 15 55.60	+34 48 15.10	C*	1506.8	20.08	2	0.857	1
12 17 29.83	+03 36 44.00	I	2411.5	17.16	1	0.077	1
12 17 56.90	+25 29 27.20	S	866.8	17.81	2		
12 18 59.22	+19 55 28.90	II	1047.0				
12 19 15.33	+05 49 40.40	I	10445.0	5.16	1	0.007	1
12 20 28.08	+09 28 26.90	II	1064.4	18.33	2	1.082	8
12 20 33.88	+33 43 10.90	II	2845.9	18.96	2	1.519	1
12 21 52.92	+31 30 56.70	II	805.8				
12 22 22.59	+04 13 17.30	C*	800.3	16.91	2	0.965	32
12 24 27.29	+42 06 10.30	II	1352.3			0.944	1
12 24 52.44	+03 30 50.10	C*	1280.3	18.05	2	0.957	2
12 24 54.62	+21 22 47.20	C*	2094.4	16.01	2	0.435	1
12 25 03.78	+12 52 35.20	I	6012.8			0.003	1
12 26 25.60	+09 40 05.70	S	1008.3				
12 27 58.78	+36 35 11.60	C*	2098.4	22.11	2	1.973	1
12 28 11.77	+20 23 19.10	II	1269.5	18.00	2	0.680	1
12 29 06.41	+02 03 05.10	C*	54991.2	11.74	2	0.158	1
12 29 32.62	+17 50 20.90	C	931.0	17.87	1		
12 29 51.84	+11 40 24.20	I	1519.0	16.06	1	0.083	1
12 30 49.46	+12 23 21.60	I	141949.3	11.08	1	0.004	1
12 32 00.13	−02 24 04.10	C*	1646.7	17.35	2	1.045	1
12 32 05.31	−01 34 55.10	I	807.4				
12 35 22.97	+21 20 18.30	II	2918.5	22.08	2	0.422	1
12 36 28.18	+16 31 35.40	I	1383.9	17.31	1	0.068	1
12 36 49.96	+36 55 18.00	II	920.2				
12 39 07.16	+ 5 19 24.50	II	938.2				
12 39 09.05	+32 30 27.30	S	827.8				
12 41 49.84	+57 30 36.90	II	1299.2				
12 42 19.68	−04 46 19.70	S	3672.1	21.28	1	0.480	1
12 43 57.63	+16 22 52.70	II	2895.8	18.63	2	0.557	1
12 44 49.18	+40 48 06.50	C*	1341.8	20.37	2	0.813	1
12 47 07.40	+49 00 18.20	C	1204.6	17.43	1	0.206	15
12 49 48.76	+33 23 15.80	II	1289.2			0.350	11
12 51 35.43	+50 34 01.40	II	1155.8			0.414	33
12 51 40.63	+08 55 58.60	II	1684.4	20.17	1		
12 52 08.60	+52 45 30.80	S	958.5				
12 52 16.81	+47 15 39.00	II	982.9				
12 52 22.78	+03 15 50.40	I	935.3	16.74	1	0.099	8
12 52 26.33	+56 34 19.70	S*	2288.3	17.93	2	0.320	1
12 53 03.55	+02 38 22.30	II	1604.9	20.50	1		
12 53 32.70	+15 42 27.30	II	1952.2	22.46	1	0.766	1
12 54 11.68	+27 37 32.70	II	2923.9	17.27	1	0.086	1
12 56 11.15	−05 47 20.10	C*	9711.2	17.57	2	0.536	1
12 58 01.96	+44 35 20.60	I	929.8	18.11	1		
13 00 32.87	+40 09 09.20	II	1368.9	18.74	2	1.667	1
13 02 28.56	+58 18 46.90	C	898.0				
13 04 28.87	+53 50 02.50	II	908.9				
13 04 43.69	−03 46 02.30	S*	826.0	18.61	2	1.250	18
13 05 36.05	+08 55 15.90	II	1461.8			1.409	1
13 07 54.01	+06 42 15.90	II	1122.0	16.54	2	0.599	7
13 09 33.94	+11 54 24.20	C*	855.0	18.52	2		
13 09 49.66	−00 12 36.60	II	1636.7	21.17	1	0.419	1
13 10 28.70	+32 20 44.30	C*	1686.6	20.08	2	0.997	1
13 11 08.56	+27 27 56.50	II	2044.6	19.32	1	0.239	1
13 13 37.88	+54 58 24.30	C*	1304.6				
13 15 01.28	+20 44 30.10	S	1098.7				
13 15 09.94	+ 8 41 44.60	II	932.8				
13 16 14.55	+07 02 19.90	I	2006.4	14.99	1	0.051	1

RA	DEC (J2000)	Radio Type	$S_{1.4\ \mathrm{GHz}}$ (mJy)	B-mag.	Opt. Type	z	Ref.
13 19 06.83	+29 38 33.80	I	1372.5	17.30	1	0.073	1
13 19 38.73	−00 49 40.90	C*	1468.9	18.20	2	0.892	1
13 19 46.40	+51 48 06.70	II	1092.6	16.59	2	1.060	15

Table B2. Data for CoNFIG-3 and CoNFIG-4 sample. The RA and DEC gives the NVSS position of the source. The sources of C* type are confirmed compact sources from the VLBA calibrator list (see Beasley et al. 2002; Fomalont et al. 2003; Petrov et al. 2005, 2006; Kovalev et al. 2007) or the Pearson-Readhead survey (Pearson & Readhead 1988). Unresolved sources (type S) are probably unresolved FRII sources. Designations I and II are Fanaroff & Riley (1974) types.

CoNFIG-3							
RA	DEC (J2000)	Radio Type	$S_{1.4\ \mathrm{GHz}}$ (mJy)	RA	DEC (J2000)	Radio Type	$S_{1.4\ \mathrm{GHz}}$ (mJy)
14 41 28.26	+10 55 24.70	S	422.7	14 55 7.32	+14 12 22.20	II	246.9
14 42 3.43	+25 5 4.30	II	204.7	14 55 55.36	+11 51 44.70	I	385.3
14 42 3.93	+13 29 17.60	C	706.0	14 56 5.65	+16 26 52.80	I	1290.3
14 42 22.99	+14 54 58.20	S	202.6	14 56 21.94	+26 35 56.40	II	345.4
14 42 27.11	+14 31 39.90	II	224.1	14 56 28.69	+13 02 41.10	S	260.7
14 42 48.37	+11 44 15.00	S	200.7	14 56 39.93	+18 08 17.50	S	408.6
14 43 1.74	+16 06 59.90	II	242.7	14 56 52.03	+24 15 19.30	S	508.3
14 43 2.77	+18 41 56.00	S	219.9	14 56 53.43	+27 41 39.20	II	321.6
14 43 5.19	+31 52 31.60	S	203.4	14 57 0.72	+13 47 6.50	II	276.2
14 43 47.18	+14 36 6.80	S	303.9	14 57 5.05	+26 58 10.60	S	295.0
14 43 56.94	+25 01 44.50	C*	361.7	14 57 23.36	+24 59 17.30	II	237.2
14 44 5.77	+20 35 18.30	C	281.7	14 57 43.45	+24 35 8.30	C*	794.4
14 44 11.04	+26 1 50.80	II	273.5	14 57 48.71	+25 06 35.10	II	580.9
14 44 14.66	+19 48 22.00	S	201.5	14 57 50.20	+28 31 8.00	II	972.1
14 44 25.07	+13 59 56.20	II	607.5	14 57 57.40	+11 44 22.10	II	559.9
14 44 34.84	+19 21 33.00	I	342.5	14 58 2.01	+29 28 31.40	S	232.9
14 44 50.95	+11 31 55.30	II	290.3	14 58 2.75	+18 39 33.30	S	253.8
14 45 4.85	+16 49 26.00	II	410.4	14 58 5.26	+14 34 10.00	S	431.1
14 45 27.03	+24 38 4.00	C	212.1	14 58 33.88	+18 30 56.10	S	499.0
14 45 32.32	+26 23 49.70	II	303.9	14 58 34.64	+14 09 51.20	II	312.6
14 45 44.74	+23 02 39.40	S	343.2	14 58 38.91	+24 58 57.40	II	236.7
14 45 57.34	+17 38 30.20	II	826.9	14 59 14.57	+23 56 33.60	S	217.2
14 45 58.32	+12 22 28.50	II	395.6	14 59 42.07	+29 03 34.10	I	367.0
14 46 19.87	+25 17 3.50	II	355.2	15 0 19.79	+20 12 1.80	I	294.1
14 46 35.32	+17 21 7.40	C*	754.1	15 00 21.36	+14 34 59.80	II	376.5
14 46 43.33	+27 57 0.70	S	1113.9	15 00 53.33	+17 39 7.60	S	206.4
14 46 50.83	+21 31 50.90	II	529.6	15 01 28.50	+21 34 20.70	I	298.5
14 46 52.13	+22 51 4.70	S	337.7	15 01 36.72	+27 44 24.00	II	342.7
14 47 8.40	+17 47 52.90	S	995.5	15 01 38.33	+13 24 49.60	S	250.2
14 47 44.55	+16 36 6.00	II	371.0	15 01 58.81	+19 14 5.30	II	312.2
14 48 4.28	+14 47 4.60	I	440.0	15 2 0.35	+24 39 17.80	II	273.6
14 48 8.62	+16 34 39.50	II	265.0	15 02 0.56	+13 11 54.30	S	314.0
14 48 27.87	+27 33 18.80	C	242.1	15 02 51.38	+25 44 14.90	II	250.7
14 48 42.66	+17 33 33.20	II	362.2	15 03 1.63	+18 20 32.40	II	316.5
14 48 50.05	+20 25 34.80	II	989.1	15 03 8.07	+12 37 2.20	S	235.3
14 49 19.01	+21 05 48.00	I	432.9	15 03 22.40	+19 33 4.10	II	232.6
14 49 27.59	+22 11 27.90	II	276.1	15 03 29.52	+10 33 31.20	S	281.8
14 50 19.92	+15 10 44.00	S	247.0	15 3 39.51	+10 16 2.80	C	340.8
14 50 31.00	+16 15 47.60	S	301.5	15 03 51.32	+12 28 7.40	II	299.0
14 51 31.48	+13 43 24.40	C	691.8	15 03 58.47	+12 30 25.60	S	268.1
14 51 38.62	+14 14 1.90	S*	359.9	15 04 17.12	+28 35 36.30	I	1698.1
14 51 39.07	+19 36 24.80	S	407.4	15 4 17.22	+10 57 35.40	S	252.8
14 52 20.42	+14 56 23.50	I	213.8	15 04 25.03	+10 29 38.50	C*	1774.2
14 52 34.57	+29 48 20.50	C	247.0	15 04 26.71	+28 54 30.60	C*	583.2
14 53 2.52	+33 10 45.10	II	455.9	15 04 58.43	+26 01 32.90	I	7613.4
14 53 6.08	+19 17 42.50	S	219.5	15 05 0.08	+11 58 43.90	S	205.9
14 53 33.41	+18 54 1.00	S	486.4	15 06 19.33	+20 27 41.50	I	294.9
14 53 38.10	+29 01 17.70	S	265.3	15 07 9.23	+16 07 16.70	S	513.1
14 53 44.24	+10 25 57.90	C*	374.8	15 07 21.88	+10 18 46.30	C	403.2
14 53 53.61	+26 48 33.40	C*	518.6	15 7 37.00	+11 3 7.00	II	226.4
14 54 8.37	+11 37 34.40	II	451.6	15 07 41.89	+12 08 4.30	S	421.0
14 54 20.30	+16 20 55.80	II	1391.3	15 07 47.06	+24 34 30.40	S	314.1
14 54 20.86	+16 24 25.10	C*	228.4	15 08 5.12	+18 52 43.80	S	220.1
14 54 22.75	+25 39 55.50	II	232.4	15 08 39.31	+18 58 60.00	S	299.4
14 54 29.16	+20 15 26.10	II	237.5	15 08 48.64	+28 50 9.50	C	391.2
14 54 32.30	+29 55 58.50	C*	730.7	15 9 0.22	+24 19 50.50	I	287.4
14 54 42.58	+27 32 11.30	I	211.1	15 09 4.80	+28 39 26.70	S	252.4

CoNFIG-3

RA	DEC	Radio Type	$S_{1.4\ \mathrm{GHz}}$ (mJy)	RA	DEC	Radio Type	$S_{1.4\ \mathrm{GHz}}$ (mJy)
(J2000)				(J2000)			
15 09 15.60	+14 06 14.80	S	402.7	15 23 58.49	+16 14 47.60	C	234.8
15 09 16.35	+16 58 57.20	II	233.5	15 24 5.26	+29 00 23.60	C	279.1
15 09 42.80	+29 39 2.80	II	205.6	15 24 12.71	+19 23 59.70	S	263.9
15 09 42.80	+15 56 59.10	C	284.9	15 24 41.60	+15 21 21.70	S	445.0
15 09 50.53	+15 57 25.70	S	386.0	15 24 54.42	+27 57 7.70	I	209.6
15 10 2.49	+23 22 3.10	S	257.6	15 25 2.88	+11 07 45.00	C*	407.7
15 10 39.49	+20 19 7.00	S	212.0	15 25 8.80	+12 53 18.10	II	219.7
15 10 43.15	+12 40 52.30	II	273.3	15 25 32.87	+15 56 11.40	S	485.7
15 10 49.12	+14 37 26.20	II	214.2	15 26 9.24	+17 2 26.70	C	317.1
15 10 50.01	+10 42 14.10	S	220.2	15 26 31.81	+14 44 59.20	S	231.0
15 10 56.69	+18 02 38.90	C	305.7	15 26 33.87	+12 53 7.60	S	234.4
15 11 5.59	+22 08 6.40	C*	411.1	15 27 15.68	+20 53 23.00	II	217.9
15 11 9.08	+18 01 53.80	I	375.9	15 27 32.48	+11 54 32.20	S	479.8
15 11 15.58	+18 08 4.90	S	281.9	15 27 40.01	+15 21 57.90	S	308.0
15 11 29.43	+10 01 43.80	II	644.7	15 27 44.61	+28 55 6.60	II	212.8
15 11 31.60	+28 22 41.40	S	207.9	15 27 57.80	+22 33 1.30	S	335.4
15 11 45.70	+21 08 3.10	S	270.6	15 28 6.39	+13 23 32.30	I	225.0
15 12 7.48	+22 47 14.60	S	280.1	15 29 9.51	+17 13 26.80	II	409.4
15 12 12.07	+15 40 25.50	S	993.5	15 29 46.19	+15 39 44.50	II	536.8
15 12 32.56	+14 56 36.70	S	223.7	15 29 51.76	+19 04 34.60	S	604.8
15 13 27.61	+22 30 23.50	S	205.4	15 30 4.69	+29 0 9.30	II	258.3
15 13 29.57	+10 11 3.90	II	221.4	15 30 5.11	+23 16 22.20	II	277.6
15 13 39.90	+26 07 33.70	I	4332.7	15 30 49.02	+27 21 27.50	C	209.6
15 13 40.20	+23 38 35.30	C*	1767.5	15 31 42.71	+24 04 27.20	II	3577.3
15 13 45.74	+24 11 2.80	II	367.3	15 31 48.52	+10 55 39.90	II	200.5
15 14 3.55	+22 23 31.50	S	268.0	15 31 49.73	+22 25 5.90	S	304.8
15 14 14.64	+23 27 11.20	I	247.0	15 32 28.50	+24 15 29.90	II	328.5
15 14 15.61	+15 41 59.60	S	278.2	15 32 34.03	+20 06 38.80	S	577.7
15 14 31.84	+12 34 17.80	S	323.0	15 32 44.30	+28 03 46.40	I	381.0
15 14 49.50	+10 17 0.90	I	436.7	15 32 50.67	+22 41 35.20	S	222.9
15 15 3.43	+22 31 45.40	I	208.4	15 32 58.12	+15 56 5.80	II	284.5
15 15 23.74	+10 18 37.30	II	237.8	15 33 14.49	+15 16 42.20	S	1055.3
15 15 54.17	+24 58 40.40	C	219.7	15 33 15.08	+13 32 24.30	II	1113.1
15 16 2.98	+14 18 22.90	II	296.3	15 34 17.83	+10 17 8.40	II	336.5
15 16 56.61	+18 30 21.60	S	1335.2	15 34 22.66	+13 49 17.10	S	809.0
15 16 56.81	+19 32 13.40	C*	464.1	15 34 46.22	+19 18 10.20	S	674.7
15 17 4.56	+21 22 42.90	I	243.3	15 34 57.26	+23 30 11.10	C	326.3
15 17 23.58	+29 55 30.40	S	320.5	15 35 19.47	+27 52 56.80	II	302.7
15 17 24.70	+17 29 28.30	II	226.0	15 35 49.55	+14 03 50.90	I	299.1
15 17 49.52	+14 27 59.30	I	201.8	15 36 11.93	+13 12 35.50	S	210.3
15 17 51.37	+10 00 26.90	II	229.5	15 36 34.02	+17 16 7.40	S	368.7
15 17 53.32	+26 48 39.50	S	284.1	15 37 7.76	+26 48 28.50	I	263.1
15 18 5.11	+19 42 43.90	S	423.2	15 37 8.01	+14 24 47.10	II	204.8
15 18 14.06	+15 49 32.60	II	219.3	15 37 32.39	+13 44 47.70	I	1805.6
15 18 23.16	+22 58 35.20	S	244.1	15 37 45.72	+23 02 24.20	C	200.2
15 18 32.14	+11 18 45.40	S	405.5	15 38 34.18	+23 18 36.80	C	259.6
15 18 35.97	+10 32 12.60	S	409.1	15 39 16.46	+14 16 22.60	II	203.7
15 18 40.02	+24 27 5.20	I	291.3	15 39 25.11	+16 04 0.30	C*	412.5
15 19 3.03	+28 49 45.50	S	214.9	15 40 9.02	+14 21 14.00	S	569.3
15 20 5.50	+20 16 5.70	S*	2688.0	15 40 49.51	+14 47 46.70	C*	1386.8
15 20 29.84	+15 26 13.20	II	556.9	15 41 4.72	+18 05 50.90	II	276.6
15 21 13.53	+22 42 46.20	S	261.8	15 41 10.39	+15 44 2.60	S	217.9
15 21 16.47	+15 12 9.90	S	347.0	15 42 19.54	+17 56 8.20	S	529.8
15 22 12.15	+10 41 31.00	II	499.4	15 42 20.49	+24 01 55.10	I	273.4
15 22 17.09	+10 13 0.50	I	333.4	15 42 56.17	+10 54 34.70	II	303.0
15 22 19.66	+21 19 57.20	S	298.0	15 43 23.83	+21 45 34.80	II	208.1
15 22 24.16	+21 58 8.80	II	333.6	15 43 28.53	+22 52 32.80	II	219.1
15 23 21.74	+13 32 29.40	S	351.2	15 43 41.41	+13 31 8.50	II	303.0
15 23 25.27	+27 04 57.70	S	347.5	15 43 43.81	+18 47 20.40	C	356.2
15 23 27.56	+11 30 23.90	I	407.2	15 44 17.49	+14 10 13.80	II	217.8
15 23 28.40	+28 36 4.10	I	835.6	15 45 2.48	+13 45 47.30	S	231.7
15 23 49.36	+32 13 50.60	C	270.0	15 45 55.05	+19 06 29.30	S	927.7
15 23 56.93	+10 55 44.10	II	1060.2	15 45 55.06	+23 11 57.90	C	228.2

CoNFIG-3

RA	DEC (J2000)	Radio Type	$S_{1.4\ \mathrm{GHz}}$ (mJy)	RA	DEC (J2000)	Radio Type	$S_{1.4\ \mathrm{GHz}}$ (mJy)
15 46 2.56	+17 54 38.40	II	229.9	15 53 19.50	+17 49 43.10	II	383.7
15 46 5.99	+27 49 17.30	S	217.1	15 53 27.68	+27 30 55.80	S	228.5
15 46 31.47	+21 57 41.30	II	427.2	15 53 32.77	+12 56 50.80	C*	947.7
15 47 7.52	+11 42 49.80	II	367.1	15 53 43.61	+23 48 4.70	I	732.1
15 47 12.96	+18 04 10.80	I	419.9	15 53 50.45	+25 01 25.30	S	367.8
15 47 21.00	+27 48 22.00	II	274.0	15 53 54.37	+21 59 27.50	II	530.0
15 47 30.07	+14 56 55.70	I	203.7	15 54 34.04	+25 19 19.40	S	394.6
15 47 42.72	+20 51 46.00	II	2396.2	15 54 39.26	+19 47 18.70	S	1094.5
15 49 4.81	+26 44 14.50	II	260.8	15 54 54.57	+14 59 40.80	II	277.7
15 48 7.46	+14 51 17.60	II	398.6	15 55 0.57	+21 41 59.50	C	233.6
15 49 36.64	+18 35 0.10	II	584.6	15 55 31.35	+27 45 40.70	S	218.6
15 49 48.98	+21 25 39.10	II	2522.0	15 55 32.85	+20 09 39.70	C	212.6
15 50 12.00	+27 17 58.20	I	282.8	15 55 43.09	+11 11 24.50	C*	312.0
15 50 38.88	+18 39 1.20	II	214.5	15 55 51.00	+24 06 15.00	II	481.9
15 50 43.51	+11 20 58.50	I	828.3	15 55 52.29	+13 18 37.50	S	202.9
15 51 11.66	+26 06 14.30	II	455.3	15 56 10.06	+20 04 21.20	II	2313.7
15 51 21.19	+20 03 12.90	II	386.6	15 56 30.55	+22 07 29.70	II	343.4
15 51 36.81	+10 36 22.70	II	530.7	15 56 37.78	+20 00 51.70	S	289.9
15 51 45.36	+12 43 25.10	S	250.1	15 56 43.27	+14 18 32.80	I	271.0
15 51 47.90	+20 04 39.90	I	834.8	15 56 47.07	+10 37 55.70	I	415.5
15 52 10.54	+18 42 7.80	S	274.7	15 57 38.81	+10 12 28.10	S	267.7
15 52 10.97	+22 45 8.00	S	248.1	15 59 6.89	+12 10 26.90	II	688.8
15 52 24.01	+11 12 45.20	S	211.9	15 59 16.81	+11 15 45.70	I	667.7
15 52 25.25	+20 06 33.20	II	3198.4	15 59 24.98	+16 24 41.30	C	321.3
15 53 5.37	+14 1 16.60	II	303.3	15 59 54.25	+16 18 38.40	C	987.1
15 53 9.93	+21 00 43.70	II	244.9				

CoNFIG-4

RA	DEC (J2000)	Radio Type	$S_{1.4\ \mathrm{GHz}}$ (mJy)	RA	DEC (J2000)	Radio Type	$S_{1.4\ \mathrm{GHz}}$ (mJy)
14 08 7.86	-04 51 28.40	II	190.1	14 11 7.85	+00 36 7.80	C*	242.0
14 08 18.51	+00 13 9.50	C	113.8	14 11 8.29	+01 24 41.10	II	187.5
14 08 28.14	+02 25 48.70	I	243.7	14 11 10.28	-00 35 59.10	II	103.3
14 08 32.29	+00 31 33.90	II	61.2	14 11 14.61	+02 17 22.50	I	86.5
14 08 32.70	-01 31 19.50	C	73.3	14 11 20.30	-04 32 36.70	II	188.3
14 08 33.31	+01 16 22.10	II	601.3	14 11 23.53	+00 42 40.10	II	426.5
14 08 37.71	+02 48 29.40	S	77.0	14 11 35.32	-03 20 19.60	II	348.2
14 08 46.83	+01 33 56.60	II	173.6	14 11 55.84	-04 23 23.30	C	58.7
14 08 51.04	-04 11 33.70	II	71.8	14 12 2.34	+02 54 39.60	S	644.3
14 08 52.43	+02 42 48.60	S	58.3	14 12 5.27	-03 19 29.10	I	360.2
14 09 14.92	-03 17 3.70	C	147.4	14 12 46.22	+02 29 26.20	II	120.9
14 09 23.53	-00 04 36.40	C	68.9	14 12 51.56	-02 08 34.50	S	388.2
14 09 28.95	-01 57 20.30	II	90.3	14 12 51.98	-00 45 7.70	II	61.8
14 09 31.43	-01 00 53.20	S	69.8	14 13 14.30	-03 45 53.90	I	52.0
14 09 48.25	-02 30 55.90	C	87.5	14 13 14.84	-03 12 27.00	I	338.8
14 09 53.30	-03 04 30.30	II	60.0	14 13 14.94	-00 22 56.60	II	233.4
14 09 56.27	-02 46 5.10	I	73.0	14 13 26.43	-01 46 46.70	II	84.3
14 09 57.00	-01 21 4.70	I	71.4	14 13 27.39	+02 37 28.80	II	55.9
14 09 58.48	-01 09 14.10	II	150.2	14 13 29.35	-02 09 31.00	C	115.6
14 09 59.53	-02 45 32.90	II	62.2	14 13 36.49	-03 54 21.50	II	59.8
14 09 59.89	+01 14 50.00	C	53.6	14 13 38.87	-02 33 15.10	II	59.1
14 10 0.72	-04 18 46.60	S	79.6	14 13 41.97	+01 11 26.60	C	195.4
14 10 4.66	+02 03 7.10	C*	333.5	14 13 52.16	+01 42 41.00	II	140.8
14 10 19.21	-01 08 3.10	C	54.0	14 13 57.18	-04 16 26.00	S	314.3
14 10 25.85	-00 41 51.50	C	66.3	14 14 9.37	+01 49 10.80	II	55.3
14 10 29.99	-04 06 24.70	C	69.7	14 14 23.04	-00 01 38.00	II	152.6
14 10 35.33	-00 41 53.30	II	178.7	14 14 35.80	+02 56 18.30	II	135.9
14 10 38.33	-04 43 47.20	C	53.6	14 14 57.34	+00 12 17.90	I	110.4
14 11 3.89	-04 15 47.90	C	74.3	14 15 10.01	+00 36 21.30	II	68.8
14 11 4.35	-03 00 43.30	I	277.3	14 15 11.41	-01 37 2.80	I	113.7

CoNFIG-4							
RA	DEC (J2000)	Radio Type	$S_{1.4\ \mathrm{GHz}}$ (mJy)	RA	DEC (J2000)	Radio Type	$S_{1.4\ \mathrm{GHz}}$ (mJy)
14 15 28.72	+01 05 54.20	II	107.2	14 26 30.42	+01 42 36.10	II	90.8
14 15 30.47	+02 23 1.30	II	153.9	14 26 49.60	-00 47 18.30	C	87.7
14 15 53.96	+02 10 31.90	C	86.5	14 26 49.84	+00 55 59.90	II	57.9
14 16 4.11	+00 29 15.40	I	107.2	14 26 55.09	-02 49 20.90	C	60.3
14 16 9.42	-01 25 13.60	I	114.2	14 26 55.47	-02 15 45.10	C	167.1
14 16 13.74	+02 19 22.50	I	256.2	14 27 11.20	-01 52 12.70	II	52.0
14 16 43.04	-02 56 11.30	C	93.6	14 27 39.70	+00 21 44.60	II	110.3
14 16 56.31	+02 22 33.30	C	60.9	14 27 44.00	-04 45 52.60	S	453.5
14 16 59.89	-00 57 31.90	II	69.9	14 27 46.92	+00 28 47.40	II	86.7
14 17 10.36	-04 28 18.90	II	619.1	14 27 46.97	+00 42 33.10	C	349.1
14 17 23.95	-04 00 46.60	S	1687.2	14 27 52.85	-01 25 26.40	S	317.3
14 17 39.24	+00 40 4.00	II	145.5	14 27 58.55	-02 00 50.50	II	51.2
14 18 24.53	-01 20 1.00	S	200.0	14 28 10.34	+02 57 41.30	C	58.0
14 18 24.69	+01 07 27.30	II	131.2	14 28 31.22	-01 24 8.70	II	3157.4
14 18 28.14	+01 27 54.30	I	240.7	14 28 41.93	-03 27 7.80	C	60.8
14 18 38.44	-02 31 5.90	S	105.9	14 28 47.61	+01 35 12.30	S	71.7
14 18 41.25	+00 23 59.20	II	52.4	14 29 4.11	+02 51 39.90	I	608.9
14 18 59.20	-03 22 51.80	C	290.3	14 29 5.53	-03 38 15.40	II	129.1
14 19 3.74	-04 13 38.10	II	78.1	14 29 27.02	-04 31 57.20	C	68.8
14 19 8.14	+01 08 55.50	C	57.1	14 29 30.20	-01 55 44.30	C	101.3
14 19 8.97	-03 14 33.00	I	145.5	14 29 43.45	-03 42 13.10	C	115.6
14 19 13.33	-00 13 52.90	I	436.1	14 29 46.17	-01 57 3.50	S	123.1
14 19 24.71	+00 16 59.90	C	178.5	14 29 48.66	-01 12 52.30	S	675.1
14 19 24.82	-01 49 32.00	I	502.7	14 29 56.08	-04 08 44.50	II	60.5
14 19 32.35	+00 31 18.10	II	70.2	14 30 0.95	+00 46 26.30	S	120.7
14 20 15.76	-04 34 9.30	C	51.8	14 30 15.69	-03 38 58.90	I	193.3
14 20 33.39	-00 32 34.80	II	77.0	14 30 23.24	-01 55 17.70	II	117.6
14 20 34.17	-00 54 59.80	C	203.4	14 30 30.32	-00 40 22.70	C	146.1
14 20 55.66	-00 09 38.90	C	53.6	14 30 30.53	+01 01 4.90	II	171.4
14 21 7.15	-04 48 43.90	S	99.4	14 30 31.45	-00 09 8.00	C	53.0
14 21 11.07	+02 48 32.80	I	332.7	14 30 36.51	+00 33 41.40	II	64.7
14 21 13.56	-02 46 46.00	S	527.9	14 30 48.92	-03 34 46.20	I	805.4
14 21 28.62	-04 31 35.10	I	55.4	14 31 10.48	-01 33 37.60	II	120.8
14 21 42.64	+01 24 42.50	II	64.9	14 31 13.10	-00 52 40.30	C	76.0
14 22 35.63	-01 52 12.40	II	113.1	14 31 33.17	-03 45 51.30	I	268.4
14 23 3.43	+01 39 58.70	C	210.4	14 31 34.19	-00 55 16.40	C	59.4
14 23 12.37	+02 20 35.40	II	170.8	14 31 38.25	-00 55 34.60	II	93.1
14 23 18.15	-04 52 37.90	II	52.4	14 31 46.86	-00 50 13.00	II	82.4
14 23 26.70	-00 49 56.50	II	492.9	14 31 53.03	-04 45 21.10	I	56.7
14 23 29.14	-02 45 21.80	II	58.0	14 31 53.62	-01 21 59.10	S	72.2
14 23 44.68	+01 20 36.80	II	53.2	14 31 55.14	-04 33 55.40	C	63.0
14 23 56.98	+00 31 15.00	II	51.4	14 32 6.30	+02 37 9.40	II	55.8
14 24 3.40	+00 29 58.70	I	95.5	14 32 21.67	-03 53 24.80	C	258.3
14 24 18.85	+00 55 12.20	C	72.7	14 32 37.84	-01 17 57.30	C	58.7
14 24 19.81	+00 25 34.20	I	157.4	14 32 38.09	-03 03 18.30	II	58.4
14 24 29.15	-03 53 3.30	C	54.8	14 32 44.31	-00 59 13.80	II	130.5
14 24 39.49	-01 44 33.40	II	67.0	14 32 49.09	+00 47 4.30	II	76.4
14 24 39.86	-04 10 53.30	C	68.7	14 32 54.19	-01 59 33.60	S	169.3
14 24 40.65	-03 23 29.80	II	550.7	14 32 59.25	+00 54 55.20	II	199.5
14 25 1.42	-02 38 36.70	II	178.1	14 32 59.93	-04 42 15.10	I	59.8
14 25 9.14	-02 27 15.80	C	52.7	14 33 1.45	-00 28 50.80	II	168.7
14 25 9.19	-01 16 1.90	I	149.9	14 33 8.83	+00 44 35.50	C	70.1
14 25 18.88	-03 39 21.70	S	50.2	14 33 14.16	-00 18 6.70	C	201.2
14 25 42.28	-03 40 33.30	S	51.1	14 33 24.80	-02 20 45.10	C	256.0
14 25 45.72	+00 22 42.00	C	70.3	14 33 29.63	-04 30 10.30	II	159.4
14 25 50.20	-00 23 15.70	I	157.4	14 33 46.59	+02 17 55.90	I	170.8
14 25 50.50	-04 29 51.30	C	58.6	14 33 46.69	-02 23 22.50	S	53.6
14 25 55.95	+02 46 56.80	S	290.9	14 33 50.13	+02 28 24.90	C	53.6
14 25 59.00	+01 38 24.00	II	97.4	14 33 52.09	+00 37 30.30	I	275.2
14 26 12.96	+02 00 39.60	C	66.8	14 34 2.62	+01 35 7.90	I	575.1
14 26 15.51	+00 50 21.70	I	96.7	14 34 3.22	+01 03 51.50	C	64.9
14 26 23.75	-03 21 28.80	S	118.3	14 34 5.22	-00 23 4.30	II	156.6

CoNFIG-4

RA	DEC	Radio	$S_{1.4\ \mathrm{GHz}}$	RA	DEC	Radio	$S_{1.4\ \mathrm{GHz}}$
(J2000)		Type	(mJy)	(J2000)		Type	(mJy)
14 34 10.14	-01 23 24.80	II	122.2	14 37 41.15	+02 17 26.70	I	67.7
14 34 32.06	-03 54 40.20	C	123.8	14 37 42.80	-00 15 4.20	I	67.0
14 34 47.71	-04 27 44.90	II	105.1	14 37 48.30	-01 47 9.40	C	52.1
14 34 49.27	-02 15 9.20	II	112.5	14 37 56.68	-00 41 16.10	II	61.6
14 34 52.84	+02 36 3.00	II	322.1	14 37 56.76	+01 56 38.30	II	86.7
14 34 59.40	-04 16 11.20	C	84.0	14 38 0.61	+02 37 3.20	II	56.9
14 35 7.84	-04 06 13.60	C	55.6	14 38 0.84	+00 23 23.80	C	111.9
14 35 21.30	-02 40 51.70	I	62.9	14 38 6.05	+01 24 30.20	C	75.2
14 35 23.20	+02 25 42.80	II	71.5	14 38 10.41	-01 42 5.30	C	58.1
14 35 36.18	-04 10 40.50	C	135.1	14 38 14.19	+01 13 30.40	C	75.1
14 35 39.83	-04 14 55.00	C*	480.1	14 38 17.17	+01 50 31.70	S	115.8
14 35 41.65	-01 47 25.90	II	132.2	14 38 20.57	-01 20 6.60	I	57.3
14 35 44.87	-04 38 30.50	C	77.1	14 38 20.96	-02 39 52.90	II	322.6
14 35 57.05	-04 12 20.70	I	234.1	14 38 25.93	-01 00 1.50	I	100.0
14 36 9.04	+01 48 49.20	C	52.7	14 38 33.63	-00 05 26.40	II	506.3
14 36 30.26	+00 35 19.80	C	123.0	14 38 33.64	+00 13 29.80	II	82.1
14 36 37.02	-02 14 31.10	C	59.8	14 38 41.86	-00 45 25.00	C	111.9
14 37 10.23	-03 04 57.80	C	50.0	14 38 43.38	+00 57 57.50	II	67.3
14 37 21.09	-00 33 18.10	S	365.0	14 38 43.41	-00 48 51.00	II	57.2
14 37 22.79	-03 03 7.30	II	120.0	14 38 48.87	+00 40 59.20	I	164.8
14 37 31.82	+01 18 58.40	C	108.8	14 38 49.11	-00 51 16.50	II	133.5
14 37 31.86	+01 43 25.20	II	443.0	14 38 53.93	-02 42 8.20	C	146.9
14 37 34.58	-04 38 55.60	C	162.4	14 39 39.50	+00 43 35.20	II	122.3
14 37 36.74	+01 45 3.20	I	276.7	14 39 43.36	-00 18 59.50	I	133.2
14 37 37.48	+02 56 10.00	II	195.4	14 39 58.03	-04 19 20.40	II	93.7

Table B3. Source counts. S_{min} and S_{max} define the flux density bins and S_{av} corresponds to the center of the bin.

$logS_{min}$	$logS_{max}$	$logS_{av}$	N	Area (sr)
All Sources				
−2.10	−1.90	−2.00	39	0.0018
−1.90	−1.70	−1.80	34	0.0018
−1.70	−1.50	−1.60	19	0.0018
−1.50	−1.30	−1.40	15	0.0213
−1.30	−1.10	−1.20	107	0.0213
−1.10	−0.90	−1.00	52	0.0213
−0.90	−0.70	−0.80	43	0.0213
−0.70	−0.50	−0.60	175	0.1340
−0.50	−0.30	−0.40	97	0.1340
−0.30	−0.10	−0.20	37	0.1340
−0.10	0.10	0.00	144	1.0202
0.10	0.30	0.20	139	1.5000
0.30	0.50	0.40	82	1.5000
0.50	0.70	0.60	30	1.5000
0.70	0.90	0.80	13	1.5000
0.90	1.10	1.00	5	1.5000
1.10	1.30	1.20	2	1.5000
1.30	1.50	1.40	4	4.3000
1.50	1.70	1.60	1	4.3000
FRI Sources				
−2.10	−1.90	−2.00	18	0.0018
−1.90	−1.70	−1.80	13	0.0018
−1.70	−1.50	−1.60	6	0.0018
−1.50	−1.30	−1.40	3	0.0018
−1.30	−1.10	−1.20	12	0.0213
−1.10	−0.90	−1.00	8	0.0194
−0.90	−0.70	−0.80	8	0.0194
−0.70	−0.50	−0.60	27	0.1322
−0.50	−0.30	−0.40	16	0.1322
−0.30	−0.10	−0.20	5	0.1322
−0.10	0.10	0.00	17	1.0202
0.10	0.30	0.20	17	1.5000
0.30	0.50	0.40	6	1.5000
0.50	0.70	0.60	7	1.5000
0.70	0.90	0.80	4	1.5000
0.90	1.10	1.00	1	1.5000
1.10	1.30	1.20	2	4.3000
1.30	1.50	1.40	1	4.3000
FRII Sources				
−2.10	−1.90	−2.00	19	0.0018
−1.90	−1.70	−1.80	20	0.0018
−1.70	−1.50	−1.60	10	0.0018
−1.50	−1.30	−1.40	8	0.0018
−1.30	−1.10	−1.20	53	0.0213
−1.10	−0.90	−1.00	30	0.0213
−0.90	−0.70	−0.80	26	0.0213
−0.70	−0.50	−0.60	122	0.1340
−0.50	−0.30	−0.40	64	0.1340
−0.30	−0.10	−0.20	26	0.1340
−0.10	0.10	0.00	93	1.0007
0.10	0.30	0.20	82	1.5000
0.30	0.50	0.40	54	1.5000
0.50	0.70	0.60	13	1.5000
0.70	0.90	0.80	4	1.5000
0.90	1.10	1.00	2	1.5000
1.10	1.30	1.20	1	1.5000
1.30	1.50	1.40	1	4.3000

APPENDIX C: CONTOUR PLOTS

C1 Contours

Contour plots from NVSS (outermost contours) and FIRST (innermost contours) of all sources in the CoNFIG sample. The contours are displayed in logarithmic intervals from 5 mJy/beam (unless specified otherwise) to the peak flux per beam of the source. The grey-scale background corresponds to the SSS optical R-band image. Sources marked with a ^{n} or a ^{v} correspond to objects for which higher resolution images were used to determine the morphology, either from the NRAO archives (^{n}) or our VLA 8 GHz observations (^{v}). The 3 sources marked by a ^{R} were removed from the sample after a closer inspection of their contour plots. They are part of the 7 deleted sources listed in Table 1. The full version of these figures can be found online on MNRAS.

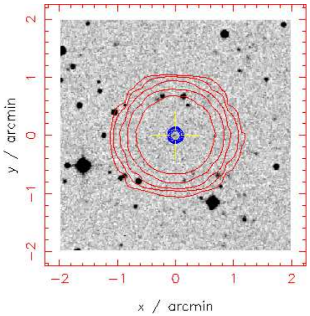

CoNFIG-001
07 13 38.15 +43 49 17.20

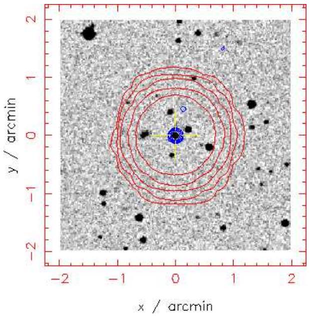

CoNFIG-005
07 41 10.70 +31 12 0.40

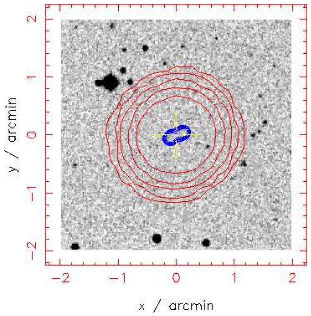

CoNFIG-009^{v}
07 59 47.26 +37 38 50.20

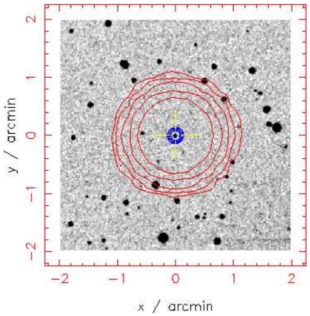

CoNFIG-002
07 14 24.80 +35 34 39.90

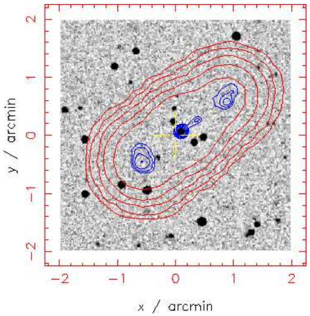

CoNFIG-006
07 45 42.13 +31 42 52.60

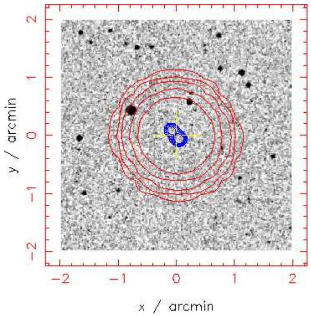

CoNFIG-010^{v}
08 01 35.32 +50 09 43.00

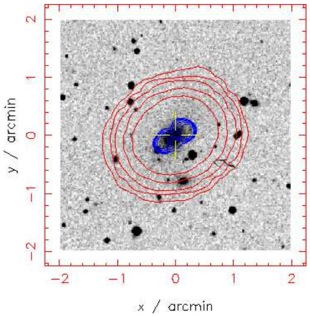

CoNFIG-003
07 16 41.09 +53 23 10.30

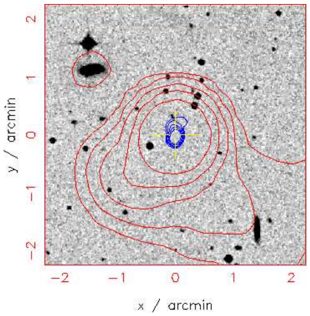

CoNFIG-007 (from 10 mJy/beam)
07 49 48.10 +55 54 21.00

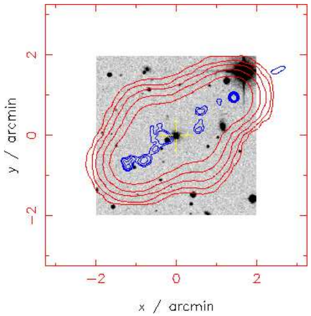

CoNFIG-011
08 05 31.31 +24 10 21.30

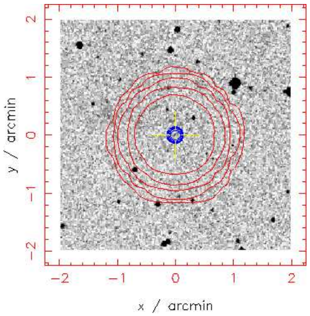

CoNFIG-004
07 35 55.54 +33 07 9.60

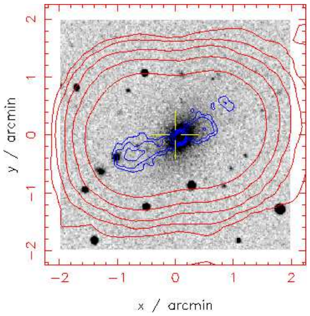

CoNFIG-008 (from 1 mJy/beam)
07 58 28.60 +37 47 13.80

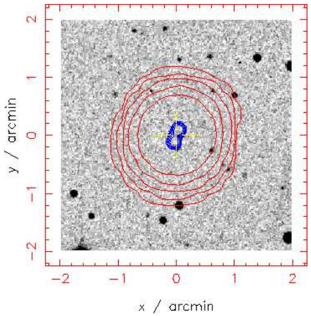

CoNFIG-012^{n}
08 10 3.67 +42 28 4.00

APPENDIX D: VLA OBSERVATIONS

D1 Comments on sources with additional VLA observations

Table D1. List of the sources with higher resolution contour plots. The sources identified by a star are part of the VLA 8 GHz A-configuration observation obtained on July 29, 2007. For these sources, the exposure time and the predicted signal-to-noise are stated. Data were extracted from the VLA archives at other frequencies and configurations for some sources for which the 8 GHz A - configuration contours were not satisfactory.

[1] Because of the very low quality of the 8 GHz data for this source, its morphology remains uncertain.

[2] The source actually consist of two separate sources with $S_{1.4\ \mathrm{GHz}} < 1.3Jy$ and was deleted from the sample.

[3] The source was classified as an FRII, but with reserve.

[4] This source was originally classified as FRI from the FIRST contours, but appeared to be an FRII when looking at the 8 GHz contours.

Source Name	RA	DEC	$S_{1.4\ \mathrm{GHz}}$ (mJy)	Frequ.	Conf.	t_{exp} (min)	S/N
CoNFIG-009*	07 59 47.26	+37 38 50.20	1691.2	8 GHz	A	5.0	14.1
CoNFIG-010*	08 01 35.32	+50 09 43.00	1471.7	8 GHz	A	10.0	10.0
CoNFIG-012	08 10 03.67	+42 28 04.00	2056.6	8 GHz	A		
CoNFIG-015*[2]	08 14 43.59	+12 58 10.00	1603.3	8 GHz	A	30.0	5.7
CoNFIG-016*[3]	08 19 47.55	+52 32 29.50	2104.2	5 GHz	B	15.0	5.7
CoNFIG-017[4]	08 21 33.77	+47 02 35.70	1787.1	8 GHz	B		
CoNFIG-025*	08 34 48.37	+17 00 46.10	1882.8	8 GHz	A	5.0	14.1
CoNFIG-034*	08 54 39.35	+14 05 52.10	2163.8	8 GHz	A	5.0	42.2
CoNFIG-036*	08 57 40.64	+34 04 06.40	1798.4	8 GHz	A	10.0	8.9
CoNFIG-037*	08 58 10.07	+27 50 50.80	1807.8	8 GHz	A	5.0	11.8
CoNFIG-045*	09 12 04.00	+16 18 29.70	1374.6	8 GHz	A	5.0	21.7
CoNFIG-048*	09 22 49.93	+53 02 21.20	1597.8	8 GHz	A	5.0	10.9
CoNFIG-050	09 30 33.45	+36 01 23.60	1875.1	5 GHz	B		
CoNFIG-054	09 42 15.35	+13 45 49.60	3336.4	5 GHz	A		
CoNFIG-055*	09 43 12.74	+02 43 27.50	1331.5	8 GHz	A	5.0	32.8
CoNFIG-060	09 51 58.83	−00 01 26.80	3152.1	5 GHz	A		
CoNFIG-068	10 11 00.36	+06 24 40.20	2964.2	8 GHz	A		
CoNFIG-070	10 17 14.15	+39 01 24.00	1392.2	8 GHz	A		
CoNFIG-080*	10 41 39.01	+02 42 33.00	2710.1	8 GHz	A	5.0	77.4
CoNFIG-083	10 58 17.46	+19 52 09.50	2143.0	5 GHz	A		
CoNFIG-084[1]	10 58 29.62	+01 33 58.20	3220.2	8 GHz	A		
CoNFIG-086*	11 02 03.91	−01 16 18.30	2799.6	8 GHz	A	5.0	13.4
CoNFIG-098	11 23 09.10	+05 30 20.30	1721.1	5 GHz	A		
CoNFIG-101*	11 34 38.46	+43 28 00.50	1567.1	8 GHz	A	5.0	36.8
CoNFIG-106*	11 41 08.23	+01 14 17.70	2690.8	8 GHz	A	5.0	94.1
CoNFIG-114	11 53 24.51	+49 31 09.50	1572.2	8 GHz	A		
CoNFIG-115*	11 54 13.01	+29 16 08.50	1620.3	8 GHz	A	10.0	6.8
CoNFIG-122*	12 04 02.13	−04 22 43.90	2141.3	8 GHz	A	30.0	4.9
CoNFIG-128*	12 15 29.80	+53 35 54.10	2755.0	8 GHz	A	5.0	18.4
CoNFIG-129	12 15 55.60	+34 48 15.10	1506.8	8 GHz	A		
CoNFIG-134	12 24 54.62	+21 22 47.20	2094.4	8 GHz	A		
CoNFIG-140	12 32 00.13	−02 24 04.10	1646.7	8 GHz	A		
CoNFIG-148*	12 53 03.55	+02 38 22.30	1604.9	8 GHz	A	30.0	5.4
CoNFIG-151	12 56 11.15	−05 47 20.10	9711.2	8 GHz	A		
CoNFIG-154	13 05 36.05	+08 55 15.90	1461.8	8 GHz	A		
CoNFIG-162*	13 20 21.45	+17 43 12.40	1573.2	8 GHz	A	5.0	9.6
CoNFIG-163	13 21 18.84	+11 06 49.40	2238.0	8 GHz	A		
CoNFIG-171	13 38 08.07	−06 27 11.20	2958.5	8 GHz	A		
CoNFIG-173	13 42 13.13	+60 21 42.30	1493.3	8 GHz	A		
CoNFIG-189	14 17 23.95	−04 00 46.60	1687.2	8 GHz	A		
CoNFIG-193	14 24 56.93	+20 00 22.70	1808.5	8 GHz	A		
CoNFIG-194*	14 25 50.67	+24 04 06.70	1558.7	8 GHz	A	30.0	5.2
CoNFIG-195	14 28 31.22	−01 24 08.70	3157.4	15 GHz	C		
CoNFIG-197*	14 36 57.07	+03 24 12.30	2797.3	8 GHz	A	5.0	66.8
CoNFIG-201*[1]	14 48 39.98	+00 18 17.90	1651.5	8 GHz	A	5.0	10.5
CoNFIG-208*	15 10 53.55	−05 43 07.10	3569.3	8 GHz	A	5.0	56.3
CoNFIG-210*[1]	15 12 25.35	+01 21 08.70	2262.7	5 GHz	A	5.0	52.3
CoNFIG-220*	15 31 25.36	+35 33 40.60	1820.7	8 GHz	A	5.0	9.1
CoNFIG-224*	15 37 32.39	+13 44 47.70	1805.6	8 GHz	A	5.0	91.5
CoNFIG-227*	15 41 45.64	+60 15 36.20	1337.4	8 GHz	A	60.0	5.0
CoNFIG-234*[1]	15 56 10.06	+20 04 21.20	2313.7	8 GHz	A	5.0	91.3
CoNFIG-244*	16 17 15.75	+21 07 29.40	1748.5	8 GHz	A	10.0	6.9
CoNFIG-257*	16 36 37.38	+26 48 06.60	1336.1	8 GHz	A	40.0	5.8

D2 1.4 GHz and 8 GHz contour plots

Contour plots from FIRST 1.4GHz (outermost contours) and VLA 8 GHz observations (innermost contours). The contours are displayed in logarithmic intervals from 5 mJy/beam to the peak flux per beam of the source. The greyscale background corresponds to the SSS optical R-band image. Stars show the FIRST positions, squares the NVSS position and triangles the optical ID from SSS. The full version of these figures can be found online on MNRAS.

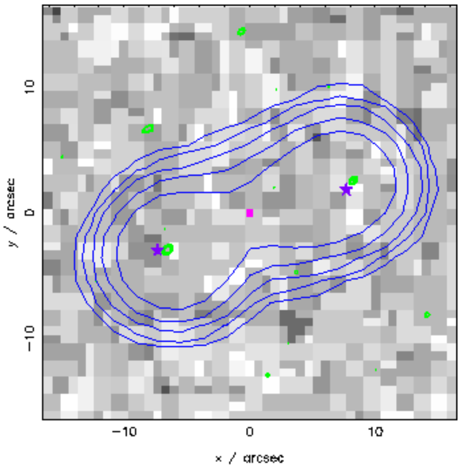

CoNFIG-009
8 GHz, A configuration

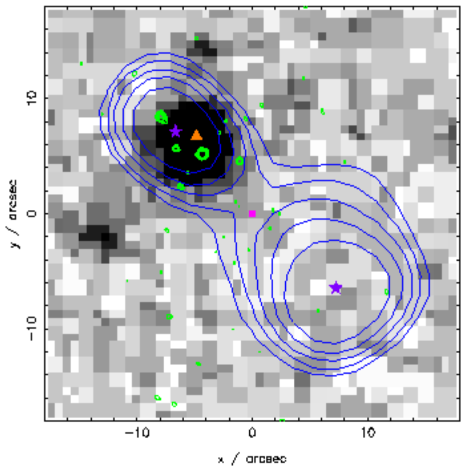

CoNFIG-015
8 GHz, A configuration

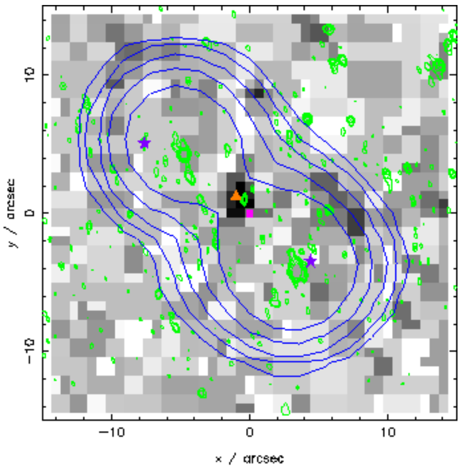

CoNFIG-010
8 GHz, A configuration

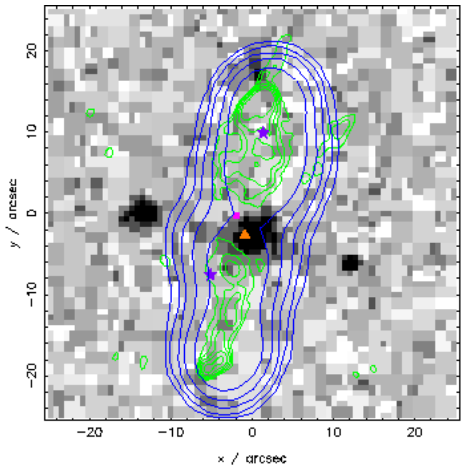

CoNFIG-016
5 GHz, B configuration

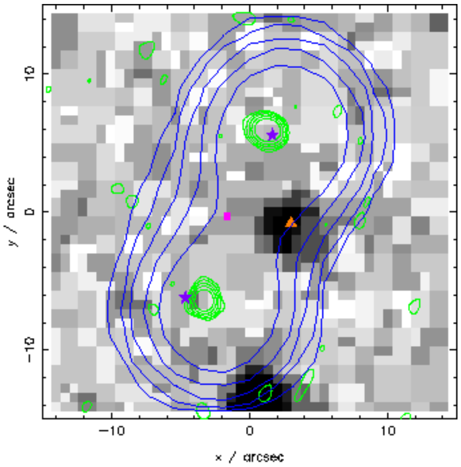

CoNFIG-012
8 GHz, A configuration

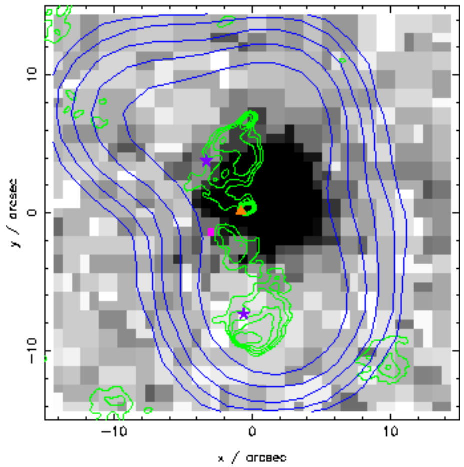

CoNFIG-017
8 GHz, B configuration